STUDIES ON
FUNCTIONAL AMINO ACID RESIDUES
AND
CATALYTIC MECHANISM OF
MAMMALIAN α-AMYLASES

KAZUHIKO ISHIKAWA

1992

STUDIES ON FUNCTIONAL AMINO ACID RESIDUES
AND
CATALYTIC MECHANISM OF MAMMALIAN α-AMYLASES

KAZUHIKO ISHIKAWA

1992

Abbreviation

PPA	porcine pancreatic α-amylase
HPA	human pancreatic α-amylase
HSA	human salivary α-amylase
TAA	Taka-amylase A (α-amylase from *Aspergillus oryzae*)
BME	*Bacillus macerans* transglycosylase
G	glucose
G_2	maltose
G_3	maltotriose
G_4	maltotetraose
G_5	maltopentaose
G_6	maltohexaose
GOH	sorbitol;
G_2OH	maltitol
G_3OH	maltotriitol
G_4OH	maltotetraitol
G_5OH	maltopentaitol
G_6OH	maltohexaitol.
α–CD	α-cyclodextrin
β-CD	β-cyclodextrin
γ-CD	γ-cyclodextrin
X	xylose
S	sorbose
D	2-deoxy-glucose
ϕ or PNP	*p*-nitrophenol
F	fructose.
M	methyl residue
HPLC	high pressure liquid chromatography
SDS	sodium dodecyl sulfate
PAGE	polyacrylamide gel electrophoresis
MW	molecular weight

CONTENT

INTRODUCTION

Amylases are the enzymes which catalyze the hydrolysis of α-(1,4) glycosidic linkages of polysaccharides such as starch, glycogen, or their degradation products (1-5). Amylases have been classified mainly into endoamylases and exoamylases (1). Endoamylases hydrolyze randomly α-(1,4) glycosidic linkages of polysaccharides and exoamylases hydrolyze polysaccharides only from the non-reducing outer chain ends. α-Amylases (EC 3.2.1.1) are one of the endoamylases and liberate the reducing hemiacetal group in α-optical configuration (Fig. 1 (A)) (6, 7). They are also able to hydrolyze (substituted)-phenyl α-maltoside into (substituted)-phenol and maltose (Fig. 1 (B)) (8). It is a synthetic substrate for α–amylases which is suitable for spectrophotometric measurement of the activity. α-Amylases are the historically earliest known enzymes. Nowadays, α-amylases are found throughout whole living organisms (1-5). α-Amylases of which sequences have been determined are listed with some characters in Table I. α-Amylases possess many common features in general. They are all slightly acidic, water-soluble proteins of molecular weight around 50,000; they contain at least 1 mole of calcium ion per mole, which is essential for their stability and activity; and their specific activities are of the similar order of magnitude (k_{cat} is 100 - 1000 s^{-1} for amylose or soluble starch at 30°C). Mammalian α–amylases differ from those of other origins in several points. Only mammalian and possibly most animal α-amylases are activated by chloride ion, and the optimum pH is neutral.
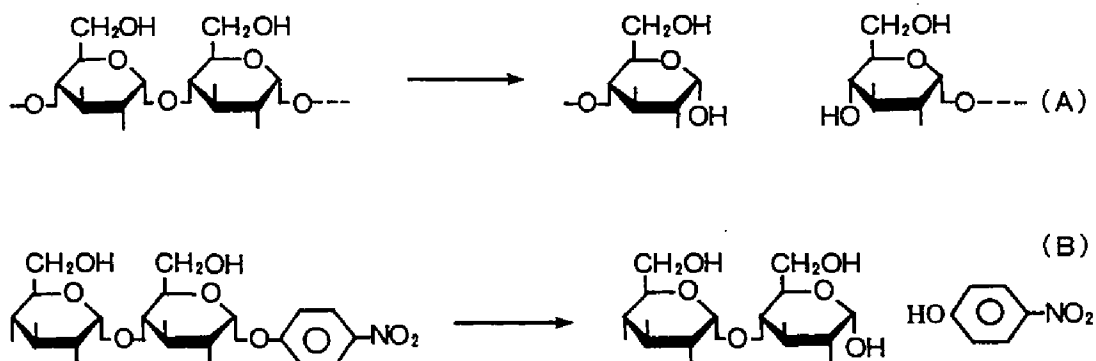

Fig. 1. Hydrolytic modes of α-(1, 4) glycoside bond in polysaccharide (A) and phenyl α-maltoside (B) by α-amylases.

Table I. Distributions and characters of α-amylases of which sequences are determined.

Kingdom	Origin	Molecular weight	Optimum pH	Activation by Cl⁻
Micro organis	A. ory. (TAA)	53,662	5.5	-
	B. amylo.	54,800	6.0	-
	B. sub.	42,000	6.0	-
	B. stearo.	61,000	6.0	-
	B. lich.	62,000	6.0	-
Plant	Barley I	45,000	5.5	-
	Barley II	45,000	5.5	-
Animal	Human p.	55,000	6.9	+
	Human s.	55,000	6.9	+
	Porcine p.	55,000	6.9	+
	Rat	58,000	6.9	+

Enzyme origins are abbreviated as: A. ory., *Aspergillus oryzae*; B. amylo., *Bacillus amyloliquefaciens*; B. sub., *Bacillus subtilis (saccharified)*; B. stearo., *Bacillus stearothermophilus*; B. lich., *Bacillus licheniformis*; s., saliva; p., pancreas.

It has been found by comparing sequences that there are conserved homology regions in α-amylases from different origins (9, 10). Homologous sequence region are surrounded by rectangles (Fig. 2). The 6 mammalian α-amylases were found to be highly homologous (80-90%). Homology was least among microorganisms, plants and animals. Nevertheless, at least four highly homologous regions were found in the amino acid sequences among whole α-amylases, despite their widely different origins. Three-dimensional structures have been determined with Taka amylase A (TAA) produced from *Aspergillus oryzae* (11) and porcine pancreas α-amylase (PPA) (12, 13). Particularly, the structure of TAA has been investigated precisely by X-ray crystallography. In TAA, the first 380 residues from the N-terminus constitute a first domain, A, and the rest make up a second domain, B. Domain A is spatially arranged from α-helices and β-strands in the $(\beta\alpha)_8$ structure, which is similar to that of triose phosphate isomerase (14) or pyruvate kinase (15). Domain B has an eight-stranded antiparallel β-sandwich structure. The two domains are linked by a single polypeptide chain with an extensive interface which is mainly composed of hydrophobic residues. A large cleft constructing the active site of TAA is located at the carboxyl end of the parallel β-barrel in domain A. From the data of the TAA crystal soaked in maltotriose solution, two carboxyl residues (Glu230 and Asp297) were proposed as the catalytic residues. In the case of PPA, the whole structure was very similar to that of TAA and the catalytic residues were also proposed as two carboxyl residues (Asp197 and Asp300) (12) (Fig. 3). Fig. 4 shows a proposed substrate binding

model of TAA and conserved amino acid residues in PPA. Furthermore, it has been inferred that the four homologous conserved regions (Fig. 2) were located around the catalytic and substrate binding sites of α-amylases from the above data.

Mammalian pancreatic α-amylase is a principal and efficient amylase relating to starch digestion and absorption of carbohydrate in small intestine. The function and its subsite pattern have been studied mainly with PPA (16, 17). PPA is a glycoprotein and consists of two isozymes (PPA I and II) which have the same molecular weight (55,000) and optimum pH (pH 6.9), but differ slightly in amino acid component and isoelectric point (18-20). In this thesis, PPA means only isozyme I purified from pancreatin

```
B.stearo.                                               M L T F H R I I R K C W H F L L A F L L T A L L F C P T C Q P A K A
B.amylo.                                         .      H I Q K R K R T V S F R L V L H C I L L F V S L P I T K T S A
B.sub.                      H F A K R F K T S L L P L F A C F L L L F H L V L A C P A A A S A E T A H K S H E
A.ory.
Rat                                                            H K F V L L L S L I C F C W A
House,s                                                      . H K F F L L L S L I C F C W A
House,p                                                        H K F V L L L S L I C F C W A
Hog
Human,s                                                      H K L F H L L F T I C F
Human,p                                                      H K F F L L L F T I C F
Barley                                                       H C K H C S L C C F S


B.stearo.   A A P F H C T H H Q Y F E H Y L P D D C T L W T K V A N E A H H L S S L C I T A L W L P P A Y K C T S R S D V C Y C V Y  60
B.amylo.       V H C T L H Q Y F E H Y T P N D C Q H W K R L Q H D A E H L S D I C I T A V W I P P A Y K C L S Q S D H C Y C P Y
B.sub.         L T A P S I K S C T I L H A W H W S F H T L K H H H-K D I H D A C Y T A I Q T S P I H Q V K E C H Q C D K S H S
A.ory.   A T P A D W R S Q S I Y F L L T D R F A R T D C S T T A T C H T A  D [D] K Y C C C T W Q G I I D K L D Y I Q C H C F T A I W I T P V T A Q L P Q D C A [V] C
Rat               Q Y D P H T A D C R T A I V H L F E W R W A D I A K E C E R Y L A P K C F C C V Q V S P P H E H I I I H H P S
House,s           Q Y D P H T Q Y C R T A I I H L F E W R W V D I A K E C E R Y L A P N C F A C V Q V S P P H E H I V V H S P S
House,p           Q Y D P H T S D C R T A I V H L F E W R W V D I A K E C E R Y L A P K C F C C V Q V S P P H E H V V V H H P S
Hog             A Y-A P Q T Q S C R T A I V H L F E W R W V D I A K E C E R Y L C P K C F C C V Q V S P P H E H V V T C H P S
Human,s       C W A Q Y S S H T Q Q C R T S I V H L F E W R W V D I A L E C E R Y L A P K C F C C V Q V S P P H E H V A I H H P F
Human,p       C W A Q Y S P H T Q Q C R T S I V H L F E W C H V D I A L E C E R Y L A P K C F C C V Q V S P Q H E I V A F H H P L
Barley   L L L L L L L A C L A S C H Q V L F Q C F H W E S W K Q S C C W Y N H H H C K V D D I A A A C V T H V W L P P P S H S V


                                                                   Region I  D A V I H H
B.stearo.   D L Y D L G E F H Q K C A V R T K Y C T X A Q Y L Q A I Q A A H A A C H Q V Y A|D V V F D H|K C C A D C T E W V D A V E  120
B.amylo.    D L Y D L C E F Q Q K C T V R T K Y C T K S E   L QDA I C S L H S R H V Q V Y C|D V V L N H|K A C A D A T E D V T A V E
B.sub.      H W Y W L Y Q P T S Y Q I C H R Y L C T E Q E F K E H C A A A E E Y C I K V.I V|D A V I H H|T T S D Y A A I S H E V K S
A.ory.      D A [V] T C Y [M] Q T D I Y S L H E H Y C T A D D L K A L S S A L H E R C H Y L H V|D V V A H H|C Y D C A C S S V D Y S V
Rat         R P W H E R Y Q P I S Y K I C S R S C H E H E F K D H V T R C H H V C V R I Y V|D A V I N H|H C C S C H S A C T H S T C
House,s     R P.W H E R Y Q P I S Y K I C S R S C H E D E F R D H V H R C H H V C V R I Y V|D A V I N H|H C C C V C A Q A C Q S S T C
House,p     R P W H E R Y Q P I S Y K I C T R S C H E D E F R D H V T R C H H V C V R I Y V|D A V I N H|H C C A C H P A C T S S T C
Hog         R P W H E R Y Q P V S Y K L C T R S C H E D E F R.D H V T R C H H V C V R I Y V|D A V I N H|H C C S C A A A C T C T T C
Human,s     R P W H E R Y Q P V S Y K L C T R S C H E D E F R H H V T R C H H V C V R I Y V|D A V I N H|H C C H A V S A C T S T C
Human,p     R P W H E R Y Q P V S Y H Y C T R S C H E D E F R H H V T R C H H V C V R I Y V|D A V I N H|H C C H A V S A C T S S T C
Barley      S H E C Y H P C R L Y D I D A S K Y C N A A E L K S L I C A L H C K C V Q A I A|D I V I N H|R C A D Y K D S R C I Y C E


B.stearo.   V H P S D R H Q E I S C T Y Q I Q A W T K F D F P C R C H T Y S S F K W R H Y H F D C V D W D E S R K L S R I Y K F R C  180
B.amylo.    V H P A H R H Q E T S E E Y Q I K A W T D F R F P C R C H T Y S D F K W H W Y H F D C A D W D E S R K I S R I F K F R C
B.sub.                                                                                        I P H W T H
A.ory.                                                    F K P F S S Q D Y F H P F C F I
Rat                                            C S Y F H P H H R E F S A V P T S A H.Y.F H D H K C
House,s                                        C S Y.F.H.P H H R D.F P C V P Y S C F D F H D C K C R T
House,p                                        C S Y L H P H H R E F P A V P Y S A W D F H D H K C
Hog                                            C S Y C H P C H R E F P A V P Y S A W D F H C H C K K T
Human,s                                        C S Y F H P C S R D F P V V P Y S C H D F H D C K C K T
Human,p                                        C S Y F H P C S R D F P A V P Y S C H D F H D C K C K T
Barley
```

- 3 -

```
                                                                                           Region 2  C F R L D A A K H
.stearo. I G K A W D W E V D T E H G H Y D Y L H Y A D L D H D H P E V V T E L K S W G K W Y V H T T H I D [G F R L D A V K H] I K 240
.amylo.  E G K A W D W E V S S E H G H Y D Y L H Y A D V D Y D H P D V V A E T K K W G I W Y A H E L S L D  G F R I D A A K H  I K
.sub     G H T Q I K H W S D R W D V T Q H S L L G L Y D H H T Q H T Q V V Q S Y L K R F L D R A L H D G A D G F R F D A A K H  I E
.ory.    Q H [YE] D Q T Q V E D C W L C [D] H T V S L P·D L D T T K D V V K H E W Y D W V C S L V S H Y S I D G L R I [D] T V [KH] V Q
rat        H G E I N H Y H D A N Q V R H C R L S G L L D L A L·D K D Y V R T·K V A D Y H H H L I D I G V A G F R L D A A K H H W
louse,s  A S G G I E H Y Q D A A Q V R D C R L S G L L D L A L E K D Y V R T K V A D Y H H H L·I D I G V A G F R L D A S K H H W
louse,p    H G E I D H Y H D A Y Q V R H G R L T G L L D L A L E K D Y V R T K V A D Y H H H L I D I G V A G F R L D A A K H H W
og       A S G G I E S Y H D P Y Q V R D G C Q V L L L D L A L E K D Y V R S H I A D Y L H K L I D I G V A G F R I D A S K H H W
uman,s   G S C D I E H Y H D A T Q V R D C R L S G L L D L A L G K D Y V R S K I A E Y H H H L I D I G V A G F R L D A S K H H W
uman,p   G S C D I E N Y H D A T Q V R D C R L T G L L D L A L Q K D Y V R S K I A E Y H H H L I D I G V A G F R L D A S K H H W
·rley                                                                                           F E G G T S [D G R L D W G Y G] H I
larley   C R D D T K Y S D G T A H L D T G A D F A A A P D I D H L H D R V Q R E L K E W L L W L K S D L G F D [A W R L D F A R C] Y S
```

```
                         Region 3  E V I D
·.stearo. F S F F P D W L S D V R S Q T G K P L F T V G [E Y W S] Y D I H K·L H H Y I H K T H G T H S L F D A P L H H K F Y T A S K 300
i.amylo.  F S F L R D W V Q A V R Q A T G K E H F T V A E Y W Q H H A G K L E H Y L H K T S F H Q S V F D V P L H F H L Q A A S S
i.sub.    L P D D G S Y C S Q F W P H I T H T S A E F Q Y G E I L Q D J A S R D A A Y A H Y H D V T A S H Y C H S I R S A
i.ory.    K D F H P G Y H K A A G V Y C I G [E W L D] G D P A Y T C P Y Q H V H D G V L H Y P I Y Y P L L H A F K S T S
rat      P G D I K A V L D K L H H L H T K W F S Q G S R P F I F Q [E V I D] L G G E A I K G S E Y F G H C R V T E F K Y G A K L G T V I R K W
louse,s  P G D I K A I L D K L H H L H T K W F S Q G S R P F I F Q E V I D L G G E A V S S H E Y F G H C R V T E F K Y G A K L G K V H R K W
louse,p  P R D I K A V L D K L H H L H T K W F S Q G S R P F I F Q E V I D L G G E A I K G S E Y F G H C R V T E F K Y G A K L G T V I R K W
dog      P G D I K A V L D K L H H·L·H·T H W F P A C S R P F I·F Q E V I D L G G·E A I·K G S E Y F S H C R V T E F K Y G A K L G T V V R K W
human,s  P G D I K A I L D K L H H L H S H W F P E G S K P F I Y Q E V I D L G G E P I K S S D Y F G H C R V T E F K Y G A K L G T V I R K W
human,p  P G D I K A I L D K L H H L H S H W F P A C S K P F I Y Q E V I D L G G E P I K S S D Y F G H C R V T E F K Y G A K L G T V I R K W
barley     P E H A K V Y I D G T S P S L A V A [E V H D] H H A T G D D C K P H Y D Q D A H R Q H L V H H V D K V G G A A S
```

```
                              Region 4  F V D H H D
l.stearo. S G C T F D H H T L H T H T L H K D Q P T L A V T [F V D H H D] T E P G Q A L Q S H V D P W F K P L A Y A F I L T R Q E G 360
l.amylo.  Q G C G Y D H R R L L D C T V V S R H P E K A V T [F V E H H D] T Q P·G Q S L E S T V Q T W F K P L A Y A F I L T R E S G
l.sub.    L K H R H L G V S H I S H Y A S D V S A D K L V T H V E S H D T Y A H D D E E S T W H S D D D I R L G W A V I A S R S G
\.ory.    G S H D D L Y H H I H T V K S D C P D S T L L G T F V E H H D H P R F A S Y T H D I A L A K H V A A F I I L H D G L P I
rat      H G E K H S Y L K H W G E G W G F V P T D R A L V [F V D H H D] H Q R G H G A C G   A S I L T F W D A R H Y K H A V G F H
louse,s  D G E K H S Y L K H W G E G W G L H P S D R A L V [F V D H H D] H Q R G H G A C G   A S I L T F W D A R H Y K H A V G F H
louse,p  H G E K H S Y L K H W G E G W G L V P S D R A L V [F V D H H D] H Q R G H G A C G   S S I L T F W D A R H Y K H A V G F H
log      S G E K H S Y L K G P L K G W G L H P S D R A L V [F V D H H D] H Q R G H G A C G   A S I L T F W D A R L Y K H A V G F H
luman,a  T G E K H S Y L K H R E E G W G F V P S D R A L V [F V D H H D] H Q R G H C A C G A C C G A T T L T F W D A R L Y H H A V G F H
luman,p  H G E K H S Y L K H W G E G W G F V P S D R A L V [F V D H H D] H Q R G H G A C G G A T S L T F W D A R L Y H H A V G F H
Barley   A G H V F D F T T K G L L H A A V E G E L W R L I D F Q G K A F G V H G W P A K A A T [F V D H H D] T G S T Q A H W P F P S D K V H Q G Y A Y I L T H P G I P
```

```
l.atearo. Y P C V F Y G D Y Y C I P Q Y H I P S L K S K I D P L L I A R R D Y A Y G T Q H D Y L D H S D I I G W T R E G V T·E K P 420
l.amylo.  Y P Q V F Y G D H Y G T KGTSPKE·I P S L K D H I E P L L K A R K E Y A Y G P Q H D Y I D H P D V I G W T R E G D S S A A
l.sub.    S T P L F F S R P E G G G H G V R F P G K S Q I G D R G S A L F E D Q A I T A V H R F H H V H A G P E E L S H P H G H
\.ory.    I Y A G Q E Q H Y A G G H [D] P A H H [R] E A T H L S G Y P T D S E L Y K L I A S A H A I R H Y A I S K D T G F V T Y K H P Y
rat      L A H P Y G F T R V H S S Y R R T R H F Q H G K D V H D W I G P P H H H G V T K E V T I H P D T T C G H D W V C E H R W
louse,s  L A H P Y G F T R V H S S Y R W H R H F Q H G K D Q H D W H V G P P H H H G K T K E V S T I H A D S T T C G H D W V C E H R W
louse,p  L A H P Y G F T R V H S S Y R W H R H F Q H G K D Q H D W H V G P P H H H G K T K E V T I H A D S T T C G H D W V C E H R W
log      L A H P Y G F T R V H S S Y R W A R H F V H G Q D V H D W I G P P H H H G V I K E V T I H A D T T C G H D W V C E H R W
luman,a  L A I L H D F T R V H S S Y R W H P R Y F E H C H D V H D W V C P P H H D H G V I K E V T I H P D T T C G H D W V C E H R W
luman,p  L A H L T D F T R V H S S Y R W P S Q F Q H G H D V H D W V C P P H H H G V I K E V T I H P D T T C G I D W V C E H R W
)arley   C I F Y D H F F H W G F K D Q I A A L V A I R K R H C I T A T S A L K I L H H E G D A Y V A E I D C K V V V K I G S R Y
```

```
).atearo. G S G L A A L I T D G P G G S K W H Y V G K Q H A G K V F Y D L T G H R S D T V T I H S D G W G E F K V H G G S V S V W 480
).amylo.  K S C L A A L I T D G P G G S K R H Y A G L K H A G E T W Y D I T G H R S D T V K I G S D G W G E F H V H D C S V S I Y
).sub.    H Q I F H H Q R G S H G V V L A H A G S S S V S I H T A T K L P D G R Y D H K A G A C S F Q V H D G K L T G T I H A R S
\.ory.    I K D D T T I A H R K C T D G S Q I V T I L S H K G A S G D S Y T L S L G A S F I A Y T A G Q Q L T E V I G C T V T V G S
Rat      R Q I R H H H V A F R H V V H G Q P F A H W W D H D S H Q V A F S R G H K G L I V F H H D D W A L S E T L Q T G L P A G T
House,s  R Q I R H H V A F R H V V H G Q P F A H W W D N D S H Q V A F S R G H K G L I V F H H D D W A L S E T L Q T G L P A G T
House,p  R Q I R H H V A F R H V V H G Q P F S H W W D H H S H Q V A F S R G H R G F I V F H H D D W A L S A T L Q T G L P A G T
Hog      R Q I R H H H V H F R H V V D G Q P F A H W W D H S H Q V A F S R G H R G F I V F H D D D Q L W S G T L Q T G L P G G T
Human,s  R Q I R H H V H F R H V V D G Q P F A H W W D H V S I Q V A F G R G H R G F I V F H H G D W T F S L T L Q T G L P A G T
Human,p  R Q I R H H V I F R H V V D G Q P F T H W W D H G S I Q V A F G R G H R G F I V F H H D E W S F S L T L Q T G L P A G T
Darley   D V G A V I P A G F V T S A H G H D Y A V W E K H G A A A T L Q R S
```

```
B.stearo. V P R K T T V S T I A W S I T T R P W T D E F V R W T E P R L V A W P
B.amylo.  V Q K
B.sub.    V A V L Y P D D I A K A P H V F L E H Y K I G V T H S F H D Q L T I T L R A D A H T T K A V Y Q I H H G P·D D R R L R H
A.ory.    D G H V P V P H A C G L P R V L Y P T E K L A G S K I C S D S S
Rat      Y C D V I S G D K V H G H C T G L K V H V G S D G K A H F S I S H S A E D P F I A I H A D S K L
House,s  Y C D V I S G D K V D G H C T G L R V Y V G H D G K A H F S I S H S A E D P F I A I H A E S K L
House,p  Y C D V I S G D K V D G H C T G L R V Y V G H D G K A H F S I S H S A E D P F I A I H A D S K L
Hog      Y C D V I S G D K V G H S C T G I K V H V S S D C T A Q F S I S H S A E D P F I A I H A Q S K L
Human,s  Y C D V I S G D K I H G H C T A I K I Y V S D D G K A H F S I S H S A E D P F I A I R A E S K L
Human,p  Y C D V I S G D K I H G H C T G I K I Y V S D D G K A H F S I S H S A E D P F I A I H A E S K L
```

```
B.sub.    E I H S Q S E K E I Q F G K T Y T I H L K G T H S D G V T R T E K Y S F V K R D P A S A K T I C Y Q H P H H W S Q V H A
B.sub.    Y I Y K H D G S R V I E L T G S W P G K P H T K H A D G I Y T L T L P A D T D T T H A K V I F H H G S A Q V P G Q H Q P
B.sub.    G F D Y V L H G L Y H D S G L S G S L P H
```

Fig. 2. Comparison of amino acid sequences of various α-amylases. Enzyme origins are abbreviated as shown in Table I. The first amino acid of extracellular amylase of *B. stearother mophilus*, Ala, is counted as +1. Signal peptides are shown in the first rows. Homologous sequence regions 1, 2, 3 and 4 are surrounded by rectangles.
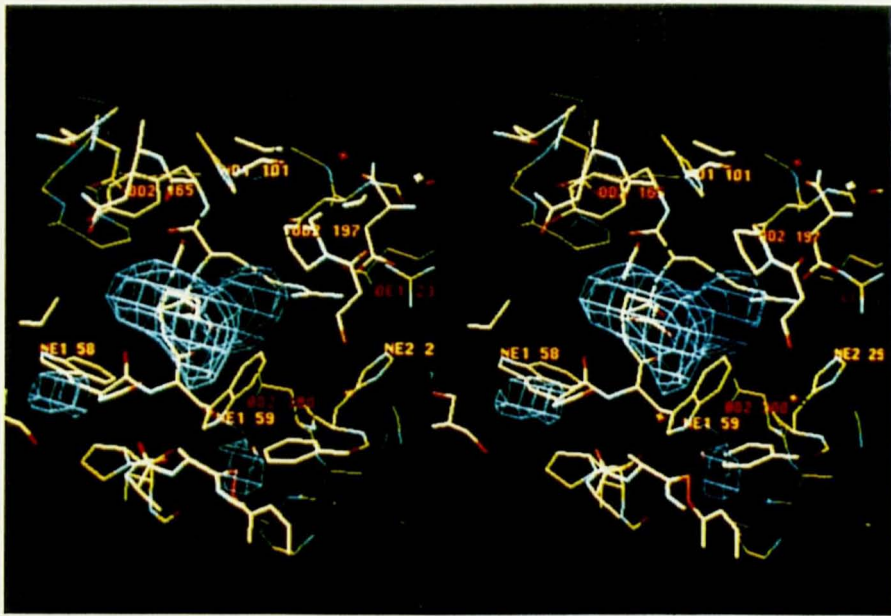
Fig. 3. Active site region of PPA superimposed on a substrate analogue (a modified maltotriose).
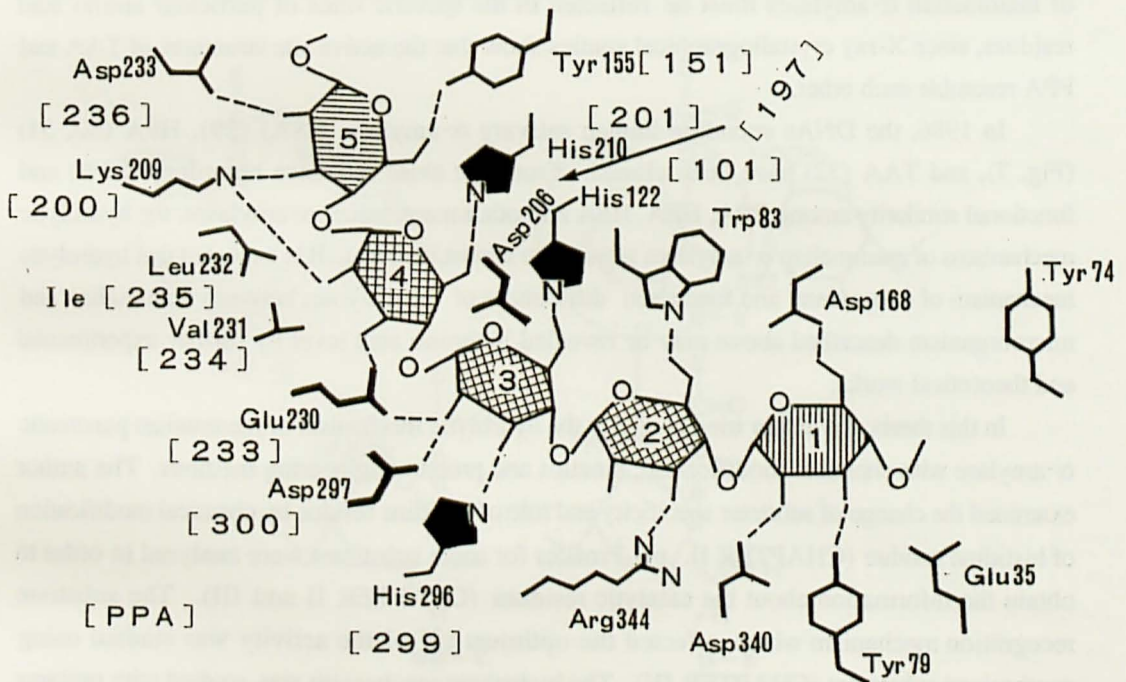This view shows the presumed catalytic aspartic acid pair (Asp197, Asp300) (12).

Fig. 4. Proposed substrate binding model of TAA (11) and conserved amino acid residues in PPA.

- 5 -

The hydrolytic mechanism and structure of α-amylase have been speculated in detail with TAA and PPA. From the sequence homology in the active sites of α-amylases among animal, plant, and microorganism (10), and from X-ray analysis of PPA and TAA (11, 12), catalytic residues of most α-amylases were assigned to be two carboxyl residues. Koshland et al. proposed a nucleophilic double-displacement mechanism with carboxylate anion and proton donor residue (1, 21) about the hydrolytic mechanism of α-amylase (Fig. 5). On the other hand, Mayer and Larger proposed an alternative mechanism employing a carbonium ion intermediate (22). The mechanism was that, after the stabilization of the extremely reactive carbonium ion intermediate, stereospecific hydration of the carbonium ion to form product was formed (Fig. 6). However, from pH profile and chemical modification studies of PPA (16, 23-25), it has been pointed out that some histidine residues which are located near the active center (12) (Fig. 3) also may contribute to the activity in α-amylases.

Furthermore, there are some functional differences between PPA and TAA in optimum pH (16, 26), regulation with an activator (chloride ion) (27) and a proteinaceous inhibitor (28), and effects of chemical modifications (23, 25) etc. in spite of the sequence homology of the active site. These differences may be related to physiological significance of mammalian α-amylases for the catalytic action in small intestine. It is expected that functional characteristics of mammalian α-amylases must be reflected in the specific roles of particular amino acid residues, since X-ray crystallographical studies show that the active site structures of TAA and PPA resemble each other.

In 1986, the DNAs encoding human salivary α-amylase (HSA) (29), HPA (30, 31) (Fig. 7), and TAA (32) have been cloned. From the close sequence homology (83%) and functional similarity among PPA, HPA, HSA and other mammalian α-amylases, the hydrolytic mechanisms of mammalian α-amylases seem to be almost identical. It is expected that hydrolytic mechanism of α-amylase and functional differences of the enzymes between mammalian and microorganism described above may be revealed in amino acid level by further experimental and theoretical works.

In this thesis, the author tried to clarify the hydrolytic mechanism of mammalian pancreatic α-amylase with chemical modification, kinetics and protein engineering methods. The author examined the change of substrate specificity and role of histidine residue by chemical modification of histidine residue (CHAPTER I). pH-Profiles for some substrates were analyzed in order to obtain the information about the catalytic residues (CHAPTER II and III). The substrate recognition mechanism which affected the optimum pH of the activity was studied using synthesized substrates (CHAPTER IV). The hydrolytic mechanism was studied with mutants of HPA from protein engineering method (Chapter V).
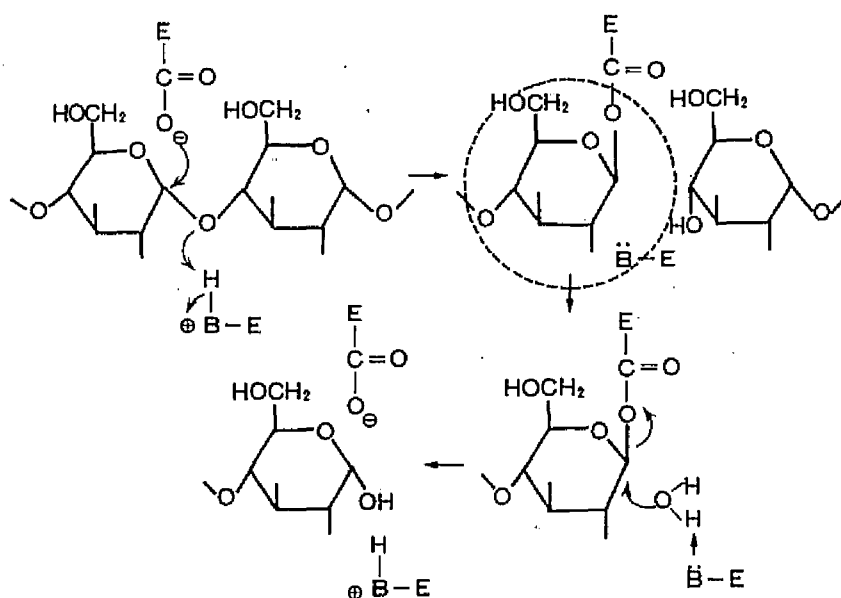
Fig. 5. Proposed nucleophilic double displacement mechanism for α-amylase by (21) (E refers to the enzyme and B refers to an electrophilic catalytic group on the enzyme. The circled structure is the proposed covalent intermediate).
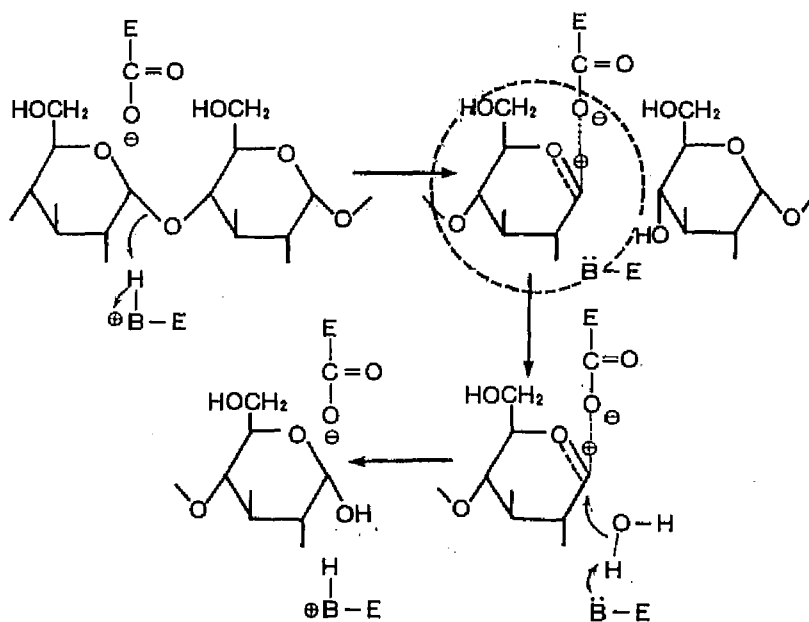

Fig. 6. Proposed carbonium ion mechanism for α-amylase by (22) (E refers to the enzyme and B refers to an electrophilic catalytic group on the enzyme. The circled structure is the proposed carbonium ion intermediate).

-7-

-200
AGGGCTCCTG AACCAGTTGT TTCCGTCTTG TCGGTCTGTC AGGGTTGGAA_GTCCAAGCCA TAGGACCCAG TTTCCTTTCT TACCTTACCT T

ATCTACCAG AGCACCGTGG GCTGTTACTT TGCCTTGAGT TGGAAGCGGT TCGCATTTAT ACCGGAATAT AAATAGTTTC TGGAAAGGAC ACTGACAACT TCAAAGCAAA

ATG AAG CTC TTT TGG TTG CTT TTC ACC ATT GGG TTC TGC TGG GCT CAG TAT TCC TCA AAT ACA CAA CAA GGA CGA ACA TCT ATT GTT CAT   90
     T   CT   C   G
Met Lys Leu Phe Trp Leu Leu Phe Thr Ile Gly Phe Cys Trp Ala Gln Tyr Ser Ser Asn Thr Gln Gln Gly Arg Thr Ser Ile Val His
         Phe   Leu   Pro

CTG TTT GAA TGG CGA TGG GTT GAT ATT GCT CTT GAA TGT GAG CGA TAT TTA GCT CCC AAG GGA TTT GGA GGG GTT CAG GTC TCT CCA CCA   180
Leu Phe Glu Trp Arg Trp Val Asp Ile Ala Leu Glu Cys Glu Arg Tyr Leu Ala Pro Lys Gly Phe Gly Gly Val Gln Val Ser Pro Pro

AAT GAA AAT GTT GCC ATT CAC AAC CCT TTC AGA CCT TGG TGG GAA AGA TAC CAA CCA GTT AGC TAT AAA TTA TGC ACA AGA TCT GGA AAT   270
            A   T
Asn Glu Asn Val Ala Ile His Asn Pro Phe Arg Pro Trp Trp Glu Arg Tyr Gln Pro Val Ser Tyr Lys Leu Cys Thr Arg Ser Gly Asn
            Tyr

GAA GAT GAA TTT AGA AAC ATG GTG ACT AGA TGC AAC AAT GTT GGG GTT CGT ATT TAT GTG GAT GCT GTA ATT AAT CAT ATG TGT GGT AAT   360
                         T   C
Glu Asp Glu Phe Arg Asn Met Val Thr Arg Cys Asn Asn Val Gly Val Arg Ile Tyr Val Asp Ala Val Ile Asn His Met Cys Gly Asn

GCT GTG AGT GCA GGA ACA AGC AGT ACC TGT GGA AGT TAC TTC AAC CCT GGA AGT AGG GAC TTT CCA GTA GTC CCA TAT TCT GGA TGG GAT   450
                                                                           C
Ala Val Ser Ala Gly Thr Ser Ser Thr Cys Gly Ser Tyr Phe Asn Pro Gly Ser Arg Asp Phe Pro Val Val Pro Tyr Ser Gly Trp Asp
                                                                         Ala

TTT AAT GAT GGT AAA TGT AAA ACT GGA AGT GGA GAT ATC GAG AAC TAT AAT GAT GCT ACT CAG GTC AGA GAT TGT CGT CTG TCT GGT CTT   540
  C   C   A
Phe Asn Asp Gly Lys Cys Lys Thr Gly Ser Gly Asp Ile Glu Asn Tyr Asn Asp Ala Thr Gln Val Arg Asp Cys Arg Leu Ser Gly Leu
                                                                                                    Thr

CTC GAT CTT GCA CTG GGG AAG GAT TAT GTG CGT TCT AAG ATT GCC GAA TAT ATG AAC CAT CTC ATT GAC ATT GGT GTT GCA GGG TTC AGA   630
  T   A   C
Leu Asp Leu Ala Leu Gly Lys Asp Tyr Val Arg Ser Lys Ile Ala Glu Tyr Met Asn His Leu Ile Asp Ile Gly Val Ala Gly Phe Arg
                 Gln

ATT GAT GCT TCC AAG CAC ATG TGG CCT GGA GAC ATA AAG GCA ATT TTG GAC AAA CTG CAT AAT CTA AAC AGT AAC TGG TTC CCG GAA GGT   720
  C   T   C   A
Ile Asp Ala Ser Lys His Met Trp Pro Gly Asp Ile Lys Ala Ile Leu Asp Lys Leu His Asn Leu Asn Ser Asn Trp Phe Pro Glu Gly
Leu   Ala

AGT AAA CCT TTC ATT TAC CAG GAG GTA ATT GAT CTG GGT GGT GAG CCA ATT AAA AGC AGT GAC TAC TTT GGT AAT GGC CGG GTG ACA GAA   810
Ser Lys Pro Phe Ile Tyr Gln Glu Val Ile Asp Leu Gly Gly Glu Pro Ile Lys Ser Ser Asp Tyr Phe Gly Asn Gly Arg Val Thr Glu

TTC AAG TAT GGT GCA AAA CTC GGC ACA GTT ATT CGC AAG TGG AAT GGA GAG AAG ATG TCT TAC TTA AAG AAC TGG GGA GAA GGT TGG GGT   900
Phe Lys Tyr Gly Ala Lys Leu Gly Thr Val Ile Arg Lys Trp Asn Gly Glu Lys Met Ser Tyr Leu lys Asn Trp Gly Glu Gly Trp Gly

TTC ATG CCT TCT GAC AGA GCG CTT GTC TTT GTG GAT AAC CAT GAC AAT CAA CGA GGA CAT GGC GCT GGA GGA_GCC TCT ATA CTT ACC TTC   990
    G A   Val   G   T
Phe Met Pro Ser Asp Arg Ala Leu Val Phe Val Asp Asn His Asp Asn Gln Arg Gly His Gly Ala Gly Gly Ala Ser Ile Leu Thr Phe
         Val   Gln

TGG GAT GCT AGG CTG TAC AAA ATG GCA GTT GGA TTT ATG CTT GCT CAT CCT TAT GGA TTT ACA CGA GTA ATG TCA AGC TAC CGT TGG CCA   1080
                                                         C
Trp Asp Ala Arg Leu Tyr Asn Met Ala Val Gly Phe Met Leu Ala His Pro Tyr Gly Phe Thr Arg Val Met Ser Ser Tyr Arg Trp Pro

AGA TAT TTT GAA AAT GGA AAA GAT GTT AAT GAT TGG GTT GGG CCA CCA AAT GAT AAT GGA GTA ACT AAA GAA GTT ACT ATT AAT CCA GAC   1170
   C G   C   C
Arg Tyr Phe Glu Asn Gly Lys Asp Val Asn Asp Trp Val Gly Pro Pro Asn Asp Asn Gly Val Thr Lys Glu Val Thr Ile Asn Pro Asp
   Gln   Gln   Asn   Asn   Ile

ACT ACT TGT GGC AAT GAC TGG GTC TGT GAA CAT CGA TGG CGC CAA ATA AGG AAC ATG GTT AAT TTC CGC AAT GTA GTG GAT GGC CAG CCT   1260
Thr Thr Cys Gly Asn Asp Trp Val Cys Glu His Arg Trp Arg Gln Ile Arg Asn Met Val Asn Phe Arg Asn Val Val Asp Gly Gln Pro
                                                                    T   Ile

TTT ACA AAC TGG TAT GAT AAT GGG AGC AAC CAA GTG GCT TTT GGG AGA GGA AAC AGA GGA TTC ATT GTT TTC AAC AAT GAT GAC TGG ACA   1350
        T   T
Phe Thr Asn Trp Tyr Asp Asn Gly Ser Asn Gln Val Ala Phe Gly Arg Gly Asn Arg Gly Phe Ile Val Phe Asn Asn Asp Asp Trp Thr
   Thr   Tyr   Gly   Asp   Asp   Ser

TTT TCT TTA ACT TTG CAA ACT GGT CTT CCT GCT GGC ACA TAC TGT GAT GTC ATT TCT GGA GAT AAA ATT AAT GGC AAC TGC ACA GGC ATT   1440
Phe Ser Leu Thr Leu Gln Thr Gly Leu Pro Ala Gly Thr Tyr Cys Asp Val Ile Ser Gly Asp Lys Ile Asn Gly Asn Cys Thr Gly Ile
                                                                                                             T

AAA ATC TAC GTT TCT GAT GAT GGC AAA GCT CAT TTT TCT ATT AGT AAC TCT GCT GAA GAT CCA TTT ATT GCA ATT CAT GCT GAA TCT AAA   1530
  T
Lys Ile Tyr Val Ser Asp Asp Gly Lys Ala His Phe Ser Ile Ser Asn Ser Ala Glu Asp Pro Phe Ile Ala Ile His Ala Glu Ser Lys

TTG TAAAATTTAAAATTAAATGCAAATCCGCAAAGCAn
              _TGTCCTCAn
Leu

Fig. 7. Nucleotide and amino acid sequences of HSA and HPA. The entire sequence for HSA is shown. Differences in the nucleotide or amino acid sequences in HPA downstream from the ATG initiation codon are presented beneath the HSA sequence (cited from (30)).

REFERENCES

1) Myrback, K. and Neumuller, G. (1950) in "*The Enzymes*" 1st ed., Vol. I, Part 1, p. 653.
2) Bernfeld, P. (1951) *Advances in Enzymo.l.* **12**, 379.
3) Meyer, K.H. (1952) *Experientia,* **8**, 405
4) Fischer, E.H., Sumerwell, W.N., Junge, J.M., and Stein, E.A. "*Proc. 4th Intern. Congr. Biochem. Vienna, (1958). Symposium 8*", p. 124, Pergamon Press, (1960).
5) Fischer, E.H. and Stein, E.A. (1960) *The Enzymes*, Academic Press New York, 2nd ed. **4**, 313-343.
6) Kuhn, R. (1924) *Ber.* **57**, 1965.
7) Kuhn, R. (1925) *Ann .* **443**, 1.
8) Matsubara, S., Ikenaka, T., and Akabori, S. (1963) *ibid.,* **46**, 425.
9) Nakajima, R., Imanaka, T., and Aiba, S., (1986) *Appl. Microbiol. Biotech.,* **23**, 355-360.
10) Svensson, B. (1988) *FEBS Lett.,* **230**, 72-76.
11) Matsuura, Y., Kusunoki, M., Harada, W., and Kakudo, M. (1984) *J. Biochem.(Tokyo),* **95**, 697-702.
12) Buisson, G., Duee, E., Haser, R., and Payan, F. (1987) *EMBO J.,* \6, 3909 -3916.
13) Buisson, G., Duee, E., Payan, F., and Haser, R. (1987) *Food Hydrocolloids,* **1**, 399-406.
14) Banner, D.W., Bloomer, A.C., Petsko, G.A., Phillips, D.C., Pogson, C.I., Wilson, I.A., Corron, P.H., Furth A.J., Milman, J.D., Offord, R.E., Priddle, J.D., and Waley, S.G. (1975) *Nature,* **255**, 609-614.
15) Stuart, D.I., Levine, M., Muirhead, J., and Stammers, D.K. (1979) *J. Mol. Biol.,* **134**, 109-142.
16) Wakim, J., Robinson, M., and Thoma, J.A. (1969) *Carbohydr. Res.,* **10**, 487-503
17) Robyt, J.F. and French, D. (1970) *J. Biol. Chem.,* **45**, 3917-3927.
18) Pasero, L., Abadie, B., Chicheportiche, Y., Mayzei, Y., Moinier, D., Bizzozero, J.P., Fougereau, M., and Marchis Mouren, G. (1981) *Biochimie,* **63**, 71-79.
19) Kluh, I. (1981) *FEBS Lett.,* **136**, 231-234.
20) Pasero, L., Mazzei-Pierron, Y., Abadie, B., Chicheportiche, Y., and Marchis-Mouren,G. (1986) *Biochim. Biophys. Acta,* **869**, 147-157.
21) Koshland, D. E. Jr. (1954) "*A Symposium on the Mechanism of Enzyme Action*" (McElroy, W. D. and Glass, B., ed.) pp. 60 - 641, The Jhons Hopkins University Press, Baltimore.
22) Mayer F. C. and Larner, J. (1958) *Biochim. Biophys. Acta,* **29**, 465.
23) Kita, Y., Sakaguchi, S., Nitta, Y., and Watanabe, T. (1982) *J. Biochem. (Tokyo),* **92**, 1499-1504.
24) Hoschke, A., Laszlo, E., and Hollo, J. (1980) *Carbohydr. Res.,* **81**, 157-166.
25) Nakatani, H. (1988) *Arch. Biochem. Biophys.,* **263**, 364-368.
26) Matsubara, S., Ikenaka, T., and Akabori, S. (1959) *J. Biochem. (Tokyo),* **46**, 425-431.
27) Levitzuki, A. and Steer, M.L. (1974) *Eur. J. Biochem.,* **41**, 171-180.
28) Marshall, J.J. and Lauda, C.M. (1975) *J. Biol. Chem.,* **250**, 8030-8037.
29) Sato, T., Tsunasawa, S., Nakamura, Y., Emi. M., Sakiyama, F., and Matsubara, K. (1986) *Gene,* **50**, 247-257.
30) Nishide, T., Emi, M., Nakamura, Y., and Matsubara, K.(1986) *Gene,* **50**, 371-372
31) Shiozaki, K., Takata, K., Omichi, K., Tomita, N., Horii, A., Ogawa, M., and Matsubara, K. (1990) *Gene,* **89**, 253-258.
32) Tada, S., Iimura, Y., Gomi, K., Takahashi, K., Hara, S., and Yoshizawa, K. (1989) *Agric. Biol. Chem.,* **53**. 593-599.

CHAPTER I Chemical Modification of Histidine Residues in Porcine Pancreatic α-Amylase
(New Substrate Specificity of Porcine Pancreatic α-Amylase)

Porcine pancreatic α-amylase (EC 3.2.1.1, abbreviated to PPA) (MW = 55,000) is able to hydrolyze not only α-D-(1,4) glycoside bonds in starch at random and but p-nitrophenyl α-D maltoside (G_2-PNP) to produce p-nitrophenol (PNP) and maltose (G_2) (1). The latter activity is designated as maltosidase activity in this thesis. From experiments of the chemical modification (2) and pH activity profile (3), it is suggested that a histidine residue (His) is one of the candidates for the catalytic groups. The primary structure (4) and crystal structure analysis at 2.9 A resolution (5) of PPA I were performed, and Asp 197 and Asp 300 were proposed as the catalytic residues. But no significant information about the active site and the catalytic mechanism have been obtained.

Proteinaceous α-amylase inhibitor phaseolamin (MW = 60,000), purified from white kidney bean, inhibits specifically α-amylase from mammalian (6). It was also reported that PPA-phaseolamin complex had a binding capacity of substrates (oligosaccharides) (7). But the binding site of PPA to phaseolamin and the inhibition mechanism of phaseolamin are not proved.

Selective inhibition study by H. Nakatani (8) with His-modified PPA showed that amylase activity was inhibited but maltosidase activity was not by phaseolamin in His-modified PPA. In this chapter, the author further investigated the roles of histidine residues and the conversion of substrate specificity with the methods of chemical (His-modification) and biochemical (phaseolamin inhibition) modifications quantitatively, using this modified PPA and other p-nitrophenyl oligosaccharides as substrates.

MATERIALS AND METHODS

Materials. PPA was purified in the crystalline state from porcine pancreatin purchased from Sigma Chemical Co., as described by Loyter et al.(9). Proteinaceous α-amylase inhibitor phaseolamin was purified from white kidney bean (*Phaseolus vulgaris*) according to the modified method described by Marshall et al. (6). TSK Gel DEAE Toyopearl 650 S and TSK-G-2000 PW column (7.5ϕ X 600 mm) were purchased from Toyo Soda Mfg. Co., Ltd. p-Nitrophenyl α-D-glycoside (G-PNP), p-nitrophenyl α-D maltoside (G_2-PNP) p-nitrophenyl α-D-maltotrioside (G_3-PNP), p-nitrophenyl α-D-maltotetraoside (G_4-PNP) and p-nitrophenyl α-D-maltopentaoside (G_5-PNP) were purchased from Calbiochem Corp.; soluble starch, maltose (G_2), maltotriose (G_3), maltotetraose (G_4), maltopentaose (G_5) and diethyl pyrocarbonate (DEP)

from Nacalai tesque Ltd. and Daiyacolor AMY (measurement kit of amylase activity) from Toyobo Co., Ltd. Other chemicals were of guaranteed or reagent grade of commercial.

Purification of the isozyme I (PPA I) from the crystalline preparation of PPA was performed by DEAE Toyopearl (10, 11). The crystalline preparation purified from pancreatin was dialyzed against 20 mM Tris-HCl buffer (pH 8.3) containing 1 mM $CaCl_2$ and applied on the TSK-Gel DEAE Toyopearl column buffered with the same buffer. Only PPA I could be eluted from this column but PPA II was adsorbed. The combined fraction of PPA I [showed a single band in polyacrylamide gel electrophoresis (pH 9.0)] was dialyzed against 25 mM phosphate buffer (pH 6.9) containing 30 mM NaCl, 1 mM $CaCl_2$ and 0.02 % NaN_3, and stored at 4° C (PPA I is simply signified by PPA in the followings).

Enzyme assay. Hydrolytic reactions of PPA were carried out at 30° C in 25 mM phosphate buffer (pH 6.9) containing 30 mM NaCl.

The hydrolysis of soluble starch was terminated by addition of 0.08 N NaOH solution and the reductometries of these hydrolysates were measured with the modified Somogyi-Nelson method (12). The hydrolytic reaction for maltopentaose (G_5) was measured by use of β-(2,4 dichlorophenyl) maltopentaoside with Daiya-color AMY measurement kit (13). The reaction was stopped by adding 2.0 mL of 10 mM KIO_3 to the 1 mL of the reaction mixture and the absorbance of the colored compound (produced from 2,4-dichlorophenyl 4-aminoantipyrine and KIO_3) was measured at 500 nm.

The hydrolytic activity for the bond between PNP and oligosaccharides in *p*-nitrophenyl oligosaccharides was calculated from the optical density of liberated PNP at 400 nm. The molar extinction coefficient of PNP was found to be 8,440 $M^{-1}cm^{-1}$ at pH 6.9.

In this thesis, the amylase and maltosidase activities signify the hydrolysis of α-(1,4) glycoside bond and the bond between PNP and oligosaccharides in *p*-nitrophenylated oligosaccharides, respectively. Units of the amylase and maltosidase activities were defined as the amount of enzyme that catalyzed the hydrolysis of 1μ moles/min of glycoside bond and the bond between PNP at 30°C, respectively. Molarity of PPA was determined from the absorbance at 280 nm on the basis of a molecular weight of 55,000 and $A^{1\%} = 24.0$ cm^{-1} (14).

Michaelis parameters (k_{cat} and K_m) were determined by the nonlinear least-squares method with the Taylor expansion (15). PPA-phaseolamin complex was performed by the incubation of PPA (10 μM) and phaseolamin (300 μM) in 25 mM phosphate buffer (pH 6.9) containing 30 mM NaCl at 25° C. After the incubation for 5 h, the activities were measured.

Chemical modification of histidine residue. Chemical modification of PPA with DEP was carried out at pH 6.0 (0.1 M phosphate buffer containing 0.1 mM $CaCl_2$) and 15° C by the

method described by Roosemount (16). DEP solution diluted 5 times with ethanol was freshly prepared before use. PPA was dialyzed against 0.1 M phosphate buffer (pH 6.0) containing 0.1 mM $CaCl_2$ and stocked as a 10 μM solution. The modification was started by the addition of the DEP solution to the PPA solution ([DEP] = 20 mM, [PPA] = 10 μM). After an appropriate interval the modification was stopped by adding excess L-histidine. After the modification, the excess histidine, modified histidine and DEP were removed by dialysis against 25 mM phosphate buffer (pH 6.9) containing 30 mM NaCl. This dialyzed solution was used for the subsequent experiments as modified PPA. The number of modified histidine residues in PPA was evaluated from the saturated absorbance increase at 240 nm as described by Roosemount (16).

Analysis of the hydrolytic products. Analysis of the hydrolytic products was carried out with the JASCO Trirotar-III High Performance Liquid Chromatography (HPLC) equipped with TSK-G-2000 PW column (7.5φ X 600 mm) (17). Separation was performed with distilled water at a flow rate of 1 mL/min. Sugars were monitored by the differential refractometer and *p*-nitrophenyl compounds were measured at 313 nm with the UV detector.
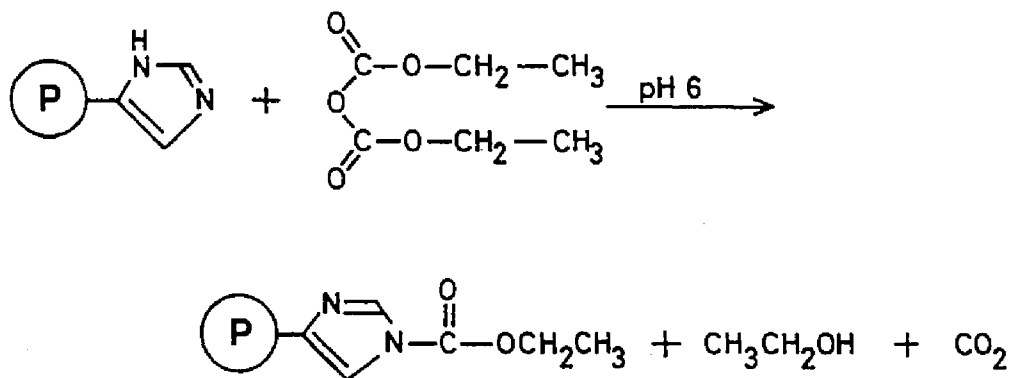
Fig. 1. Chemical modification of histidine residue with DEP.

RESULTS

Chemical modification of PPA

The ethoxyformylation of histidine residues in PPA with DEP was carried out with 20 mM DEP at pH 6.0 and 15°C (Fig. 1). As shown in Fig. 2, the amylase activity for starch

gradually decreased and at the end of the modification five of eight histidine residues in PPA were modified. The amylase activity of modified PPA was less than 1%. In the presence of G_3, three histidine residues were protected from this modification, and the amylase activity remained 40% of that of the native enzyme. On the other hand, the maltosidase activity for G_2-PNP increased to 3.5 and 2 times of native one for the former and latter modification, respectively (Fig. 2). Relationship between the activities and the number of His residues modified is shown in Fig. 3. These activities became stationary state, when the number of modified histidine residues reached to four.

No transglycosylation of G_2-PNP catalyzed by the native and modified PPA was found by HPLC under the employed condition (see legend to Fig. 2).

When the modified PPA (mod-PPA) was treated with 0.5 M HCl-hydroxylamine for 45 min at pH 6.0 and 25 °C, the ethoxyformyl residues were released from the modified histidine residues. The resulting PPA gave the same amylase and maltosidase activities as those of native one. The ethoxyformyl groups of the modified lysine residues could not be released with the same treatment. Since SH residues do not exist at the surface of PPA in the presence of Ca^{2+} (18, 19), they are not considered to be modified by DEP. Thus, it is concluded that the changes of the activities in Fig. 2 and 3 are due to the ethoxyformylation of histidine residues in PPA. Furthermore, from the circular dichroism spectra (200 - 250 nm), no destruction of the tertiary structure of PPA was thought to be influenced by the modification .

Inhibition experiments with phaseolamin

The effect of the proteinaceous α-amylase inhibitor ,phaseolamin, on the activities was examined (Table I). When PPA and phaseolamin were incubated according to the described method, both amylase and maltosidase activities disappeared completely, in contrast to the case of the inhibitor from red kidney bean (7). On the other hand, with the mod-PPA, the amylase activity (less than 1% remaining) was also inhibited completely by the inhibitor but no decrease in the maltosidase activity was observed. Similar results were obtained for the mod-PPA in the presence of G_3. These suggest that only the amylase activity of mod-PPA is inhibited specifically by phaseolamin.

Hydrolytic action for p-nitrophenyl oligosaccharides by PPA

As shown in Fig. 4 (A), the TSK-G-2000 PW column could separate the free sugars with one to five glucose residues and the corresponding p-nitrophenyl compounds. PNP was not detected with this column because of the adsorption on it. HPLC analysis of the hydrolysis products revealed the hydrolysis modes of the p-nitrophenyl oligosaccharide with PPA, as shown in Fig. 5 (A). G-PNP and G_2 were not hydrolyzed by PPA, but G_2-PNP was
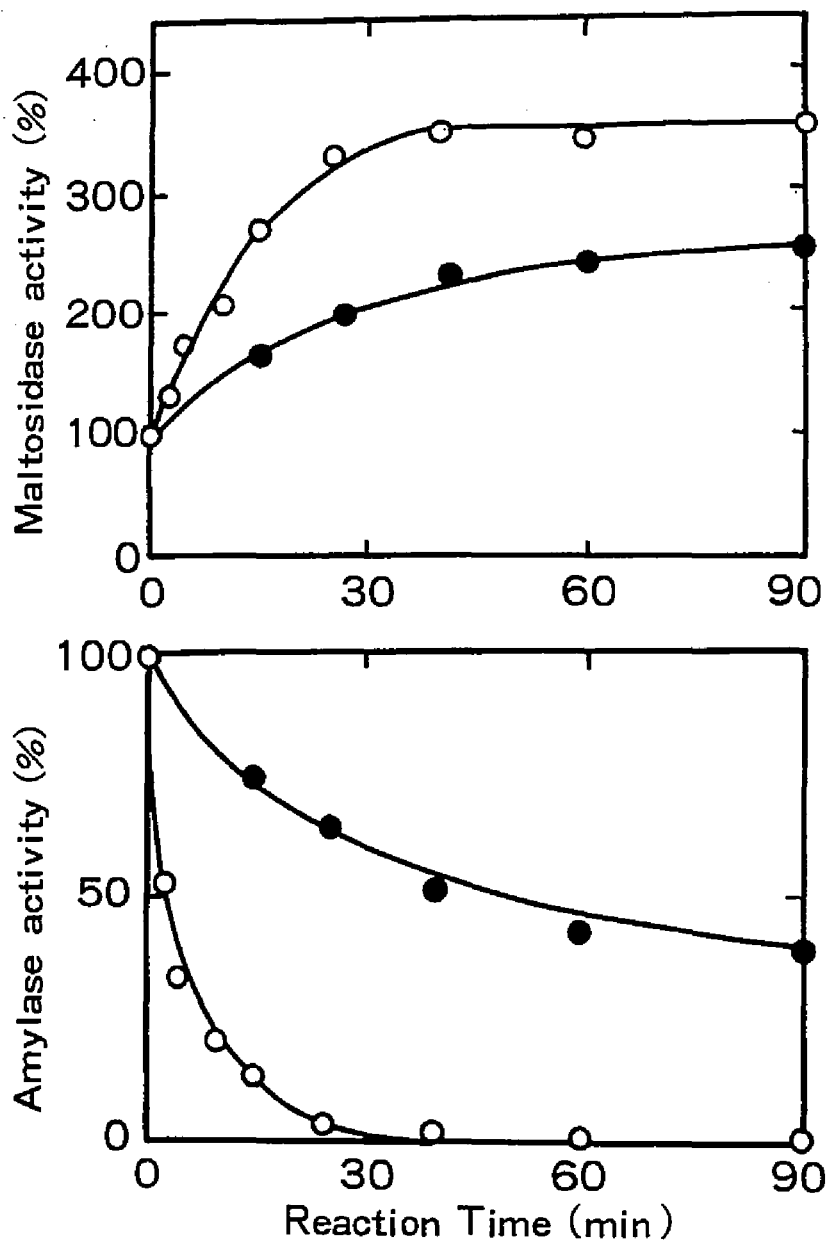
- 13 -

Fig. 2. Changes in maltosidase and amylase activities by chemical modification of PPA with DEP. PPA (1×10^{-5}) was incubated with DEP (20 mM) in the absence ($\bigcirc$) and presence ($\bullet$) of G_3 (100 mM) at pH 6.0 15°C. After the appropriate time, aliquots of modified PPA were removed and the activity for hydrolysis of starch (amylase activity) and of G_2-PNP (maltosidase activity) were determined. At the end of the modification, five and two histidine residues in PPA were modified in the absence and presence of G_3, respectively.
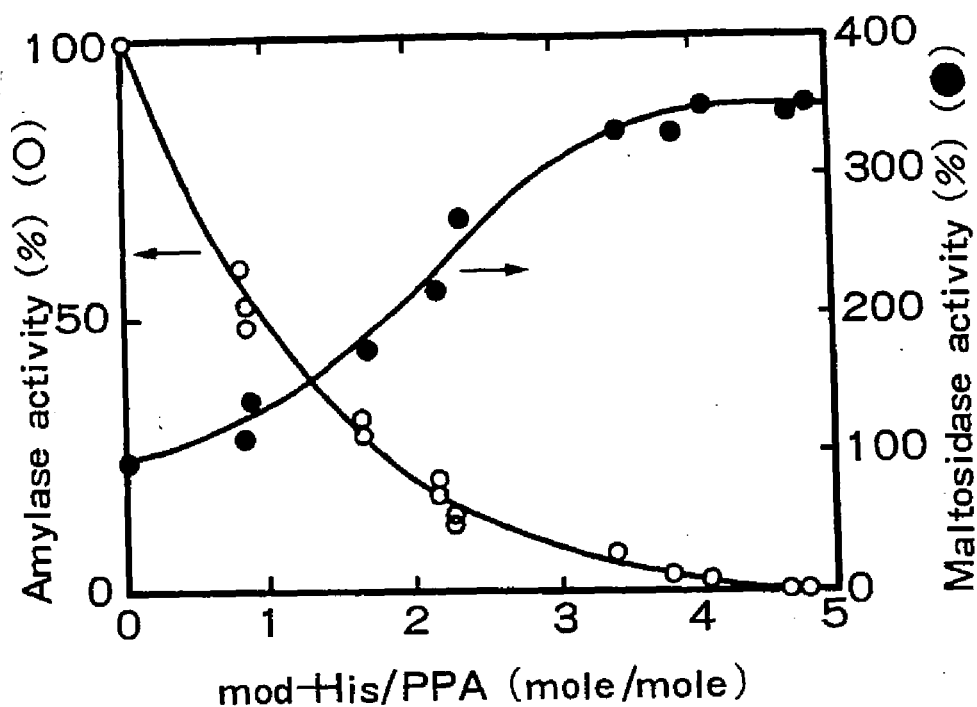
Fig. 3 Relationship between the activities and the number of modified histidine residues in PPA. was modified with DEP in the absence of G_3, and amylase (O) and maltosidase (●) activities were measured. The modification conditions are described in MATERIALS AND METHODS.

hydrolyzed to G_2 and PNP by PPA. G_3-PNP, G_4-PNP and G_5-PNP were preferentially hydrolyzed by the native PPA at arrows in Fig. 5 (A) since the amylase activity was stronger than the maltosidase activity. The HPLC analysis of the hydrolysis products (G_3 and G_2-PNP) from G_5-PNP was shown in Fig. 4 (B). The affinity of PPA for PNP was very weak compared with that for glucose; thus, the hydrolysis mode of the p-nitrophenyl oligosaccharides by PPA was the same as that of the corresponding free oligosaccharides (20).

The specificity of mod-PPA for p -nitrophenyl oligosaccharides was examined. Mod-PPA hydrolyzed the bond between G_2 and PNP of G_2-PNP as the substrate, and the k_{cat} increased 5 times of that of the native PPA and the K_m increased about 2 times of that of the native PPA (Table II). When the amylase inhibitor phaseolamin was incubated with mod-PPA, the values of k_{cat} and K_m for the hydrolysis of G_2-PNP were almost unaltered but the amylase activity remaining less than 1% disappeared completely (Table I). Therefore, mod-PPA bound to phaseolamin (mod-PPA-I) was used for the subsequent experiments. Since mod-PPA-I had no amylase activity for G_3-PNP, G_4-PNP and G_5-PNP, the author proposed a hydrolysis mode designated in Fig. 5 (B), which was supported by the HPLC analysis of the hydrolysis

products [G_5 and PNP (not determined with this column)] from G_5-PNP by mod-PPA-I shown in Fig. 4 (C). That is, PPA which mainly hydrolyzes α-(1,4) glycoside bonds between glucose residues was converted by both the chemical modification with DEP and biochemical modification with the amylase inhibitor, phaseolamin, into a new enzyme which hydrolyzes only the bond between PNP and oligosaccharides of the p-nitrophenylated oligosaccharides. The values of k_{cat} and K_m of mod-PPA-I for G_3-PNP, G_4-PNP and G_5-PNP were about 10 times larger and 20 times smaller than those for G_2-PNP, respectively. In the case of maltosidase activity of G_3-PNP, the value of k_{cat} was not altered so much but the value of K_m was decreased by the chemical modification.

Table I. Amylase and maltosidase activities of PPA influenced by DEP and phaseolamin (I)[a].

Enzyme	Amylase activity (units/mg)	Maltosidase activity (units/mg)
PPA	520	0.089
PPA-I	0	0
mod-PPA[b]	3.12	0.31
mod-PPA[b]-I	0	0.31
mod-(G_3+PPA)[c]	265	0.23
mod-(G_3+PPA)[c]-I	0	0.21

[a] Those activities using β-(2,4-dichlorophenyl) maltopentaoside (4 mM) and G_2-PNP (30 mM) were detected in phosphate buffer (pH 6.9, 25 mM) containing 30 mM NaCl at 30° C. Those activities for complex of PPAs and I were performed at pH 6.9 and 25 °C as described in MATERIALS AND METHODS.

[b] Five histidine residues were modified in the absence of G_3.

[c] Two histidine residues were modified in the presence of G_3.

Table II. Kinetic parameters for hydrolysis of the bond between PNP and oligosaccharides by native and mod-PPA-I[a].

Substrate	PPA		mod-PPA-I[a]	
	k_{cat}(s^{-1})	K_m(mM)	k_{cat}(s^{-1})	K_m(mM)
G_2-PNP	0.0773 ± 0.0015	6.01 ± 0.26	0.260 ± 0.012	10.9 ± 0.92
G_3-PNP	2.80 ± 0.054	1.53 ± 0.055	3.19 ± 0.065	0.537 ± 0.032
G_4-PNP			2.08 ± 0.040	0.472 ± 0.025
G_5-PNP			2.42 ± 0.054	0.425 ± 0.026

[a] All parameters were determined at pH 6.9 and 30° C as described in MATERIALS AND METHOD. The values of k_{cat} were measure as moles of PNP liberated per mole of enzyme per second
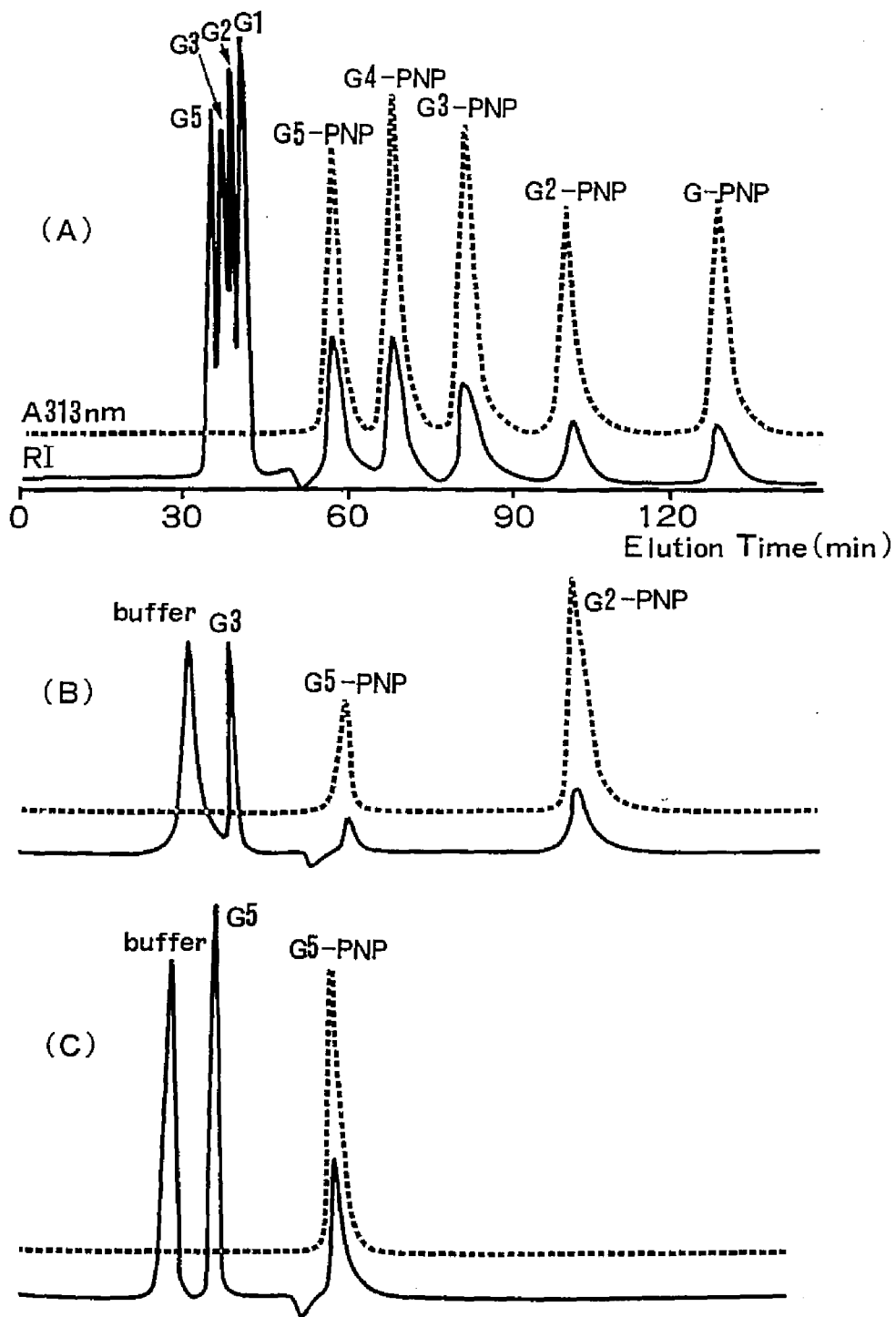
Fig. 4. Analysis of the hydrolysis products with HPLC. (—) Refractive index; (---) uv spectrometry (A_{313nm}). (A) Simultaneous separation of free sugars (1%) with one to five glucose residues and corresponding p-nitrophenylated oligosaccharides (1%) on TSK-G-2000 PW column. (B) Product distribution of G_5-PNP after hydrolysis (extent of reaction, ca. 75%) with native PPA. (C) Product distribution of G_5-PNP after hydrolysis (extent of reaction, ca. 40%) with mod-PPA-I. The hydrolysis conditions and separation conditions are described in MATERIALS AND METHODS.
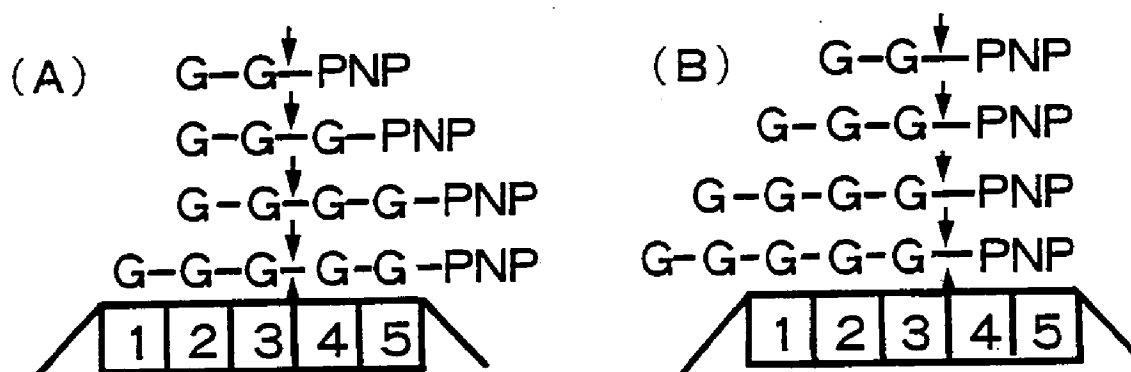
Fig. 5. Hydrolysis modes of *p*-nitrophenyl oligosaccharides by native PPA (A) and mod-PPA -I (B). Subsites per glucose residue (G) are numbered 1-5 from nonreducing end. The catalytic residue is located between subsite 3 and 4.

Experiments on inhibition of maltosidase activity

G_2 is not hydrolyzed by PPA but it is a competitive inhibitor of PPA. The maltosidase activity of native and mod-PPA were also inhibited competitively by G_2 as shown in Fig. 6 and the inhibition constants K_i were identical (Table III). In the case of mod-PPA, the hydrolyses of G_3, G_4 and G_5 were suppressed and these substrates were also used as inhibitors of mod-PPA. The maltosidase activity of mod-PPA was inhibited competitively by G_3, G_4 and G_5, and the values of K_i are shown in Table III. The same results were obtained for the case of mod-PPA-I. Therefore, mod-PPA and mod-PPA-I could not hydrolyze G_2, G_3, G_4 and G_5 but have binding site and capacity to them. From these results, it was speculated that the active site of native PPA was the same as that of mod-PPA and mod-PPA-I.

Table III. Inhibition constants, K_i, of maltosidase activity for G_2-PNP.

| Inhibitor | K_i (mM) | | |
	PPA	mod-PPA	mod-PPA-I
G_2	34.1 ± 4.9	37.1 ± 5.8	36.3 ± 5.4
G_3		0.692 ± 0.090	0.668 ± 0.087
G_4		0.804 ± 0.113	0.731 ± 0.102
G_5		1.24 ± 0.48	1.19 ± 0.36
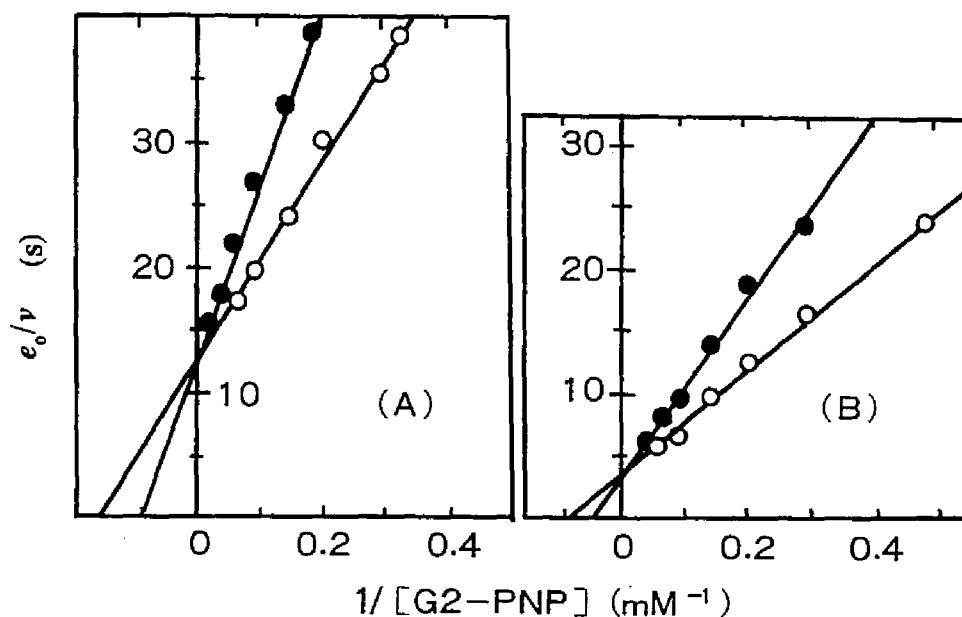
Fig. 6. Inhibition of the maltosidase activity of native (A) and modified (B) PPA with G_2. Activities for G_2-PNP in the presence (●) (28 mM) and absence (○) of G_2; double-reciprocal plot.

The activation parameters for k_{cat}

It has been reported that k_{cat} of PPA for the hydrolysis of G_2-PNP represents the conversion of enzyme-substrate complex to the very similar enzyme-product complex (1). The activation parameters for k_{cat} of PPA and mod-PPA were determined thermodynamically and revealed an increase in maltosidase activity by chemical modification . The activation parameters were calculated using the equations

$$\Delta G' = 2.303 \, RT \, [\log (k \, T \, / \, h) - \log k_{cat}]$$
$$E_A = -2.303 \, R \, d \, (\log k_{cat}) \, / \, d \, (1/T)$$
$$\Delta H' = E_A - RT$$
$$\Delta S' = (\Delta H' - \Delta G')/T$$

where E_A, $\Delta G'$, $\Delta H'$, $\Delta S'$, R, k and h represent the activation energy, the activation Gibbs energy, the activation enthalpy, the activation entropy, gas constant, Boltzman constant and Planck constant, respectively.

The temperature dependence of k_{cat} of PPA and mod-PPA on G_2-PNP was determined in the range of 10°C to 37°C. The activation parameters (Table IV) were calculated from the

Arrhenius plots (Fig. 7). In this temperature range no curvature of the Arrhenius plots was observed. The values of K_m for G_2-PNP were not affected by the temperature range.
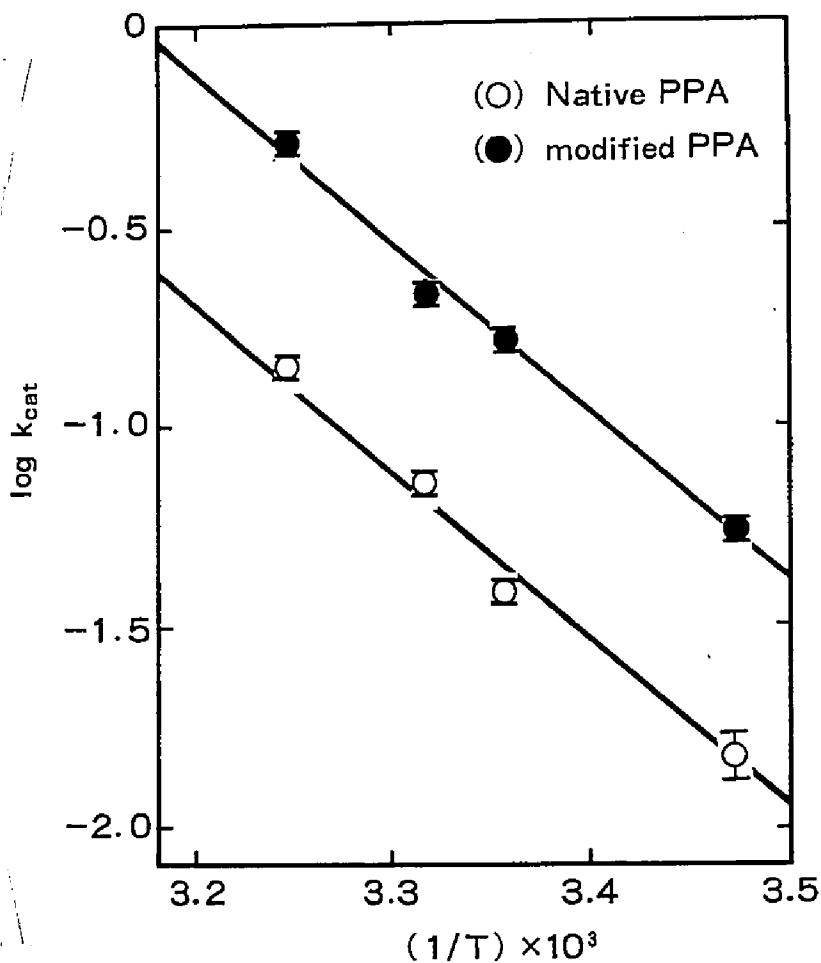
Fig. 7. Temperature dependence of maltosidase activity for G_2-PNP of native (O) and modified (●) PPAs.

Table IV. Activation parameters for PPA and mod-PPA-catalyzed hydrolysis of G_2-PNP at pH6.9 and 30°C

	PPA	mod-PPA
E_A (kcal/mol)	19.19 ± 1.44	19.18 ± 0.95
$\Delta H^\dagger$ (kcal/mol)	18.59 ± 1.44	18.58 ± 0.95
$\Delta G^\dagger$ (kcal/mol)	19.30	18.51
$\Delta S^\dagger$ (e.u.)	-2.34 ± 4.75	0.23 ± 3.14

DISCUSSION

On the basis of results that three of the five histidine residues modified by DEP in PPA were protected by G_3, it is speculated that five of eight histidine residues in PPA exist at the surface of PPA and at least three of the five histidine residues are masked by G_3 or made less reactive with conformation changes induced by G_3. The reversibility of this chemical modification with HCl-hydroxylamine reveals that the change of the activities are due to the ethoxyformylation of histidine residues in PPA.

The binding site of PPA to the amylase inhibitor phaseolamin has not been proved completely. However, from the inhibition study of Wilcox and Whitaker (7) and the measurements of fluorescence intensity of PPA-inhibitor complex influenced by substrates (unpublished observation), it can be speculated that PPA-phaseolamin complex has a binding capacity of oligosaccharides. On the basis of the specific inhibition of the amylase activity of mod-PPA by phaseolamin (Table I), it is suggested that the inhibition mechanism by phaseolamin is altered by the modification of histidine residue and at least one of the histidine residue is related to the inhibition by phaseolamin in PPA.

The reasons of the increase of the maltosidase activity of G_2-PNP may be that the decrease in the probability of the nonproductive binding mode of G_2-PNP, the increase of the affinity for G_2-PNP in the productive binding mode, or slight conformational change "wobble", in the active site by this chemical modification. The data for G_3-PNP (decrease of K_m value by the chemical modification) (Table II) supports the increase of the affinity for the substrate (p-nitrophenyl oligosaccharides) in the productive binding mode by the chemical modification. From the data ,however, the details are ambiguous.

For the mod-PPA and phaseolamin complex, the values of k_{cat} and K_m for G_3-PNP, G_4-PNP and G_5-PNP were about 10 times larger and 20 times smaller than those for G_2-PNP, respectively (Table II). These results indicate that a great affinity for glucose exists at subsite 1 in the complex and the subsites 1 - 3 are not disrupted or masked by the chemical modification and with phaseolamin. The reason of the slight decrease of k_{cat} for G_4-PNP and G_5-PNP compared with that for G_3-PNP is thought to be the inhibition strength of the nonproductive binding mode of the substrates (nonproductive binding affinity of PPA for G_4-PNP and G_5-PNP is larger than that for G_3-PNP).

The amylase and maltosidase activities of the native PPA are competitively inhibited by G_2 and their K_i values are approximately identical (20). These results indicate that the active site of the hydrolysis of α-(1,4) glycoside bond in starch and oligosaccharide is the same as that of the bond between PNP and oligosaccharide. Furthermore, competitive inhibition of maltosidase activity of mod-PPA by G_3, G_4 and G_5 indicates that these oligosaccharides bind to

the same site to which G_2 bind. The K_m values of G_3, G_4 and G_5 are approximately same as the K_m values of these substrates for native PPA (20). So the active site, that is, the binding site of PPA against these oligosaccharides, is not thought to be much changed by the modification. In addition, given that the K_i values of the above oligosaccharides of mod-PPA are same as those of mod-PPA-I, it is speculated that phaseolamin does not act on the oligosaccharide binding site in the mod-PPA.

Given the activation parameters (Table IV), the increase of the maltosidase activity is attributable to the increase of the activation entropy. However, the standard deviations are so large that an accurate estimation can not be obtained from the data.

It was revealed that the histidine residue which can be modified by DEP exists around the active center and plays an important role in determining the specificity of cleavage of α-(1,4)glycoside bond. Furthermore, the amylase inhibitor phaseolamin is thought to bind around the subsite 4 and 5 of PPA (Fig. 5). A comparison of the hydrolysis of G_3 with G_2-PNP reveals that this modification can reverse the order of the values of k_{cat} for G_3 and G_2-PNP (the k_{cat} of native PPA for G_3 (0.16 s^{-1}) (20) is larger than that for G_3-PNP (0.0773 s^{-1}; Table II) but the k_{cat} of mod-PPA for G_3 (<<0.16 s^{-1}) is smaller than that for G_2-PNP (0.260 s^{-1}; Table II)). This observation indicates that substrate specificity is altered by this chemical modification. Further, by modifying the histidine residue in PPA (chemical modification) and binding amylase inhibitor to PPA (biochemical modification), the author can create a new enzyme which hydrolyzed only the bond between PNP and oligosaccharides of p-nitrophenyl oligosaccharides (Fig. 5 (B)).

SUMMARY

Conversion of the substrate specificity of porcine pancreatic α-amylase (PPA) was studied using chemical modification of His residues. Diethyl pyrocarbonate modified His residues in PPA and the activity of the modified PPA for the hydrolysis of the α-D-(1,4)glycoside bond in starch or oligosaccharides decreased to less than 1% of that of the native enzyme. However, the activity for the hydrolysis of the bond between p-nitrophenol and oligosaccharides in p-nitrophenyl oligosaccharides was increased by chemical modification. When the modified PPA was incubated with a proteinaceous α-amylase inhibitor (M_r 60,000) purified from white kidney bean (*Phaseolus vulgaris*), it bound to the inhibitor. As a result, the remaining less than 1% hydrolytic activity of the modified PPA for the starch disappeared completely but that for p-nitrophenyl oligosaccharides remained unaltered. The hydrolytic activity of the native PPA for the α-D-(1,4) glycoside bond in oligosaccharides was stronger than that between p-nitrophenyl

and oligosaccharides in p-nitrophenyl oligosaccharides. Therefore, when p-nitrophenyl oligosaccharides (three to five glucose residues) were used as substrates for the native PPA, the α-D-(1,4)glycoside bonds in the oligosaccharides were hydrolyzed. However, the modified PPA-inhibitor complex hydrolyzed only the bond between p-nitrophenol and oligosaccharides in p-nitrophenyl oligosaccharides. The above results mean that, by chemical modification with diethyl pyrocarbonate and biochemical modification with a proteinaceous amylase inhibitor, α-amylase can be converted to a new exo-type enzyme which hydrolyzes only the bond between p-nitrophenol and oligosaccharides in p-nitrophenyl oligosaccharides.

REFERENCES

1) Levitzki, A. and Steer, M.L. (1974) *Eur. J. Biochem.*, **41**, 171-180.
2) Hoschke, A., Laszlo, E., and Hollo, J. (1980) Carbohydr. Res., **81**, 157-166.
3) Wakim, J., Robinson, M., and Thoma, J.A. (1969) *Carbohydr. Res.*, **10**, 487-503.
4) Pasero, L., Mazzei-Pierron, Y., Abadie, B., Chicheportiche, Y., and Marchis-Mouren, G. (1986) *Biochim. Biophys. Acta*, **869**, 147-157.
5) Buisson, G., Duee, E., Haser, R., and Payan, F. (1987) *EMBO J.*, **6**, 3909-3916.
6) Marshall, J.J. and Lauda, C.M. (1975) *J. Biol. Chem.*, **250**, 8030-8037.
7) Wilcox, E.R. and Whitaker, J.R. (1984) *Biochemistry*, **23**, 1783-1791.
8) Nakatani, H. (1988) *Arch. Biochem. Biophys.*, **263**, 364-368.
9) Loyter, A. and Shram, M. (1962) *Biochim. Biophys. Acta* **65**, 200-206.
10) Marchis-Mouren, G. and Pasero, L. (1967) *Biochim. Biophys. Acta*, **140**, 366-368.
11) Sakano, Y., Takahashi, S., and Kobayashi, T. (1983) *J. Jpn Soc. Starch Sci.*, **30**, 30-37.
12) Hiromi K., Takahashi Y., and Ono S. (1963) *Bull. Chem. Soc. Jpn.* **36**, 563-569.
13) Nakagiri, Y., Kanda, T., Otaki, M., Inamoto, K., Asai, T., Okada, S., and Kitahata, S. (1982) *J. Japan, Soc. Starch Sci.*, **29**, 161-166.
14) Elodi, P., Mora, S., and Kryzteva, M. (1972) *Eur. J. Biochem.*, **24**, 572-581.
15) Sakoda, M. and Hiromi, K. (1976) *J. Biochem. (Tokyo)*, **80**, 547-555.
16) Roosemount, J.L. (1978) *Anal. Biochem.* **88**, 314-320.
17) Wallenfels, K., Laule, G., and Meltzer, B. (1982) *J. Clin. Chem. Clin. Biochem.*, **20**, 581-586.
18) Granzer, M., Abadie, B., Mazzei, Y., and Marchis-Mouren, G. (1975) *FEBS Lett.*, **50**, 276-278.
19) Steer, M.L., Nathan, T., and Levitzki, A. (1974) *Biochem. Biophys. Acta*, **334**, 389-397.
20) Prodanov, E., Seigner, C., and Marchis-Mouren, G. (1984) *Biochem. Biophys. Res. Commun.*, **122**, 75-81.

CHAPTER II   Substrate-Dependent Shift of Optimum pH in Porcine
Pancreatic α-Amylase-Catalyzed Reaction

From the primary structure (1) and crystal structure with 2.9 Å resolution (2), the catalytic residues of PPA were proposed to be the carboxyl groups of Asp 197 and Asp 300. PPA resembles TAA in terms of the crystal structure and sequence homology around the active site (3). Therefore, two carboxyl residues are speculated to be the catalytic residues in the both enzymes. Unlike TAA, however, PPA is activated by the chloride ion (4) which is binding to the catalytic site (2). The optimum pH's of PPA and TAA for the hydrolysis of soluble starch and amylose is 6.9 (4) and 5.5 (5), respectively. The pH profile of the rate parameter for PPA is not a simple bell shape expected from the two catalytic residues mechanism. Therefore, it is important to obtain information on catalytic residues from kinetic analysis of enzyme actions. The values of pK's and enthalpy change for that can indicate probable catalytic amino acid residues. For the analysis of pH-profiles, small substrates with only one possible cleavage site are useful because the complexity of "multiple attack" action (6, 7) on amylose and starch and other effects due to different productive binding modes (8) may be eliminated. In this chapter, the author reports the detailed analysis of pH profiles of PPA by using low molecular substrates and the probable amino acid residues related to the catalysis function determined from thermodynamic data.

MATERIALS AND METHODS

Materials. PPA is the same as that described in CHAPTER I. TSK Gel DEAE Toyopearl 650 S and TSK-G-2000 PW column (7.5 φ x 600 mm) were purchased from Toyo Soda Mfg. Co., Ltd. p-Nitrophenyl α-D-maltoside (G$_2$-PNP) was purchased from Calbiochem Corp. Soluble starch, amylose A (MW = 2,900), maltotetraose (G$_4$), maltopentaose (G$_5$), maltohexaose (G$_6$) and γ-cyclodextrin (γ-CD) were purchased from Nacalai tesque Ltd. Maltotetraitol (G$_4$OH), maltopentaitol (G$_5$OH) and maltohexaitol (G$_6$OH) were prepared by the reduction of G$_4$, G$_5$ and G$_6$ with sodium borohydride according to the method by Walfolm and Thompson (9), respectively. Other chemicals were of commercial guaranteed or reagent grade.

Enzyme assay. The hydrolytic reaction was initiated by mixing a PPA solution with a substrate solution in a 25 mM Tris-acetate buffer (pH 3.5 - 9.0) or in a 25 mM sodium-borate buffer (pH 9.0 - 11.0), containing 30 mM NaCl and 1 mM CaCl$_2$ at 30° C. The reactions for soluble starch, amylose and the oligosaccharides (G$_5$, G$_4$OH, G$_5$OH and G$_6$OH) were terminated by the addition of the same volume of 0.08 N NaOH solution. The activities for the substrates

were determined by reductometry; for soluble starch and amylose the modified Nelson-Somogyi method (10) was used and for the oligosaccharides the method of Dygert et al.(11) was used. For G_2-PNP, the reaction was terminated by pouring 0.5 mL of the reaction mixture into 1 mL of the 0.01 N NaOH solution and the activity was measured by the 400 nm absorption of the product p-nitrophenol liberated within the 2 min. The alkaline hydrolysis of G_2-PNP was negligible. The hydrolysis of γ-CD was determined by utilizing the fluorescence of 2-p-toluidinylnaphthalene-6 sulfonate (TNS) (12). Since the fluorescence emission (450 nm) of TNS excited at 366 nm is increased by the addition of CD, the amount of γ-CD is measurable from the increment of the fluorescence emission at 450 nm. The kinetic parameters (k_{cat} and K_m) were determined with the same method described in CHAPTER I. Analysis of oligosaccharides was carried with the same method described in CHAPTER I.

RESULTS

Influence of the buffer on the hydrolytic activity

The hydrolytic activity of PPA for G_5 were measured in some buffers with the modified Nelson-Somogyi method (10). The kinetic parameters (k_{cat} and K_m) were examined at some pH's in sodium-acetate buffer (pH 5.1), sodium-phoshate buffer (pH 6.9), sodium-borate buffer (pH 9.0) and Tris-acetate buffer (pH 5.1, 6.9 and 8.9) containing 30 mM NaCl and 0.1 mM $CaCl_2$ (Fig. 1). The parameters were independent of these buffer system. However, the parameters were slightly dependent on concentration of the buffer. In the case of Tris-acetate buffer, k_{cat} decreased in more than 125 mM buffer and K_m increased in more than 100 mM buffer (Fig. 1). The same results were obtained for soluble starch as substrate. These effects were negligible at low concentrations (10 - 50 mM) of the buffer. Therefore, subsequent experiments were carried out in 25 mM of Tris-acetate and sodium phosphate buffer containing 30 mM NaCl and 0.1 mM $CaCl_2$.

Hydrolysis of amylose and soluble starch

The pH profile for the hydrolytic activity of PPA for amylose A (MW = 2,900) showed that the optimum pH is 6.9. The similar profile was obtained with soluble starch and the optimum pH of 6.9 was confirmed as reported by Wakim et al., (4). However, the pH profiles of PPA for these substrates does not reflect exactly the initial hydrolytic activity for the cleavage of their α-(1,4) glycoside bonds because the "multiple attack" action of PPA on these long chain substrates depends on pH (6, 13). Therefore, the author used oligosaccharide conjugates with sorbitol and p-nitrophenol, and γ-CD as substrates to analysis pH-profiles without "multiple attack" action.
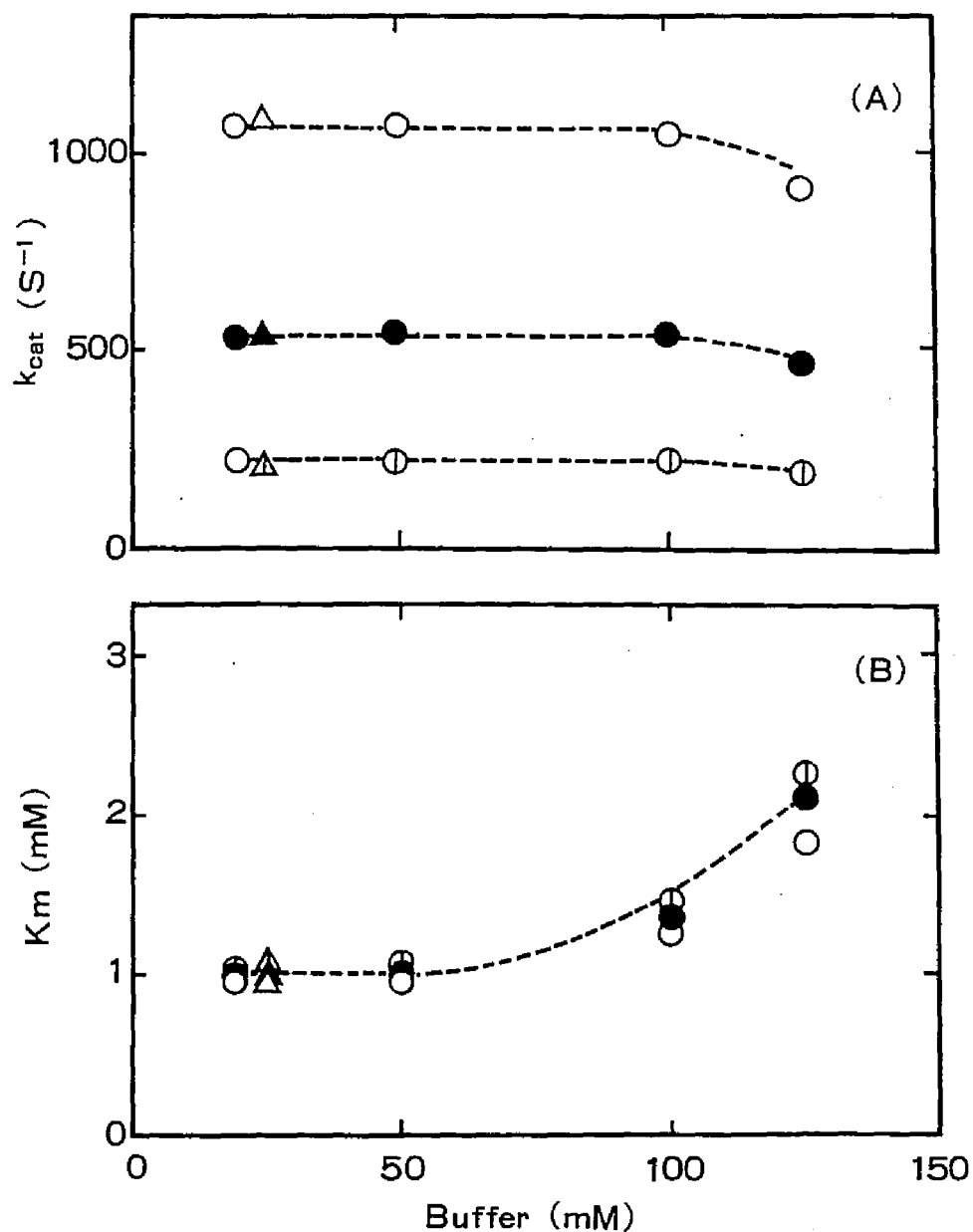
Fig. 1. Influence of the buffer on kinetic parameters k_{cat} (A) and K_m (B) in the hydrolytic activity for G_5. ●, ○ and ⦶ represent Tris-acetate buffer at pH 5.1, 6.9 and 8.9, respectively. ▲, △ and ⊿ represent sodium-acetate buffer (pH 5.1), sodium-phosphate buffer (pH 6.9) and sodium-borate buffer (pH 9.0), respectively. All buffers contain 30 mM NaCl and 0.1 mM CaCl$_2$. The reactions were carried out at 30°C.

Hydrolysis of G_2-PNP

G_2-PNP is favorable to study the hydrolytic activity of PPA, since it is the smallest substrate that can be hydrolyzed at one position shown in Fig. 2 (A) to give p-nitrophenol (14). The increase of the 400 nm absorbance due to the liberated p-nitrophenyl was linear within 10 % conversion. The initial rate of the hydrolysis was obtained from the slope of the linear plot. The optimum pH of the rate constant (k_{cat}) for G_2-PNP was 5.2 unlike that for soluble starch and amylose, and the value of Michaelis constant (K_m) was 5.0 mM all over the pH range examined (Fig. 3 (A)). Furthermore, the pH profile of k_{cat} deviates at around pH 7 from the theoretical profile based on the two ionizing group catalysis mechanism (15).

Hydrolysis of γ-CD

γ-CD was hydrolyzed at the one cleavage position in the cyclic α-(1,4) glycoside bonds (Fig. 2 (B)) to linear maltooctanoside, which was then decomposed to smaller oligosaccharides by the "multiple attack" action of PPA (16). Thus, the decrease rate of γ-CD measured by the TNS fluorescence method reflects directly the initial hydrolysis rate for γ-CD within 10-20 % conversion. The optimum pH of the k_{cat} for γ-CD was 5.2 in accord with that for G_2-PNP and the value of K_m was also independent of pH (Fig. 3 (B)). This pH profile also shows deviation at around pH 7 from the theoretical curve obtained by assuming two catalytic groups.
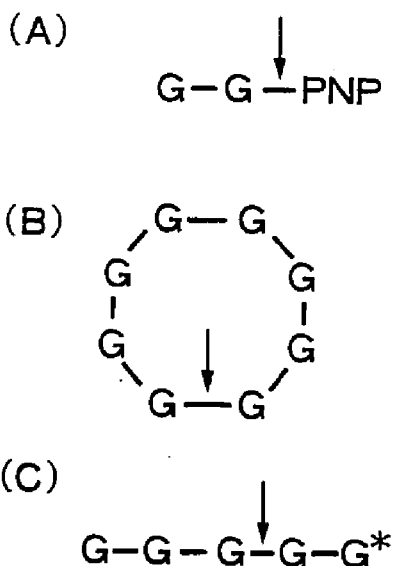
Fig. 2. Hydrolytic patterns of G_2-PNP (A), γ-CD (B) and G_5 (C). Glucose residue, reducing end of oligosaccharide, p-nitrophenol and α-(1,4) glycoside bond are shown as G, *, PNP and —. The bond scissible by PPA are shown by arrows.

Hydrolysis of G_5, G_4OH, G_5OH and G_6OH

For G_5, the hydrolysis occurred at one cleavage position without multiple attack (Fig. 2 (C)) as reported by Robyt et al. (8) in the pH 4.0 to 9.3 region. The initial hydrolysis rate was calculated from the slope of the linear time course plot obtained with reductometry within 10-20 % conversion. The optimum pH of k_{cat} was 6.9, identical with those for soluble starch and amylose, and the value of K_m was independent of the pH examined (Fig. 3 (C)).
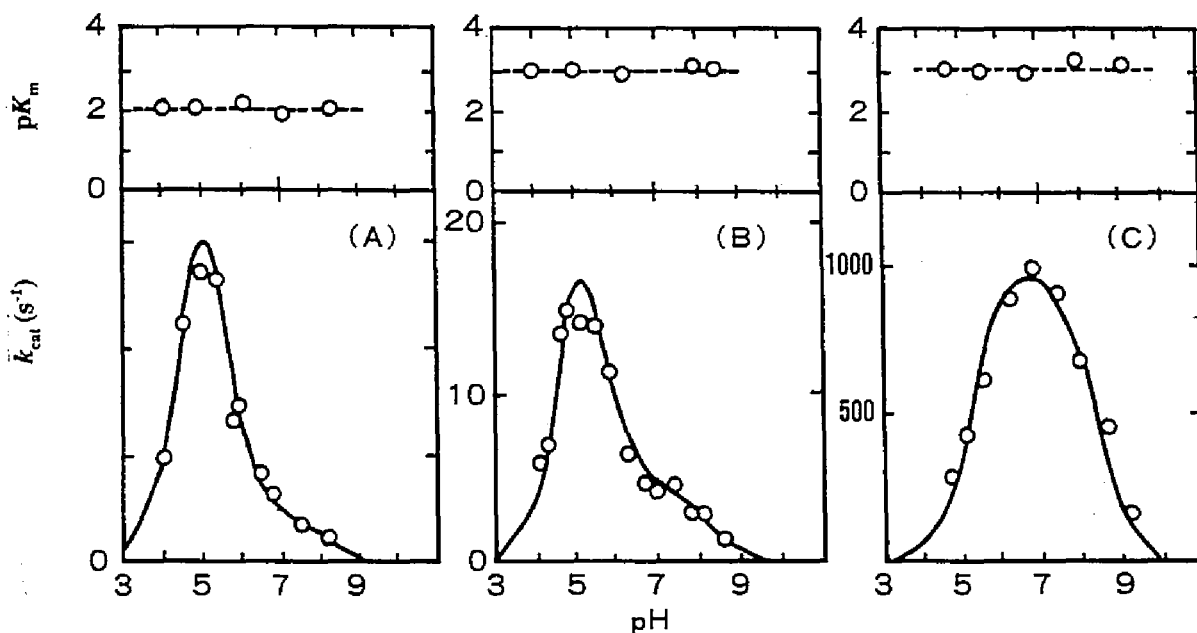

Fig. 3. Effect of pH on the K_m and k_{cat} of the hydrolytic reaction of G_2-PNP (A), γ-CD (B) and G_5 (C). The theoretical curves fitting these data were calculated by using eq. (1) and the estimated parameters (pK_1=4.90, pK_2=5.35, pK_3=8.55, (A) k_1=0.608 s^{-1}, k_2=0.040 s^{-1}, (B) k_1=32,6 s^{-1}, k_2=4.2 s^{-1}, (C) k_1=368 s^{-1}, k_2=1010 s^{-1}).

Next, the author used some substrates without reducing end, G_4OH, G_5OH and G_6OH to measure the initial rate of the hydrolysis of α-D-(1,4) glycosidic bond at 10, 20, 30 and 37° C by the reductmetric method. For these substrates, the initial rate of the hydrolysis of α-D-(1,4) glycoside bond could be measured accurately from the reductmetric determination because there was no reducing end. The hydrolysates from these substrates were analyzed by HPLC, although reduced oligosaccharides (GnOH) were not separated from the corresponding oligosaccharides with reducing end (Gn). In the case of G_4OH, the products G_2 and G_2OH appeared at the same position. Similarly, the products from G_6OH were G_3 and G_3OH, which also eluted as one peak. In the case of G_5OH, two peaks at the positions of G_2 and G_3 were

(A) G—G—G—GOH

(B) G—G—G—G—GOH

(C) G—G—G—G—G—GOH

Fig. 4. Hydrolytic patterns of G₄OH (A), G₅OH (B) and G₆OH (C). GnOH indicates reduced oligosaccharide with sodium borohydride from Gn. The bond scissible by PPA are shown by arrows.

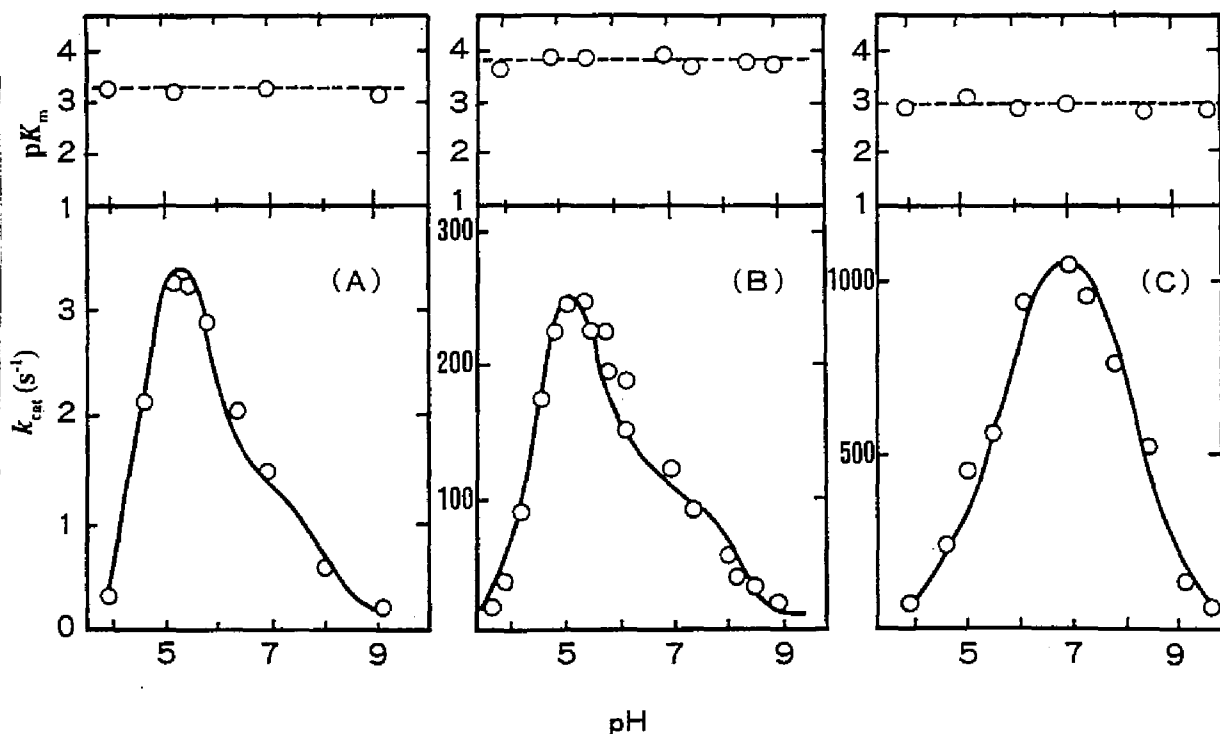Fig. 5. Effect of pH on the K_m and k_{cat} of the hydrolytic reaction of G₄OH (A), G₅OH (B) and G₆OH (C). The theoretical curves fitting these data were calculated by using eq. (1) and the estimated parameters (pK_1=4.90, pK_2=5.35, pK_3=8.55, (A) k_1=6.23 s⁻¹, k_2=1.47 s⁻¹, (B) k_1=490 s⁻¹, k_2=98 s⁻¹, (C) k_1=482 s⁻¹, k_2=912 s⁻¹).

- 30 -

detected. The analysis of the products from G_5OH with paper chromatography indicated that they were G_2OH and G_3 since the product at the G_3 position had a reducing end but that at G_2 had not. The product analysis proved that these substrates were hydrolyzed at a single cleavage site shown in Fig. 4, regardless of the pH, substrate concentration and reaction temperature examined. The K_m values for the substrates were invariable in the range of pH 4 to 10. The k_{cat} values strongly depended on the pH and the optimum pH for the hydrolysis of G_4OH and G_5OH was 5.2 (Fig. 5 (A), (B)) whereas that for G_6OH was 6.9 (Fig. 5 (C)).
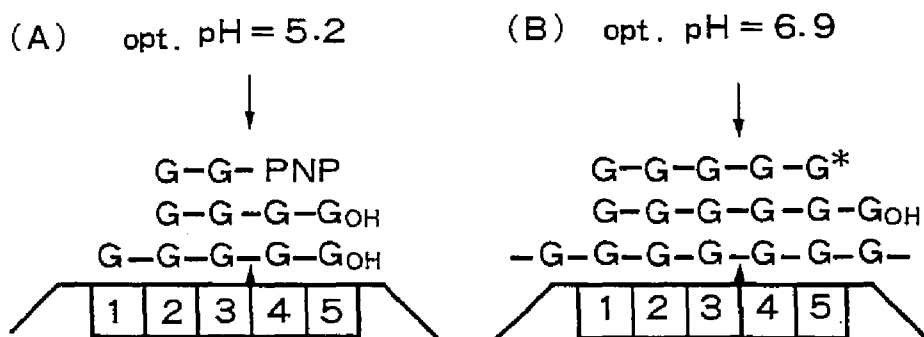
Fig. 6. Schematic representation of the active site of PPA and the productive binding mode of substrates. Subsites per glucose residue (G) of the substrates are numbered 1-5 from the nonreducing end. The catalytic residue is located between subsite 3 and 4. (A) Productive binding modes of G_2-PNP, G_4OH and G_5OH. Optimum pH of the hydrolytic activity is 5.2. (B) Productive binding modes of G_5, G_6OH and amylose. The optimum pH of that is 6.9.

DISCUSSION

The optimum pH for the hydrolytic activity of PPA under the physiological conditions has long been believed to be around neutrality on the basis of the study on soluble starch and amylose (4). However, the author found that it shifts to 5.2 in the case of some low molecular substrates (Fig. 3) and the shift depends on the occupancy of one enzyme subsite critical for the difference of only one glucose residue in the substrates (Fig. 5). Analysis of the products from the substrates, $G_{4-6}OH$ indicates that the shift of the optimum pH from 6.9 to 5.2 occurs when the subsite 5 of PPA is not occupied by a glucose residue of the substrates in the productive binding mode (Fig. 4, 6). This rule holds also for the other substrates (amylose, starch, G_5 and G_2-PNP) as shown in Fig. 6. The optimum pH for γ-CD is 5.2, suggesting that

the subsite 5 is not occupied in the productive binding mode. If the catalytic ionization groups are two, the pH profiles must be bell-shaped and the optimum pH should be substrate-independent like TAA, because the fact that the K_m values of PPA are independent of pH indicates that the pK values of the ionization groups contributing to the catalytic function of PPA are substrate-independent. Actually, PPA is showing a substrate-dependent shift of the optimum pH without any change in the pK values of the catalytic groups. The substrate-dependent shift of the optimum pH, the pH-independent K_m and the deviation of pH-profiles from the theoretical curves based on the contribution of two ionizing groups to the catalytic activity (G_2-PNP, γ-CD, G_4OH and G_5OH) led to the modified reaction mechanism with three ionization groups shown in scheme I:

Scheme I
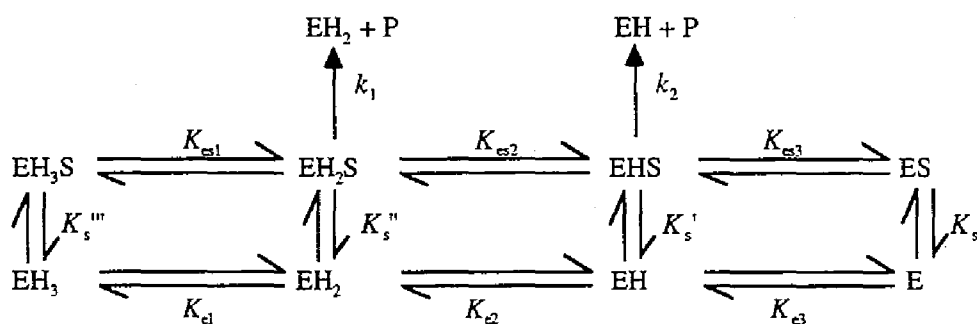
E = enzyme (PPA); S = substrate; P = product; H = proton.

In the scheme I, the author assumes that three ionization groups contribute to the enzyme activity. K_{e1}, K_{e2} and K_{e3} are the ionization constants of the enzyme at the first, second and third ionization stages, respectively. K_{es1}, K_{es2} and K_{es3} are those of the enzyme-substrate complexes. K_s, K_s', K_s'' and K_s''' are the dissociation constants between the substrate and the enzyme in the successive ionized states, E, EH, EH_2 and EH_3, respectively. Hydrolysis of the substrates occurs only from the complex EH_2S and EHS with the rate constants k_1 and k_2, respectively. The relative values of k_1 and k_2 determine the apparent optimum pH of the hydrolysis. When the substrate is large enough to occupy subsite 5 of PPA, the complex EHS is more active than the complex EH_2S; the k_2 value is greatly increased and the optimum pH shifts towards neutrality. Thus, the substrate dependent shift of the optimum pH observed for the hydrolytic activity of PPA can be explained quantitatively by the scheme I.

The fact that K_m is independent of pH allows us to assume $K_s=K_s'=K_s''=K_s'''$, $K_{e1}=K_{es1}$, $K_{e2}=K_{es2}$ and $K_{e3}=K_{es3}$. Then, the following rate equation (eq. (1)) can be derived from the scheme 1 by use of the method of stationary state.

- 32 -

$$k_{cat} = \cfrac{k_1}{\cfrac{K_{e2}K_{e3}}{[H^+]^2} + \cfrac{K_{e2}}{[H^+]} + 1 + \cfrac{[H^+]}{K_{e1}}} + \cfrac{k_2}{\cfrac{K_{e3}}{[H^+]} + 1 + \cfrac{[H^+]}{K_{e2}} + \cfrac{[H^+]^2}{K_{e1}K_{e2}}} \qquad (1)$$

Here K_{e1}, K_{e2}, K_{e3}, k_1 and k_2 are functions of temperature as shown:

$$pK_{1-3} = -\log K_{e1-3}$$
$$\Delta H_{1-3} = 2.3R \, d \, (pK_{1-3}) / d \, (1/T)$$
$$E_{1-2} = -R \, d \ln k_{1-2} / d \, (1/T) \qquad (2)$$

here ΔH_1, ΔH_2 and ΔH_3 are enthalpy change for pK_1, pK_2 and pK_3, E_1 and E_2 are activation energies for k_1 and k_2, and R and T are the gas constant and temperature, respectively. The kinetic constants and their standard errors can be calculated using eq. (1) and (2) and a non-linear least squares method "program system SALS" with Gauss-Newton variation (17). The rate parameters pK_1, pK_2, pK_3, k_1 and k_2, the enthalpy changes for pK_1, pK_2 and pK_3, and the activation energies for k_1 and k_2 are determined most accurately using the pH-profile data for G_6OH and G_5OH at 10 - 37°C since they are the substrates with different optimum pH's and rather small differences between their k_1 and k_2 values. The values of pK_1, pK_2 and pK_3, based on the dissociation constants of the free enzyme itself, are independent of substrates. Therefore, the author must obtain the following 14 parameters; pK_1, pK_2, pK_3, ΔH_1, ΔH_2, ΔH_3, and k_1, k_2, E_1 and E_2 for G_5OH and G_6OH, from the temperature depending pH-profile data for G_5OH and G_6OH at 10, 20, 30 and 37°C using eq. (1) in which eq. (2) is substituted. As a result of the computer analysis of the pH profiles, we obtained above parameters for G_5OH and G_6OH shown in Table I. The experimental data and theoretical line computed from eq. (1) and (2) with the parameters (Table I) are shown in Fig. 7. The values of k_1 and k_2 for other substrates at 30°C can be determined by using these same values of pK_{1-3}. As shown in Fig. 3 and 5, theoretical curves (solid lines) (values of pK_1, pK_2, pK_3, k_1 and k_2 are described in the figure legends) fit in well with the experimental values. The scheme I and Table I show that the catalytic residue of pK=8.55 acts as a proton donor of PPA. The amino acid sequences at the active site of PPA and TAA are quite similar and the amino acid residues near the catalytic site of PPA are compared to be the three dimensional structure of TAA (2, 3). Comparison of TAA with PPA indicates that the three histidine residues (101, 201 and 299 in PPA) and three carboxyl residues (197, 233 and 300 in PPA) are close enough to form hydrogen bonding pairs. The enthalpy changes of the pK's and the information of the three dimensional structure strongly suggest that the residues with pK values of 4.9 and 5.35 are carboxylates (Asp197 or

- 33 -

Asp300) and His, Cys and Tyr are candidates for the residue with pK value of 8.55. However, the most probable residue is His since Cys and Tyr residues are not located in the catalytic site of PPA (2).

PPA whose five histidine residues were modified chemically by diethyl pyrocarbonate at pH 6.0 (18, CHAPTER I) showed a decrease in amylase activity and an increase in maltosidase activity. If the catalytic residue with the pK value of 8.55 is histidine residue, it can not be modified by the reagent since the chemical modification reagent is specific for the deprotonated histidine residue at pH 6.0; normal histidine residues (pK =6-7) can be modified but the catalytic one with pK=8.55 must be practically unmodified at pH 6.0. Therefore, steric hindrance around the histidine residue (one of catalytic residues) may reduce the reactivity with the modification. Furthermore, pH profile for the increased maltosidase activity of His modified PPA (CHAPTER I) was similar to that of native one (unpublished data). This result also supports the above consideration. The optimum pH of PPA for soluble starch shifted from 6.9 to 5.5 when the chloride ion binding to PPA was eliminated, although the enzyme activity was much lowered (4). Therefore, chloride ion also affects the relative values of the two parameters k_1 and k_2 in the scheme I. Since the chloride ion binding site is near the active site (2) far from the subsite 5, the molecular mechanism for the optimum pH shift due to the chloride ion may be different from that in the substrate effect; chloride ion binding is an additional indispensable factor for being optimum pH around 7. Drastic differences in the k_1 and k_2 values and the optimum pH's between maltopentaitol and maltopentaose (Fig. 3 and 5) suggest that the binding modes are not the same despite the fact that the substrates are quite similar in apparent structure. Subtle difference in the end group of these substrates, glucose and sorbitol, as well as the binding of chloride ion has pronounced influence on the catalytic mechanism. TAA shows simple bell-shape pH profiles with the optimum pH around 5.5, regardless of the characters of substrates (5); its catalytic residues are composed of two carboxyl groups (3). The present data and analysis show that the catalytic function of PPA consists of at least three ionizable residues. Previously proposed catalytic mechanisms which assume only two catalytic residues (2, 19) should be extended so as to include additional modulation factor. The residue of pK_3 acting as a proton donor is His, and the other two residues of pK_{1-2} are probably carboxyl residues as a proton acceptor and its modulator. Therefore, the catalytic mechanism of PPA should be constructed including additional modulation mode to distinguish characters of substrates at productive binding mode by protonation and deprotonation of the probable carboxyl residue at the active site. Our data and X-ray structure suggest that the proton donor for the catalysis of PPA is a histidine residue, one of His101, 201 and 299 and the active carboxyl residues are two of three residues Asp197, Glu233, and Asp300. To clarify the detailed catalytic mechanism of PPA, further structural and biochemical investigations are

necessary. Furthermore, it has been found that binding of a glucose residue to the subsite 5 in the productive binding mode affects the transition-state of hydrolysis at the catalytic site (Fig. 6). It is reasonable to assume that the interaction between each subsite and a glucose residue in the enzyme-substrate complex is not rigid and not independent in PPA, but flexible especially at the subsites 3 and 4 in which the catalytic site locates. The productive binding mode covering the subsite 5 with a glucose residue must change configurations between catalytic residues and glycosidic bond hydrolyzed. The molecular mechanism will be discussed at the last section (SUMMARY AND CONCLUSION) of this thesis.
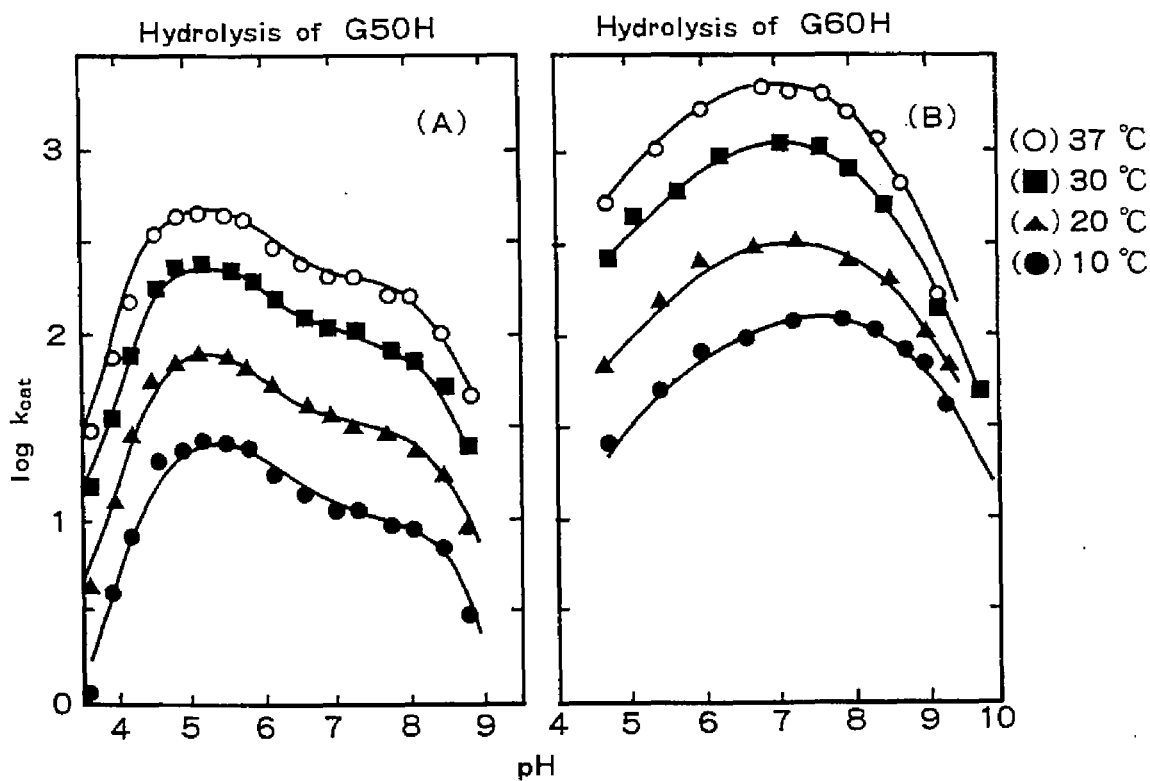
Fig. 7. Effect of temperature on pH-profiles of k_{cat} for G_5OH (A) and G_6OH (B). The experimental points (●;10°C, ▲;20°C, ■;30°C and O;37°C) were determined at the condition of the substrates concentrations much excess than the value of K_m. The theoretical curves fitting these data were calculated by using eq. (1) and (2) and the parameters estimated (Table I).

Table I. Kinetic parameters computed from the data of k_{cat} for G_5OH and G_6OH

Substrate	G_5OH	G_6OH
pK_1	4.90 ± 0.05	
pK_2	5.35 ± 0.06	
pK_3	8.55 ± 0.02	
ΔH_1 (kcal/mol)	0.0 ± 0.07	
ΔH_2 (kcal/mol)	2.87 ± 0.12	
ΔH_3 (kcal/mol)	7.33 ± 0.10	
k_1 (s^{-1})	490 ± 37	482 ± 30
k_2 (s^{-1})	98 ± 3.8	912 ± 14
E_1 (kcal/mol)	19.7 ± 0.066	19.5 ± 0.13
E_2 (kcal/mol)	20.1 ± 0.11	18.8 ± 0.026

The 14 kinetic parameters on the activity of PPA including their standard errors were obtained from the k_{cat} values at the different pH and temperature using eq. (1) and (2) and a non-linear least squares method with Gauss-Newton variation. The values of pK_{1-3} and k_{1-2} were those at 30°C.

SUMMARY

PPA hydrolyzes α-D-(1,4)glycosidic bonds in starch and amylose at random, and the optimum pH for the substrates is 6.9. The optimum pH, however, shifted to 5.2 for the hydrolytic reaction of low molecular weight oligosaccharide substrates such as p-nitrophenyl α-D-maltoside, γ-cyclodextrin, maltotetraitol, and maltopentaitol. The optimum pH for the oligosaccharides consisting of more than five glucose residues, such as maltopentaose and maltohexaitol, was 6.9. From the analysis of the hydrolysates, it was clear that the shift of the optimum pH occurred only when the fifth subsite of PPA in the productive binding modes was occupied by a glucosyl residue of the substrates. The value of K_m was independent of pH between 4 and 10 but than of k_{cat} was dependent on pH. The pH profiles of k_{cat} for the above substrates did not fit a simple bell-shaped curve predicted by a two-catalytic-group mechanism. Instead, they were well analyzed theoretically by three pK values and two intrinsic k_{cat} values. Enthalpy changes for the three pK'_s (4.90, 5.35, and 8.55 at 30°C) were determined from the temperature dependence of pH profiles for maltopentaitol and maltohexaitol to be 0.0, 2.87, and 7.33 kcal/mol, respectively. These results indicate that productive binding modes of the substrates directly affect the catalytic function of the enzyme. From the present thermodynamic analysis and reported three-dimensional structure at the active site of PPA [Buisson,G. et al.

(1987) *EMBO J.* **6**, 3909-3916], one can assume that a histidyl residue (101, 201, or 299) acts as a proton donor and two carboxyl groups (Asp197, Glu233, or Asp300) act as proton donors or acceptors, and the productive binding mode covering the fifth subsite changes configurations between the catalytic residues and the glycosidic bond to be hydrolyzed and modulates kinetic parameters depending on pH.

REFERENCES

1) Pasero, L., Mazzei-Pierron, Y., Abadie, B., Chicheportiche, Y., and Marchis-Mouren, G. (1986) *Biochim. Biophys. Acta.* **869**, 147-157.
2) Buisson, G., Duee, E., Haser, R., and Payan, F., (1987) *EMBO J.,* **6**, 3909-3916.
3) Matsuura, Y., Kusunoki, M., Harada, W., and Kakudo, M. (1984) *J. Biochem. (Tokyo)* , **95**, 697-702.
4) Wakim, J., Robinson, M., and Thoma, J. A. (1969) *Carbohydr. Res.* **10**, 487-503.
5) Matsubara, S., Ikenaka, T. and Akabori, S. (1959) *J. Biochem. (Tokyo)* **46**, 425-431.
6) Robyt, J.F. and French, D. (1967) *Arch. Biochem. Biophys.* **122**, 8-16.
7) Robyt, J. F. and French, D. (1970b) *Arch. Biochem. Biophys.* **138**, 622-670.
8) Robyt, J. F., and French, D. (1970a) *J. Biol. Chem.* **45**, 3917-3927.
9) Walform, M. L. and Thompson, A. (1963) *Method in Carbohyd. Chem.* **2**, 65-68.
10) Hiromi, K., Takahashi Y., and Ono S., (1963) *Bull. Chem. Soc. Jpn.,* **36**, 563-569.
11) Dygert, S., Li, L. H., and Thoma, J. A. (1965) *Anal. Biochem.,* **13**, 367-374.
12) Kondo, H., Nakatani, H., and Hiromi, K. (1976) *J. Biochem.(Tokyo)* **79**, 393-405.
13) Kondo, H., Nakatani, H., Hiromi, K. and Matsuno, R. (1978) *J. Biochem. (Tokyo),* **84**, 403-417.
14) Levitzki, A., and Steer, M. L., (1974) *Eur. J. Biochem.,* **41**, 171-180.
15) Dixon, M., Webb, E., Thorne, C. J. R., and Tipton, K. F.,(1979) *"Enzymes "* , Academic Press, New York San Francisco,   pp138-164.
16) Abdullah, M., French, D., and Robyt, J. F. (1966) *Arch. Biochem. Biophys.* **114**, 595-598.
17) Nakagawa, T and Oyanagi, Y., "Program System SALS for Nonlinear Least-Squares Fitting in Experimental Sciences" in Recent Developments in Statistical Inference and Data Analysis, Matusita, K., editor, p221-225 (North Holland Publishing Company, (1980)
18) Nakatani, H. (1988) *Arch. Biochem. Biophys.* **263**, 364-368.
19) Thoma, J. A. (1968) *J. Theoret. Biol.,* **19**, 297-310.

CHAPTER III   The pH-Dependence of Action Pattern in Porcine Pancreatic α-Amylase-Catalyzed Reaction for ^{14}C Labeled Maltooligosaccharide Substrates

From the detailed analyses of the data on pH-profiles for some substrates, a three catalytic residue model was proposed that contains a histidine residue in addition to two carboxyl residues for the catalytic action (CHAPTER II).   In fact, three carboxyl residues (Asp197, Asp300 and Glu233) and three histidine residues (His101, His201 and His299) are located in the active site (1).   However, identification of catalytic amino acid residues and the reaction mechanism are not well clarified.   Therefore, it is important to confirm the three catalytic residue model for PPA by use of natural linear maltooligosaccharide substrates composed only of glucosyl residues.   In this chapter, the author examine the three catalytic residue model of PPA by analyzing the pH dependencies of hydrolytic patterns and activities on maltotriose (G_3), maltotetraose (G_4), maltopentaose (G_5) and maltohexaose (G_6) substrates having a ^{14}C-labeled glucose at their reducing ends.

MATERIALS AND METHODS

Materials. PPA and α-CD are the same as those described in the previous chapter. ^{14}C-Glucose was purchased from Daiichi Kagaku Chemicals. Other chemicals were of commercial guaranteed or reagent grade.

Synthesis of maltooligosaccharides with ^{14}C-labeled reducing end glucose. Maltooligosaccharides (G_3, G_4, G_5 and G_6) with a labeled glucose (G) at their reducing ends were synthesized from α-CD and ^{14}C-labeled G by utilizing *Bacillus macerans* transglycosylase (2). Labeled G (10 μCi), 10 mg of α-CD and 20 THU (Tilden-Hudson Units) of transglycosylase were mixed to make a 1 mL reaction mixture and kept at 50°C and pH 6.0 for 3h. After the mixture was put in a boiling bath for 10 min to inactivate the enzyme, the products with reducing end labeled G were separated by multiple ascending paper chromatography on Whatman 3MM (30x30 cm) with aqueous 60% n-propanol at room temperature. The portions showing radioactivities were cut into small segments, and the products were extracted with distilled water.

Enzyme assay and product analysis. The hydrolytic reaction of PPA for the reducing end-labeled maltooligosaccharides (G_3, G_4, G_5 and G_6) was carried out at 30°C and the products were quantitatively analyzed by radioactive paper chromatography. The reaction was initiated

by mixing aliquots of the enzyme solution with the substrate (1 - 60 μM) in 25 mM tris-acetate buffer (pH 3.5 - 9.0), 25 mM sodium-acetate buffer (pH 3.5 - 5.5), 25 mM sodium-phosphate buffer (pH 6.0 - 8.0), or 25 mM sodium-borate buffer (pH 9.0 - 11.0), all containing 30 mM NaCl and 0.1 mM CaCl$_2$, and terminated by adding the same volume of 1.0 N acetic acid solution to the reaction mixture. The reaction products were separated by multiple ascending paper chromatography (Whatman 3MM, 30x30 cm) with aqueous 60 % n-propanol. After irrigation twice, the strip of paper was cut into segments (0.5 - 1.0 cm), placed in a glass vial containing toluene, 2,5 diphenyloxazole and dimethyl-1,4-bis-2-(5-phenyloxazole)-benzene, and its radioactivity was counted for 5 min with a liquid scintillation counter.

The value of k_{cat}/K_m was determined from the measurement of hydrolytic rate at sufficiently low concentration of substrate to exclude possible condensation and transglycosylation effects (3). Under the condition of s<< K_m, the Michaelis-Menten equation can be written as:

$$dp/dt = V s / (K_m + s) \cong (V / K_m) s = (k_{cat} / K_m) e_0 s$$

where p, s, e_0 and V are the concentrations of product, substrate and enzyme, and the maximum velocity of the reaction, respectively. This equation shows that, under the specific reaction conditions, the hydrolytic reaction can be regarded as a first order reaction with a rate constant $(k_{cat}/K_m) e_0$.

The first-order kinetics can also be represented in an integrated form (4):

$$k \, t = ln \, (s_0/s) = ln \, [1 / (1 - Ex)]$$

where k, s_0, s and Ex are the first-order rate constant, the substrate concentrations at time 0 and t, and the extent of the hydrolysis, $(s_0-s) / s_0$, respectively. Thus, the value of $(k_{cat}/K_m) e_0$ may conveniently be obtained as the first-order rate constant k from the slope of a plot of $ln[1/(1-Ex)]$ against time.

RESULTS

Bond cleavage pattern

The optimum pH of the hydrolytic activity of PPA is dependent on the structure of substrates. For soluble starch, amylose, maltohexaitol and G$_5$, the optimum pH is 6.9, while for maltopentaitol, maltotetraitol, γ-CD and G$_2$-PNP, it is 5.2 at 30°C (CHAPTER II). In order to know details of the substrate dependent shift of the optimum pH, the author examined pH dependence of the bond cleavage pattern for a series of oligosaccharides. The bond

cleavage pattern means a distribution of the position and normalized frequency of the cleavage bond in a substrate. The cleavage patterns of G_3, G_4, G_5 and G_6 at pH 6.9 and pH 5.2, determined by the radioactive analysis of the digestion products that resulted from the initial action of PPA on the labeled substrates, are shown in Fig. 1. For the hydrolysis of G_3, G_5 and G_6, the cleavage patterns are independent of pH and agree well with those obtained at neutral pH by Robyt and French (6), except that labeled G_2 production from G_3 is negligible under our conditions. For G_4 hydrolysis, however, the cleavage pattern is dependent on pH; at pH 6.9 the production of labeled G_2 is superior to that of labeled G1 whereas at pH 5.2 the situation is reversed. The values shown in Fig. 1 were independent of the substrate concentrations (1 - 60 μM) used in this work. These results suggest that G_4 is hydrolyzable in two productive binding modes with different pH dependency.
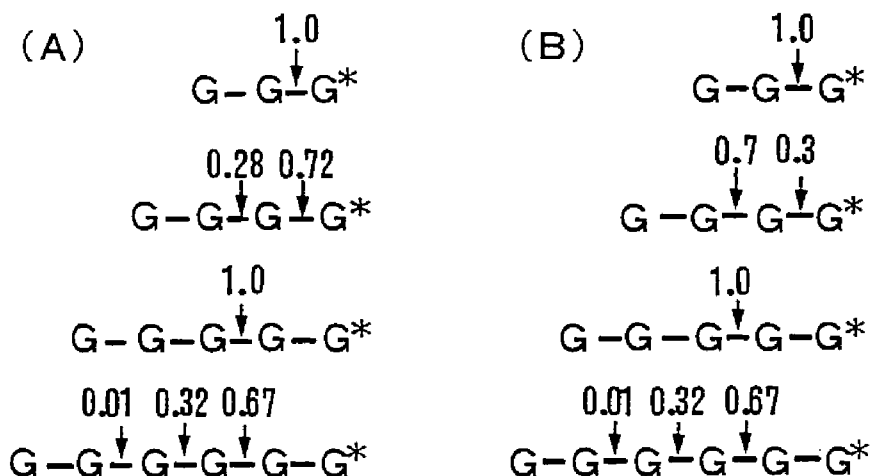
Fig. 1. Frequency distribution of the cleavage for linear maltooligosaccharides at pH 5.2 (A) and 6.9 (B). G, G* and - represent unlabeled, labeled glucose residues and α-1,4 glycoside bond, respectively. The numerals indicate the fractional cleavage distribution. PPA concentration was 5 nM and the concentrations of reducing end-labeled G_3, G_4 G_5 and G_6 were 7.2, 6.8, 5.1 and 4.2μM, respectively. The reactions were carried out at 30° C.

pH Profile of the activity

The pH profiles of the hydrolytic activities for G_3 - G_6 are shown in Fig. 2. They were not dependent on the buffer system used. Their optima were dependent on the chain-length of substrates G_3 - G_6. The optimum pH for G_3 was around 5.2, while for G_5 and G_6 it was around 6.9 like that for soluble starch and amylose. Furthermore, the pH profiles for the three

cleavage patterns of G_6 and for the single pattern of G_5 were identical. For G_4, however, the pH profiles for the two cleavage patterns were different from one another and the optimum pH of the total activity of the two productive binding modes is around 5.5 - 6.5, in contrast with that of G_3, G_5 and G_6. The pH profile for the labeled G production from G_4 is quite similar to that of G_3 and shows an optimum at around pH 5.2. However, the pH profile for the production of labeled G_2 from G_4 resembles those of G_5 and G_6 which have an optimum pH around 6.9 regardless of the cleavage patterns. These pH profiles and values of k_{cat}/K_m, and cleavage patterns were unchanged over the substrate concentration (1 - 60 μM) used. Therefore, contribution of condensation reactions is excluded that must occur depending on the substrate concentration. These results indicate that the shift of the optimum pH depends on the occupation of subsite 5 with a glucose residue of the substrate in the productive binding mode as described previously for the hydrolysis of maltopentaitol and maltohexaitol (CHAPTER II). The substrate-dependent optimum pH shift involving subsite 5 in the hydrolysis by PPA cannot be explained by the mechanism based on a simple two catalytic residue model where the shape of pH profile for k_{cat}/K_m is independent of the substrates (4).

DISCUSSION

In the previous chapter, the author proposed a three catalytic residue model to interpret the substrate dependent shift of optimum pH which allows the participation of three ionization groups in the hydrolytic activity. In this paper, The author consider the microscopic environment of these ionization groups and propose a slightly modified mechanism, as shown in Scheme I, by assuming that the three catalytic groups with low, middle and high pK values are ionizable independently from any ionization stage of the enzyme. In the mechanism, an inactive form, EH_1H_3, deprotonated in the middle pK group is taken into consideration in addition to an active form, EH_2H_3, deprotonated in the low pK group since the difference between the low and middle pK values is insufficiently small to neglect the ionization into the EH_1H_3 form.
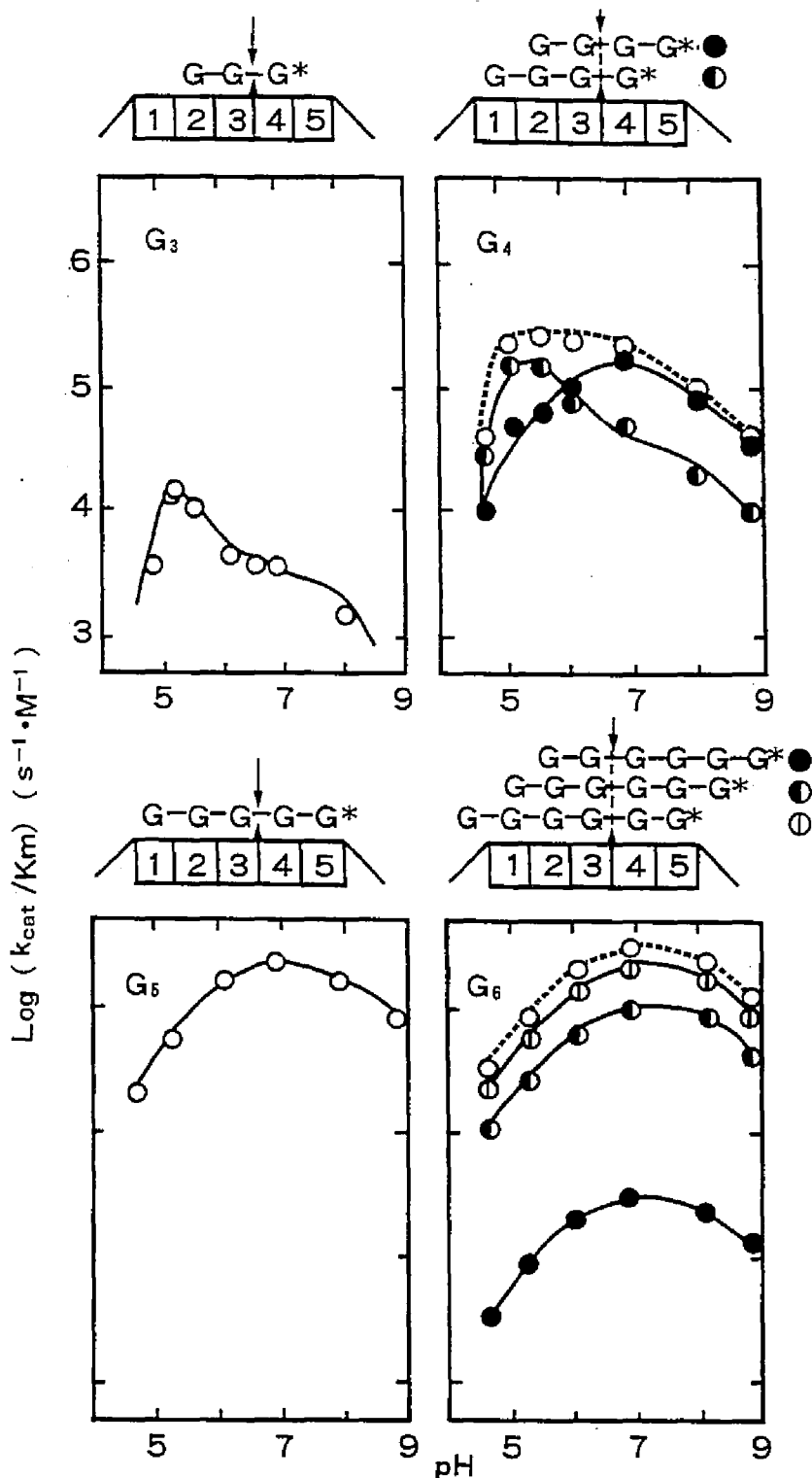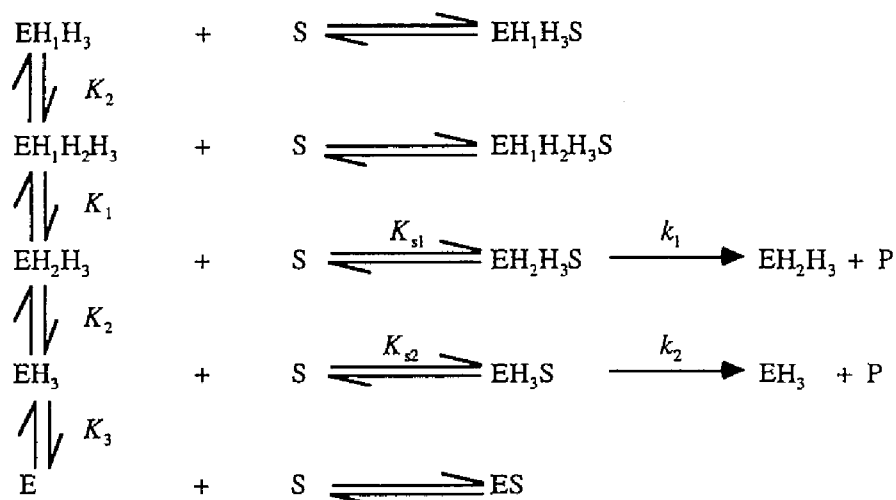
Fig. 2. Cleavage positions of maltooligosaccharides and pH profiles of the cleavage activities. The wedge (▲) shows the catalytic site and the boxes represent the subsites, numbered from the nonreducing end as indicated. Total hydrolytic activities calculated from the decrease of the substrate are indicated as open circles (○) for G_4 and G_5. Other symbols represent the hydrolytic activities from the binding modes indicated above. Solid lines indicate the theoretical lines calculated by using eq. (2) with the estimated parameters (Tables I and II).

- 43 -

Scheme I.

$$
\begin{array}{ccccc}
EH_1H_3 & + & S & \rightleftharpoons & EH_1H_3S \\
\Big\updownarrow K_2 & & & & \\
EH_1H_2H_3 & + & S & \rightleftharpoons & EH_1H_2H_3S \\
\Big\updownarrow K_1 & & & & \\
EH_2H_3 & + & S & \xrightleftharpoons{K_{s1}} EH_2H_3S \xrightarrow{k_1} EH_2H_3 + P \\
\Big\updownarrow K_2 & & & & \\
EH_3 & + & S & \xrightleftharpoons{K_{s2}} EH_3S \xrightarrow{k_2} EH_3 + P \\
\Big\updownarrow K_3 & & & & \\
E & + & S & \rightleftharpoons ES
\end{array}
$$

Here $K_{1\text{-}3}$, $k_{1\text{-}2}$ and $K_{s1\text{-}2}$ are the ionization constants for protons $H_{1\text{-}3}$ in the three catalytic residues, the hydrolytic rate constants of hydrolysis and dissociation constants of enzyme-substrate complexes, respectively.

Since K_m was independent of pH, it was suggested that $K_m = K_{s1} = K_{s2}$. The rate equation deduced from Scheme I is

$$
k_{cat} = \frac{(k_1 \cdot K_1)/[H^+] + (k_2 \cdot K_1 \cdot K_2)/[H^+]^2}{1 + (K_1 + K_2)/[H^+] + (K_1 \cdot K_2)/[H^+]^2 + (K_1 \cdot K_2 \cdot K_3)/[H^+]^3} \tag{1}.
$$

The values of $pK_{1\text{-}3}$ and their enthalpy changes $\Delta H_{1\text{-}3}$ for eq. (2) in CHAPTER II were reestimated by applying eq (1) to the pH profile plots of the hydrolysis of maltopentaitol and maltohexaitol reported chapter. Values of these parameters were calculated directly from initial velocity data by a nonlinear least squares method (APPENDIX), as shown in Table I. The reestimated values are practically not different from those of the previous chapter.

Table I. pK and enthalpic parameters for Scheme I computed with eq. (1) from data for maltopentaitol and maltohexaitol.

pK_1	4.78 ± 0.04
pK_2	5.54 ± 0.05
pK_3	8.62 ± 0.02
ΔH_1	0.09 ± 2.18 (kcal/mol)
ΔH_2	1.52 ± 2.24 (kcal/mol)
ΔH_3	6.86 ± 0.94 (kcal/mol)

Next, the author examined validity of the three catalytic residue model (Scheme I) for the hydrolysis of G_3 - G_6 with pK_1, pK_2 and pK_3 values in Table I obtained from eq. (1). From a steady state treatment for the enzyme-substrate complexes in Scheme I, k_{cat}/K_m can be written

$$k_{cat}/K_m = \frac{(k_1 \cdot K_1)/(K_m \cdot [H^+]) + (k_2 \cdot K_1 \cdot K_2)/(K_m \cdot [H^+]^2)}{1 + (K_1 + K_2)/[H^+] + (K_1 \cdot K_2)/[H^+]^2 + (K_1 \cdot K_2 \cdot K_3)/[H^+]^3} \qquad (2).$$

The values of k_1/K_m and k_2/K_m in eq. (2), which relate to the hydrolysis rate of the substrate in the individual productive binding modes, were obtained for G_3 - G_6 from their pH profile plots by the non-linear least squares method using the $pK_{1\text{-}3}$ values in Table I from eq. (1). The results are summarized in Table II. Theoretical curves computed from eq. (2) by use of these values of kinetic parameters fit well with the experimental data (Fig. 3). These results show that the three catalytic residue (two carboxyl and one histidine) model of PPA is also well adapted for the hydrolysis of the substrates composed of linear maltooligosaccharides.

This model assumes that there are two different hydrolytic modes depending on pH. The productive binding modes for G_3 - G_5 are illustrated in Fig. 3; one mode (A) with unoccupied subsite 5 results in labeled G production at the optimum pH 5.2, while another mode (B) with occupied subsite 5 results in labeled G_2 production at the optimum pH 6.9. The structural difference between the two productive binding modes ((A) and (B)) should be minor because subsites other than 5 are common to them as shown in Fig. 3. These facts suggest that the occupation of subsite 5 by a glucosyl residue of the substrate may switch the composition of the active site in PPA from one pair of catalytic residues to another pair exhibiting different pH dependence. Furthermore, the data for the hydrolysis of G_4 proved that affinities of each subsite were not determinable solely from k_{cat} and K_m for linear maltooligosaccharides. For PPA, therefore, the simple subsite theory (7) cannot be used to determine subsite affinities, because each affinity is defined independently and the functions of catalytic residues are assumed to be independent from the binding modes. Furthermore, it is clear that subsite 5, which is rather remote (about 4-7 Å) from the catalytic site between subsites 3 and 4, controls the catalytic activity including the optimum pH through binding with a glucose residue of the substrate. This control of the activity and shift of optimum pH of PPA by occupation of subsite 5 suggests an example of the induced fit mechanism for conformational change of enzyme-substrate complexes (8). Although a detailed catalytic mechanism of PPA cannot be elucidated at present, possible roles of each catalytic residue are estimated. The histidine residue with pK_3 in scheme I, which the author assigned in the previous chapter, must be a proton donor as a general acid, and the carboxyl residue with pK_1 in an anion form should

stabilize the carbonium intermediate assumed in the reaction of α-amylase-related carbohydratases (9). The role of carboxyl residue with pK_2 is rather complex; it may modulate the catalytic power of PPA by either protonation or deprotonation. In a protonated state, it can act as another proton donor, and in a deprotonated state it can assist the pK_1 carboxyl residue as an anion to stabilize the carbonium intermediate. The optimum pH shift from the acidic to the neutral region through occupation of subsite 5 by a glucosyl residue is related to the relative values of k_1/K_m and k_2/K_m; in the productive binding mode with occupied subsite 5, the k_2/K_m value is larger than k_1/K_m value and the optimum pH is around neutral, whereas in the unoccupied mode the k_2/K_m value is smaller than the k_1/K_m value and the optimum pH is acidic (Table II). This difference suggests that the occupation of subsite 5 by a glucosyl residue enhances the k_2/K_m value to shift the optimum pH to neutral. It is interesting that a sorbitol residue instead of a glucose is ineffective in eliciting the optimum pH shift (CHAPTER II). Taka α-amylase A (TAA), a fungal amylase produced by *Aspergillus oryzae*, resembles PPA in the three dimensional structure of the active site. However, pH profiles for the activity of TAA on soluble starch and G_2-PNP (10) were of simple bell-shape for a mechanism based on a two catalytic residue model (two carboxyl residues) (4). It is interesting that the catalytic mechanism of PPA must be different from that of TAA, even though the active site structures are similar (1, 11). Human pancreatic α-amylase also displays a substrate-dependent shift of the optimum pH (unpublished data, Ishikawa et al.), as may be expected from the sequence homology (12, 13). The very close sequence homologies (14) among porcine, mouse, rat and human α-amylases suggest that these mammalian enzymes may, in general, possess three catalytic residues.
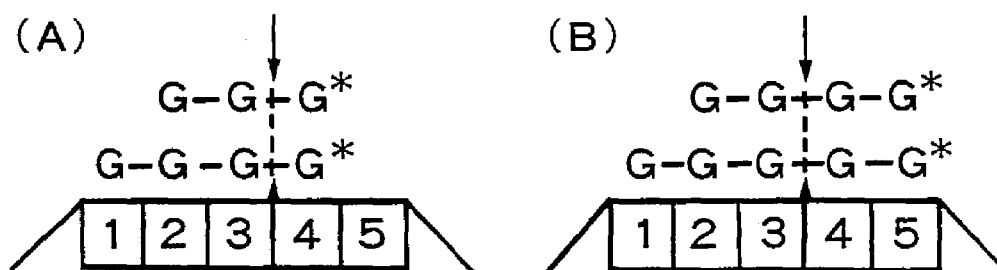

Fig. 3. Schematic binding mode of PPA and maltooligosaccharides (G_3, G_4 and G_5).

Table II. Kinetic parameters computed with eq. (2) by use of the values of Table I.

Cleavage positions of the maltooligosaccharides	k_1/K_m $(s^{-1} \cdot M^{-1})$	k_2/K_m $(s^{-1} \cdot M^{-1})$
G-G↓G*	2.6×10^4	1.8×10^3
G-G↓G-G*	3.1×10^5	2.2×10^4
G-G↓G-G*	6.2×10^4	1.9×10^5
G-G-G↓G-G*	7.8×10^5	2.1×10^6
G-G-G↓G-G-G*	5.4×10^5	1.5×10^6
G-G↓G-G-G-G*	2.6×10^5	7.0×10^5
G-G↓G-G-G-G*	8.1×10^3	2.2×10^4

SUMMARY

PPA displays an optimum at pH 6.9 for the majority of substrates. The optimum pH, however, shifted to 5.2 for the hydrolysis of some low molecular substrates (CHAPTER II). Details of the substrate-dependent shift of the optimum pH in PPA were studied by use of a series of maltooligosaccharides with ^{14}C-labeled reducing end glucose as substrates. The optimum pH for maltotriose was 5.2, whereas that for maltopentaose and maltohexaose was unchanged at pH 6.9. The pH profile for the intermediate size substrate maltotetraose showed abnormality; the apparent optimum pH was broadened between 5.5 and 6.5 and the bond cleavage pattern depended on pH, unlike that for the other substrates examined. These results were independent of either buffer systems or substrate concentration. Analyses of the hydrolysates of the maltooligosaccharides revealed that the shift of the optimum pH to the neutral region occurred only when the fifth subsite of PPA in the productive binding modes was occupied by a glucosyl residue of a substrate. The three-catalytic residue model of PPA deduced from the analysis of the hydrolysis of some modified maltooligosaccharides (p-nitrophenyl-α-D-maltoside, γ-cyclodextrin, maltopentaitol, and maltohexaitol) (CHAPTER II) was successfully adapted to the linear maltooligosaccharides used in this work. These results indicate that the different productive binding modes of the linear oligosaccharide substrates affect directly the catalytic power and the optimum pH of PPA.

REFERENCES

1) Buisson, G., Duee, E., Haser, R., and Payan, F., (1987) *EMBO J.*, **6**, 3909-3916.
2) Pazur, J. H.(1955) *J. Am. Chem. Soc.*, **7 7**, 1015-1017
3) Suganuma, T., Matsuno, R., Ohnishi, M., and Hiromi, K.,(1978) *J. Biochem.(Tokyo)*, **8 4**, 293-316, (Suganuma, T. (1978) Ph. D. Thesis, Kyoto University)
4) Dixon, M., Webb, E., Thorne, C. J. R., and Tipton, K. F.,(1979) *Enzymes* , Academic Press, New York San Francisco
5) Hiromi, K., Takahashi, Y., and Ono, S., (1963) *Bull. Chem. Soc. Jpn.* **3 6**, 563-569
6) Robyt, J. F., and French, D. (1970) *J. Biol. Chem.*, **4 5**, 3917-3927.
7) Prodanov, E., Seigner, C., and Marchis-Mouren, G., (1984) *Biochem. Biophys. Res. Commun.*, **1 2 2**, 75-81
8) Koshland, D. E., Jr. and Neet, K. E. (1968) *Ann. Rev. Biochem.*, **3 7**, 359-410
9) Thoma, J. A. (1968) *J. Theor. Biol.*, **1 9**, 297-310
10) Matsubara, S., Ikenaka, T. and Akabori, S. (1959) *J. Biochem. (Tokyo)*, **46**, 425-431
11) Matsuura, Y., Kusunoki, M., Harada, W., and Kakudo, M. (1984) *J. Biochem.(Tokyo)*, **9 5**, 697-702.
12) Pasero, L., Mazzei-Pierron, Y., Abadie, B., Chicheportiche,Y. and Marchis-Mouren, G. (1986) *Biochim. Biophys. Acta.*, **8 6 9**, 147-157.
13) Nishide, T, Emi, M., Nakamura, Y., and Matsubara, K (1986) *Gene*, **5 0**, 371-372
14) Svensson, B. (1988) *FEBS Lett.* **2 3 0**, 72-76

CHAPTER IV Substrate Recognition at the Binding Site of Mammalian Pancreatic α-Amylases

The main physiological function of the mammalian α-amylase is to produce fragments of oligosaccharides from starch for membrane digestion in small intestine (1). The optimum pH of PPA is 6.9 for starch, amylose and maltopentaoside, but is around 5.2 for maltopentaitol, γ-cyclodextrin and *p*-nitrophenyl maltoside in the presence of chloride ion (CHAPTER II). On the other hand, the optimum pH of α-amylases from microorganism are around 5.0 - 6.0 for whole types of substrates examined, in spite of the conserved amino acid sequence regions around active sites and substrate binding sites among these α-amylases (2). These differences are important in point of functional evolution of α-amylases, because characters or roles of catalytic residues might be modified or changed during biological evolution toward mammalian. From the analysis of the pH profile of the activity and rate parameters, it was revealed that the apparent catalytic residues of the α-amylase consists of at least 3 amino acid residues, and a binding at terminus of substrate binding site correlates with the catalytic activity and its optimum pH (CHAPTER II and III). This control of the optimum pH by the substrate binding site far from the catalytic residues may be a potential function of mammalian α-amylases. Optimum pH shift of the mammalian α-amylase may have biologically significant for starch digestion *in vivo* since the optimum pHs of hydrolytic enzymes for oligosaccharides working membrane digestion in small intestine are distributing from pH 5.5 to 7.0 (3).

For the clarification of the mechanism of the optimum pH shift in mammalian α-amylase, it is needed to reveal systematically the recognition pattern at the selected binding site. For this purpose, synthetic hetero-oligosaccharides (mimic to maltopentaose) with different reducing end residues were synthesized, and used for analysis of pH profiles and optimum pHs of PPA and HPA.

MATERIALS AND METHODS

Materials PPA is the same as that described in the previous chapter. The plasmid pAMPA2 which directed production and secretion of HPA under PHO5 promoter by yeast was provided from Dr. K. Shiozaki and Dr. K. Matsubara (4) of Institute for Molecular and Cellular Biology of Osaka University. *Saccharomyces cerevisiae* strains KK4 (MAT α , ura3, his3 trp1, leu2, gal80) (5), A2-1-1A (MATa, SUC2, CUP2, mal, leu2) (6) and KSC22-1C (MATa, ssl1, leu2, his3, ura3) (7) were used as recipient strains for transformation. The ssl1 is a recessive single gene mutation causing a supersecretion of lysozyme. α-Cyclodextrin (α-CD), maltopentaose (G_5), maltohexaose (G_6) and monosaccharides were purchased from Nacalai Tesque Ltd.

p-Nitrophenyl-α-D-maltopentaoside (G$_4$-φ) was from Calbiochem Co. Restriction enzymes were from Toyobo Co. (Osaka, Japan). MCI GEL column for HPLC was purchased from Mitsubishi Kasei Co., Ltd. (Tokyo, Japan). Enzyme-immunoassay kit for HPA (right assay "P-Amylase") was from Sankyo Junyaku Co., Ltd. (Tokyo, Japan) (8). Other chemicals were of commercial guaranteed or reagent grade.

Construction of recombinant plasmid which produces HPA in yeast. Construction of YEp-HPASIG and pESH-HPASIG plasmids, designed to express pre-HPA gene in yeast, from pAMPA2 is shown in Fig. 1. This plasmids were transformed into the yeast by the method of Kushner et al. (9) and Leu$^+$ transformants were selected.

The transformed yeast cells were cultured in synthetic media containing 0.67% Bacto yeast nitrogen base without amino acid, supplemented with an amino acid mixture (20-375μg/ml) lacking leucine (13), sodium phosphate buffer (pH 7.0, 0.1 M), CaCl$_2$ (0.1 mM) and glucose (4%) or galactose (4%) as a carbon source.

Purifications of HPA. HPA was purified from the yeast culture medium with the method of Matsuura et al. (14). The culture medium was centrifuged at 6,000 rpm. for 10 min to remove yeast, and solid ammonium sulfate was added to the supernatant to 0.25 saturation adjusting the pH 6.5 with a sodium hydroxide solution. To the solution was added a suspension of corn starch which had been heated at 70°C for 30 min in 15% ammonium sulfate solution, pH 7.8, and then cooled. The mixture was left at 4°C overnight gently stirring to adsorb HPA. At this condition, no further reaction proceeded. The precipitated HPA-starch complex was collected by centrifugation at 4°C. HPA adsorbed on the starch was liberated by digestion of starch with enzymatic hydrolysis, adding equal volumes of 0.02 M sodium chloride solution containing 0.01 M calcium acetate, pH 6.5, and incubating at 40°C for 1 h. The supernatant solution which contains liberated HPA was dialyzed against 20 mM Tris-HCl buffer (pH 8.3) containing 0.1 mM CaCl$_2$. The dialyzed solution was applied to a column of DE52 cellulose (Whatman) equilibrated with the same buffer. HPA was eluted with NaCl gradient (0-0.2 M) in the same buffer.

Synthesis of hetero-oligosaccharides with glucose analogue at the position of reducing end glucose of maltopentaose. Hetero-oligosaccharides with L-sorbose (S), D-xylose (X), 2-deoxy-D-glucose (D), sucrose (G-F), cellobiose (G β -G) and 1-O-methyl-D-glucose (G-M) at their reducing ends (Fig. 2) were synthesized from α-CD and the acceptors (S, X, D, G-F, G β -G and G-M) by transglycosylation reaction. 1g of α-CD, 1g of the acceptor and 300 THU (Tilden-Hudson Units) (15) of *Bacillus macerans* transglycosylase

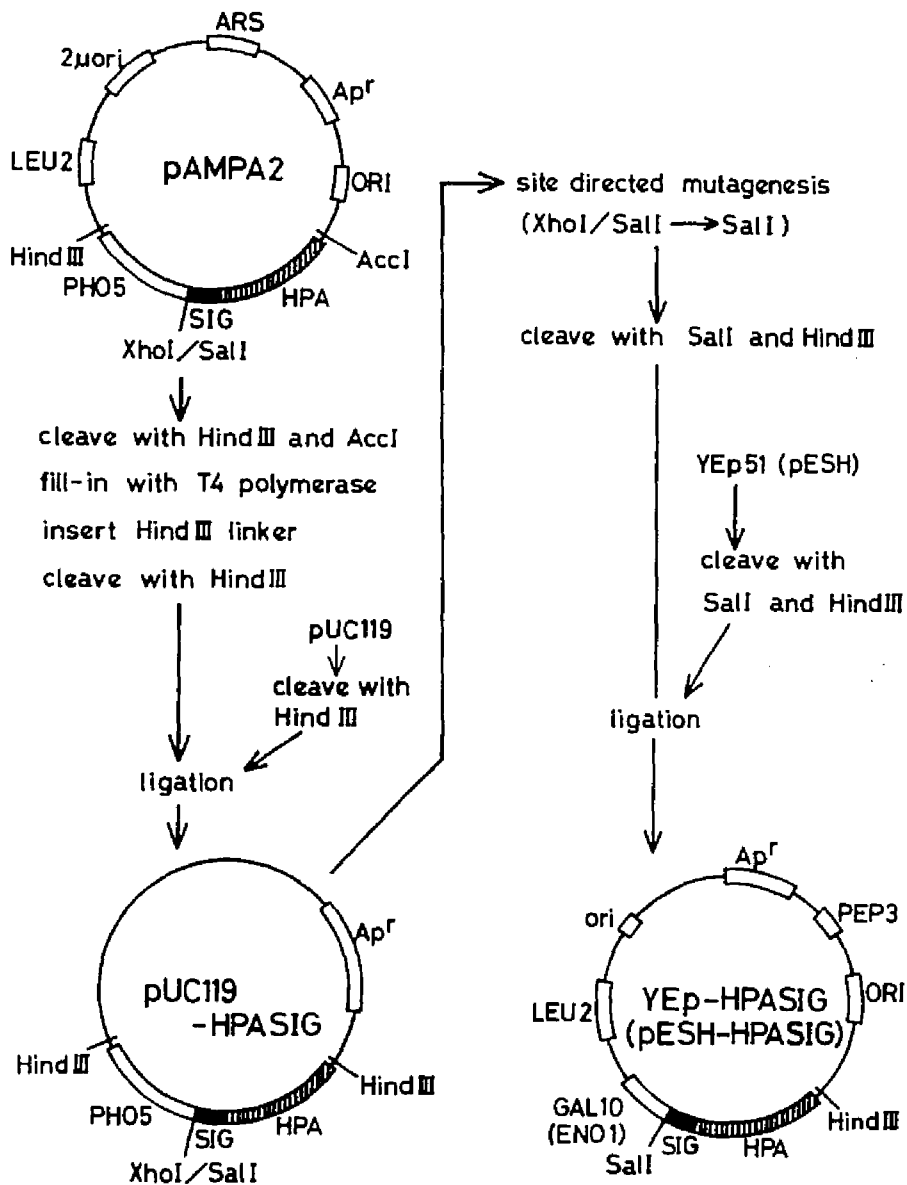(BME) were mixed to make a 100 ml reaction mixture and kept at 50° C and pH 6.0 for 17h.

Fig. 1. Construction of YEp-HPASIG and pESH-HPASIG. The 4.3 kb HindIII-AccI fragment carrying HPA structural gene (HPA), signal sequence (SIG) and PHO5 promoter (4) was isolated and filled in with T4 DNA polymerase. HindIII linker was inserted to the fragment and cleavaged with HindIII. The fragment was purified and cloned into HindIII segment of pUC119. The XhoI/SalI site was converted into SalI site using site-directed mutagenesis (10). The 1.8 kb SalI-HindIII fragment carrying HPA and SIG was cloned into *S. cerevisiae-E. coli* shuttle vector YEp51 (11) and pESH (12). The resultant plasmids, YEp-HPASIG and pESH-HPASIG, have GAL10 and ENO1 promoter, respectively.
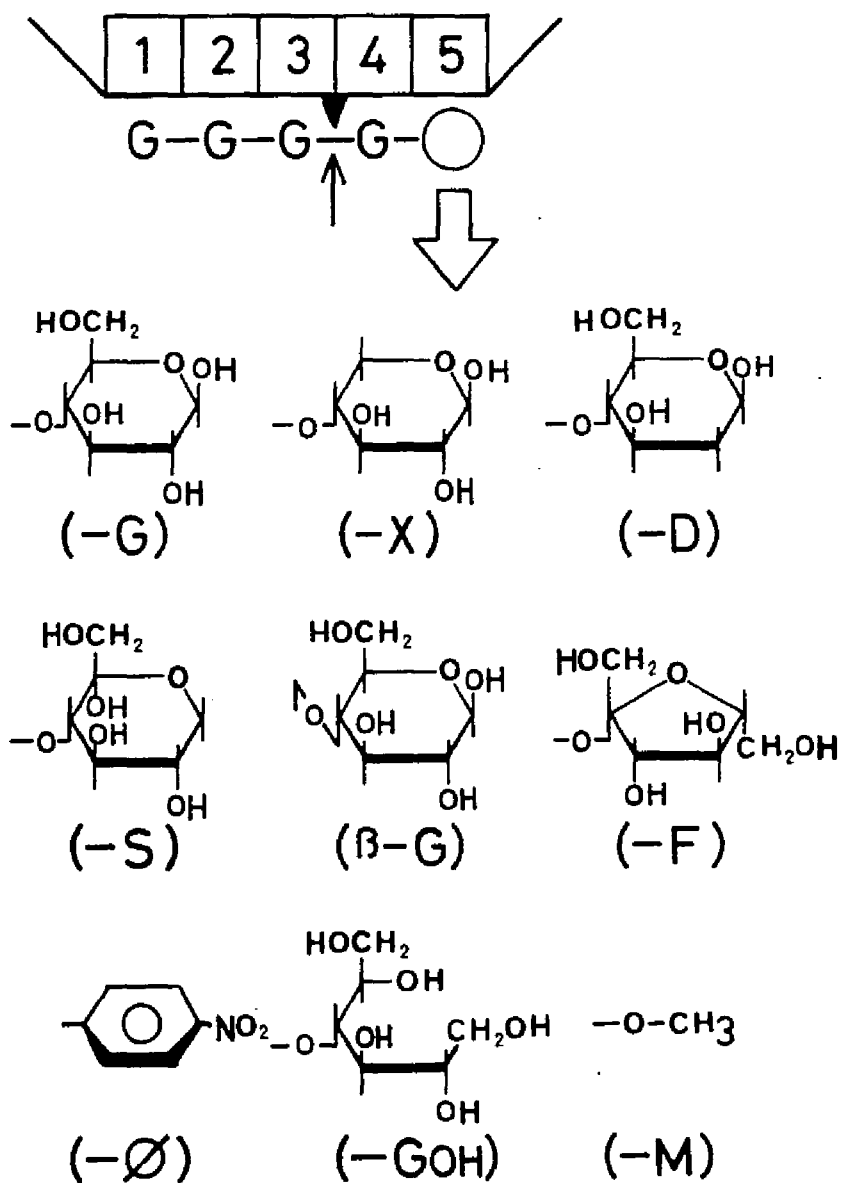
Fig. 2. Schematic representation of the active site of PPA and significant productive binding mode of hetero-oligosaccharides (upper figure) and structures of reducing end glucose analogues examined (lower figure). Subsites per glucose residue (G) of the substrate are numbered as 1 to 5 from the nonreducing end. The probable catalytic residues are located between subsite 3 and 4. The noticeable productive binding mode is show under the active site, where the reducing end glucose analogue O is located on subsite 5. Glucose and glucose analogues are D-glucose (G), D-xylose (X), 2-deoxy-D-glucose (D), L-sorbose (S), fructose (F), p-nitrophenol (φ) D-sorbitol (GOH), and methyl residue (M). The α- and β-glycosyl linkages are shown as - and β-.

- 52 -

Then the solution was put in a boiling bath for 10 min to inactivate BME, products was precipitated by adding acetone to 90%. The collected precipitate was dissolved with a small amount of distilled water, and remaining α-CD was removed as precipitate by adding tetrachloroethane (16). From the products mixture, malto-hetero-pentaoses and -tetraoses (Fig. 2) were separated and purified with HPLC equipped with MCI GEL column.

Maltopentaitol (G_5OH or G_4-GOH) and maltohexaitol (G_6OH) are that described in the previous chapter.

Enzyme assay and product analysis. The hydrolytic reactions of PPA and HPA for the synthetic malto-hetero-oligosaccharides were carried out at 30°C and the products were quantitatively analyzed by HPLC equipped with MCI GEL column at 65°C. The reaction was initiated by mixing aliquots of the enzyme solution with the substrate in 25 mM Tris-acetate buffer (pH 4.0 - 9.0) containing 30 mM NaCl and 0.1 mM $CaCl_2$, and terminated by adding the same volume of 1.0 N sodium hydroxide solution to the reaction mixture. The reductometry of the products was measured with the method of Dygert and Thoma (17). The molarity of PPA and HPA was determined from the absorbance at 280 nm on the basis of the same molecular weight of 55,000, $A^{1\%} = 24.0$ cm^{-1} (18) and 21.0 cm^{-1} (14), respectively.

RESULTS

Expression and purification of HPA

Plasmid pAMPA2 which have PHO5 promoter and signal sequence can secrete HPA (4). However, the amount of secreted HPA was not so large (Table I) and the induction method with low Pi (19) was tedious for large scale culture. Therefore, the author constructed two plasmids, YEp-HPASIG and pESH-HPASIG, which had strong promoters, GAL10 and ENO1, respectively, in addition to signal sequence derived from pAMPA2. Using some S. *cerevisiae* strains, these plasmids expressed a large amount of HPA in small scale cultures, compared with that for pAMPA2 (Table I). The plasmid YEp-HPASIG and strain KSC22-1C were selected for large scale production of HPA. After 5 days shaking culture (1 l) at 30°C, yeast was removed from the culture medium by centrifugation and HPA was purified with the modified method of Matsuura et al. (14), described in MATERIALS AND METHODS. From 1 l culture medium, about 1 mg of purified HPA was obtained. The purified HPA showed 58-61 kDa component in SDS-PAGE (Fig. 3). The difference in the molecular weight predicted from the amino acid sequence (55-kDa) was responsible for glycosylated protein, as indicated by Shiozaki et al. (4).

From the similarity of the primary structure of HPA to that of PPA (2), the author assumed that the active site structures of HPA is same as that of PPA. Purified HPA was stable in cold neutral buffer solution for at least a few months.

Table I. Secretion of HPA

Promoter	strain	secreted HPA (mg/l)
PHO5[a]	KK4	0.4
ENO1[b]	KK4	1.0
	A2-1-1A	1.5
	KSC22-1C	2.0
GAL10[c]	KK4	1.0
	KSC22-1C	2.5

The yeasts were grown in L-shaped test tube (10 ml) containing 5 ml of culture medium with shaking for 5 days at 30°C. The amount of secreted HPA was determined from the amylase activity of the culture medium using HPA purified from human pancreas (20) as an indication of the activity.

[a] Burkholder minimum medium was used for culture medium containing 4% glucose. Induction with low Pi medium was carried out with the method of Miyanohara et al. (19). pH of the medium was kept at around 7 with sodium hydroxide.

[b] Glucose (4%) was used as carbon source.

[c] Galactose (4%) was used as carbon source.
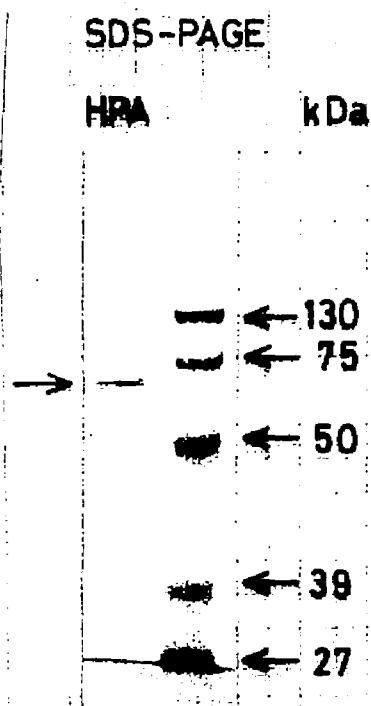
Fig. 3. SDS-PAGE of the purified HPA secreted by yeast. The purified HPA was electrophoresed in a SDS-PA gel (15% PA gels with 25 mM Tris-glycine buffer pH 8.3, containing 0.1% SDS) and made visible by Coomassie brilliant blue staining. The following molecular weight standards (Bio-Rad) were used; phospholylase b (130 kDa), bovine serum albumin (75 kDa), ovalbumin (50 kDa), carbonic anhydrase (39 kDa), soybean trypsin inhibitor (27 kDa), and lysozyme (17 kDa).

Synthesis of hetero-oligosaccharides

Hetero-pentaosides or -tetraosides, as shown in Fig. 2, were prepared in order to examine the recognition for glucose analogue at subsite 5. BME recognizes the C2-, C3- and C_4-OH of glucose as an acceptor for transglycosylation reaction (15). Therefore, the yield of the purified product from the acceptors, S, X, G-F, Gβ-G and G-M, was about 1% of the total products but that from D was less than 0.3%. About 20-10 mg of the purified oligosaccharides (purities > 95%) were obtained by two times chromatography with HPLC.

Bond cleavage pattern of the hetero-oligosaccharides

At first, bond cleavage patterns for a series of the hetero-oligosaccharides by PPA and HPA at pH 6.9 were examined in order to know the roles of the recognition at subsite 5. The bond cleavage pattern of a substrate means a distribution of the position and its normalized frequency to be cleavaged. The cleavage patterns determined by the HPLC analysis of the digestion products from initial actions of PPA and HPA, are shown in Fig. 4. The cleavaged site of G_5 has been shown to be only between second and third glucose units, by the analysis of ^{14}C labeled G_5 (CHAPTER III). For the hydrolysis of G_5, G_4-S, G_4-X and G_4-D, these amylases mainly hydrolyzed them at the same cleavage position. For G_5OH, G_4-F and G_4-ϕ, however, the main cleavage positions by PPA and HPA were different. These results suggest that the affinity of subsite 5 for G in HPA is a little stronger than that of PPA or that of subsite 1 is weaker than that of PPA, compared with that for GOH, F and ϕ at subsite 5. This difference reflects minor differences of active site structures. The bond cleavage pattern of G_4-M was the same as that of G_4 for PPA (CHAPTER III, 21) and HPA.

pH Profile of the activity and recognition for glucose analogues

In order to examine the influence of the glucose analogues at subsite 5, the author focused one cleavage pattern producing G_3 and disaccharides composed of glucose and a substance (glucose analogue) shown in Fig. 2, where glucose analogue is located on subsite 5 in a productive binding mode. pH Profiles of the hydrolytic activities at the selected one hydrolytic position (Fig. 2) for these substrates are shown in Fig. 5. HPA and PPA had similar pH profiles of the activities for these substrates. G_5 examined was the best substrate over other pentamer substrates. Their optimum pH's were dependent on the character of the substance at the reducing ends. Their optimum pH's for G_5OH and G_4-F were around 5.2, while for G_4-X, -S, -D, -ϕ, β-G and G_5 it was around 6.9 like that for soluble starch and amylose. These results show that both PPA and HPA hydrolyze above substrates essentially with the similar mechanism. Subsite 5 tends to recognize X, S, D, ϕ and β-G with the same manner as a glucose residue and kept the optimum pH at 6.9, but poorly recognizes F and

GOH. pH Profiles of the hydrolytic activities of HPA and PPA for G_4-M were the same as those for G_4. Therefore, the interaction between subsite 5 and methyl residue is negligible. For all substrates, the values of K_m were almost independent on pH examined. The values of K_m for G_4-X, -S, -2D, -F, -ϕ and β-G were around 1 mM.
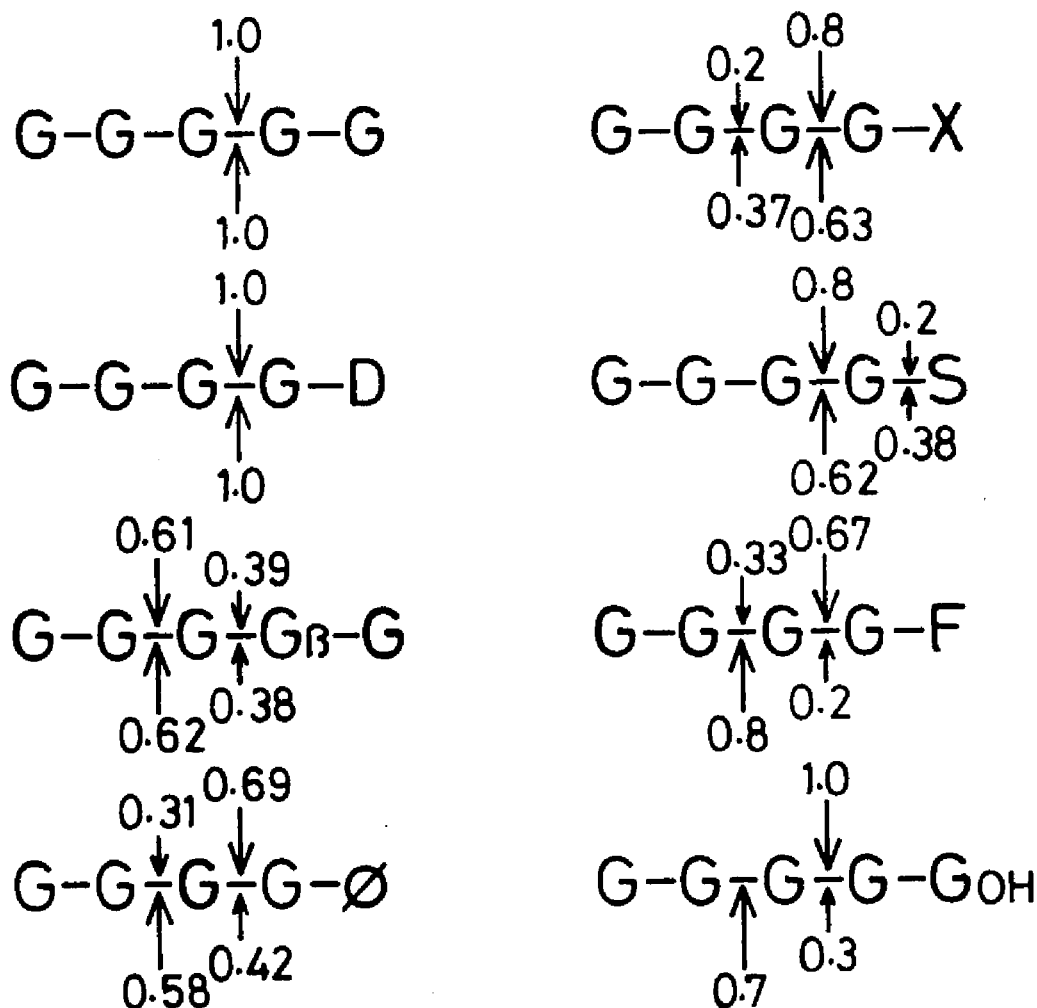
Fig. 4. The frequency distribution of bond cleavage during initial action of PPA (upper allows, ↓) and HPA (lower allows, ↑). The reaction was carried out at pH 6.9 and 30°C. The concentration of the hetero-oligosaccharides was 7 mM.
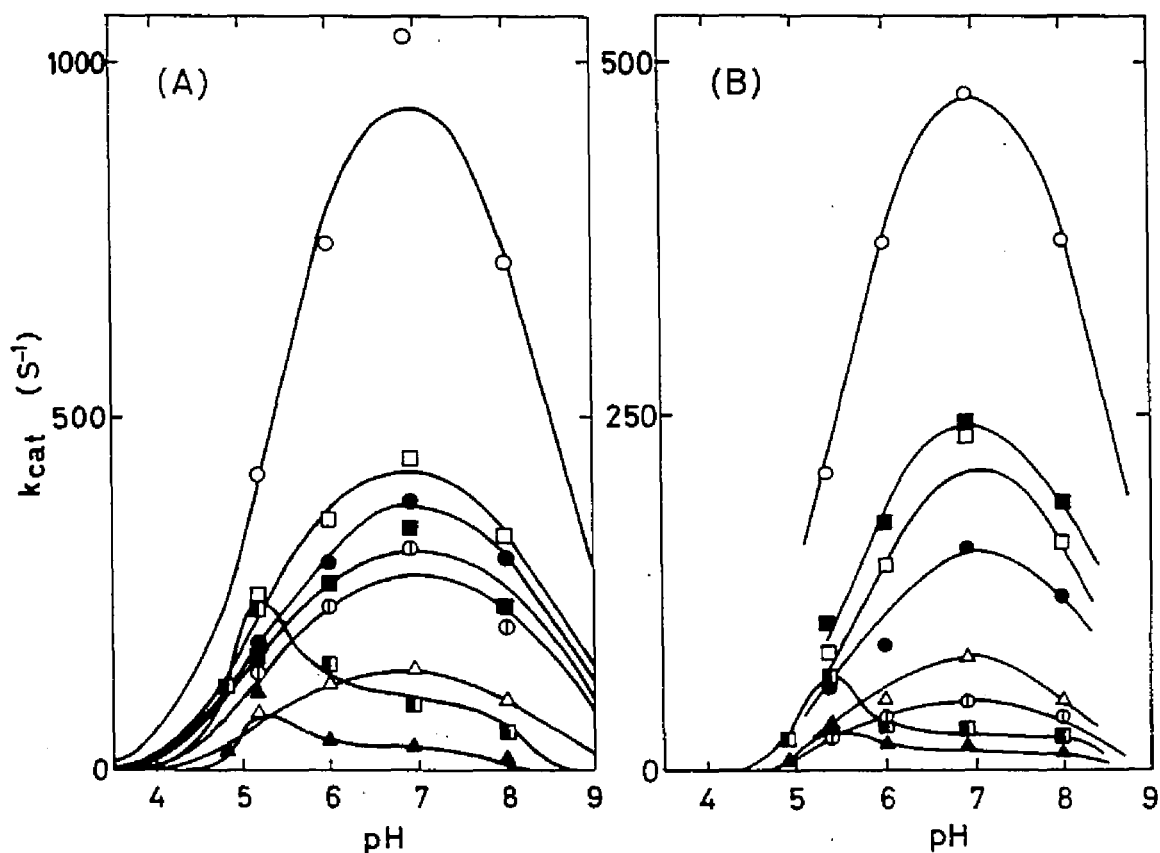
Fig. 5. pH Profiles of the cleavage activity for the hetero-oligosaccharides by PPA (A) and HPA (B). The values of k_{cat} were the those from the productive binding mode, as shown in Fig. 2.   The reaction was carried out at 30°C.   (○)G_5; (□)G_4-S; (●)G_4X; (■)G_4-D; (⏀)G_4-φ; (△)G_4β-G; (▣)G_4-GOH; (▲)G_4-F. Solid lines in (A) indicate theoretical lines calculated by using eq. (1) with the estimated parameters (Table II).   Solid lines in (B) are not the theoretical lines.

DISCUSSION

Analysis of pH Profile

        In our previous chapters, a three-catalytic residues model for the analysis of substrate dependent shift of optimum pH of PPA was proposed. Since the values of K_m for all substrates so far examined were independent of pH, the pH dependency of k_{cat} was deduced as follows (CHAPTER III),

$$k_{cat} = \frac{(k_1 \cdot K_1)/[H^+] + (k_2 \cdot K_1 \cdot K_2)/[H^+]^2}{1 + (K_1 + K_2)/[H^+] + (K_1 \cdot K_2)/[H^+]^2 + (K_1 \cdot K_2 \cdot K_3)/[H^+]^3} \qquad (1).$$

eq. (1) is applicable to all substrates using the same pK_{1-3} values (CHAPTER III). The values of k_1 and k_2 in eq. (1) which relate to the overall hydrolysis rate constant of the individual substrates were determined from the analysis of pH profiles by nonlinear least squares method, using pK_{1-3} values determined in the previous chapters. The results are listed in Table II. Theoretical curves using eq. (1) and values in Table II fit well with experimental data as shown in Fig. 5. In the case that the value of k_1 is smaller than that of k_2 the optimum pH is around 6.9 and in the reverse case the optimum pH is around 5.2. Thus the mechanism shown in the previous chapter is supported well with present systems.

It was found that approximately linear relationship between values of k_1 and k_2 for different substrates exists, as shown in Fig. 6, except those for maltopentaitol of which ring structure at the terminus is broken (Fig. 2). From a least-squares method, following linear relation was deduced

$$k_2 = a + b \cdot k_1 \quad (a = -168 \pm 139, \ b = 2.85 \pm 0.58) \qquad (2).$$

Since a<0, b>1, relative value of k_2 to k_1 turns over at $k_1 = -a/b = 58.9$. When $k_2 > k_1$, optimum pH is around 6.9, and when $k_2 < k_1$, the optimum pH is around 5.2. At the condition, $k_2=0$ and $k_1=58.9$, only two catalytic residues contributes to the pH profile, like mold α-amylase (22). Deviation toward the low activity from eq. (2) on G_5OH is due to the lack of a ring structure at the terminus. Therefore, six or five members sugar-like ring structures are fundamental prerequisite for the effective catalysis through structure recognition at subsite 5. The mechanism of substrate recognition for GOH (lack of a ring structure) might be slightly different from that for the ring structures (K_m for G_5OH is 0.2 mM (CHAPTER II), compared to 1mM for other ring structure substrates). These correlation between the catalytic site and the part of binding site for the effective catalytic action may be regarded as an example of induced-fit mechanism (23). As a result, the optimum pH of PPA is controlled by the interaction at subsite 5 in enzyme-substrate complex.

Comparison of PPA and HPA

Using GAL10 promoter and *S. cerevisiae* strain KSC22-1C (supersecretion mutant; containing ss11 mutation which shows a supersecretion of human lysozyme and causes a missorting of vacuolar protein, carboxypeptidase, into the cell surface) (7), over 2 - 2.5 mg of

Table II. Kinetic parameters computed from the pH profiles of PPA

Reducing end of the substrate	k_1 (s^{-1})	k_2 (s^{-1})
G	342 ± 115	985 ± 84
S	293 ± 46	431 ± 18
X	175 ± 34	387 ± 13
D	187 ± 65	325 ± 26
ϕ	142 ± 66	296 ± 26
β-G	107 ± 12	141 ± 5
GOH	490 ± 37	98 ± 3.8
F	75 ± 8.1	33 ± 5.8

The values of k_1 and k_2 in Equation 1 were determined from the pH profile plots by the nonlinear least squares method using the fixed pK_{1-3} values (pK_1=4.78, pK_2=5.54, pK_3=8.62) from CHAPTER III.
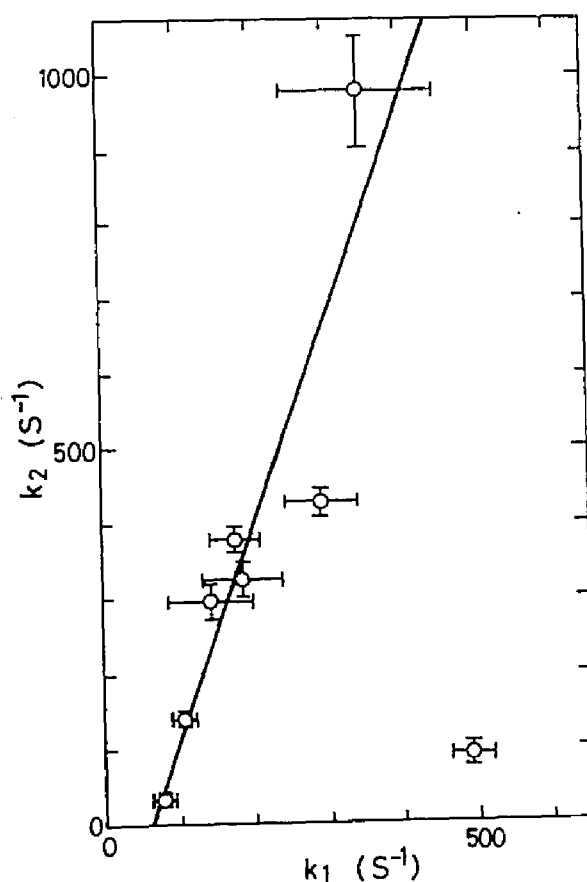
Fig. 6 Relationship between k_1 and k_2 in eq. (1) of PPA. The solid line is the theoretical line using eq. (2).

- 59 -

HPA per 1 l culture medium was obtained, as well as in the case of lysozyme (24). From the result of SDS PAGE (Fig. 3) and two potential site for N-glycosylation of HPA (25, 26), HPA produced from yeast was glycosylated protein (high mannose type) somewhat different from HPA purified from human pancreas juice. However, its activity for G_5 was same as that of HPA purified from human pancreas (20) and wild-type and mutant HPAs specifically cross-reacted with HPA-antibody (8) used in clinical analysis of human serum α-amylase. Therefore, these HPA produced by yeast are regarded as HPA from human pancreas, at least, as far as the functions which hydrolyze maltooligosaccharide substrates. Overall amino acid sequence of HPA has 83% homology with PPA, and amino acid residues at the active site are almost completely corresponding each other (2). The pH profiles of HPA for the synthetic substrates are also similar to those of PPA. Therefore, the recognition mechanism of HPA is thought to be identical to that of PPA and results based on mutant HPA's can be applied for the analysis of the catalytic mechanism of both PPA and HPA.

Structure recognition at subsite 5

The activity of the mammalian α-amylase varies with the interaction at subsite 5 for the reducing end of the pentamer substrate composed of maltotetraose and additional residues. Cleave and pH profile patterns of G_4-M were same as those of G_4, since the methyl residue bound at subsite 5 is not recognized as a part of a substrate. In the intermediate structures (G_4-X, -S, -2D, β-G, -ϕ, -F and -GOH) of the substrates between G_5 and G_4-M , the interaction at subsite 5 correlates with catalytic functions at the active center. Subsite 5 can recognize the whole shape of the molecule and the optimum pH shifts gradually according to eqs. (1) and (2). Fig. 7 shows ball and stick models of glucose, PNP, GOH and F. Since rate parameters of G_4-ϕ is close to those of G_5 than those of G_4-F and G_5OH, flat-6-members-ring structures such as benzene and glucose analogues are favorite with the interactions at subsite 5 rather than compact structure of fructose or flexible sorbitol chain. For realization of optimum pH around pH 6.9 with high activity, steric adaptability and additional hydrogen bonds between the glucosyl residue and amino acid residues composing subsite 5 are fundamentally needed (22). Catalytic function and binding mode at each subsite are correlating ingeniously and skillfully in α-amylase-substrate complexes. The fundamental factor for the recognition is a flat-6-members-ring structure.

The very close sequence homologies among porcine, human and rat α-amylases (2) suggest that these mammalian α-amylases possess, in general, the same recognition and control mechanism. These functional characteristics of mammalian α-amylases must have physiological meanings and may be important for digestion of some artificially modified oligosaccharides in foodstuff (27) in small intestine.
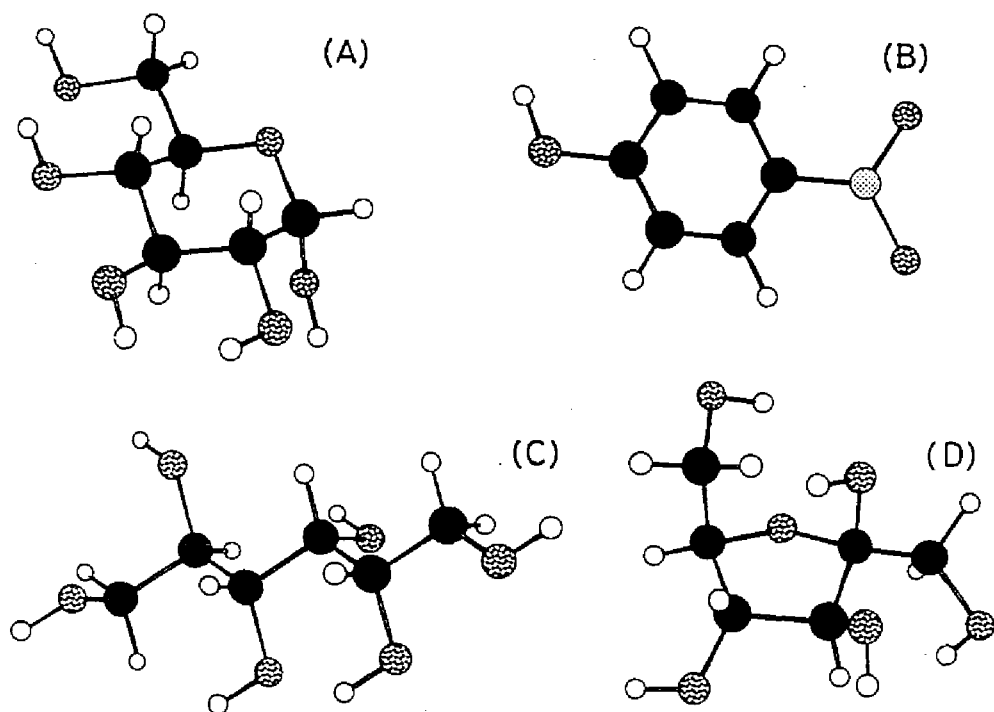
Fig. 7. Ball and stick models of G (A), PNP or φ (B), GOH (C) and F (D).

SUMMARY

The optimum pH of PPA and HPA, as described previously, shifts from neutrality to acidity when a substrate is too small to occupy a substrate recognition site, the subsite 5. It is very interesting that substrate recognition at the subsite 5 rather remote from the catalytic site changes the optimum pH of the enzyme. Thus the author studied the substrate recognition mechanism of the enzymes by using the following synthetic substrates; maltopentaose (G_5) and its analogs 4-O-α-maltotetraosyl-D-xylose (G_4-X), 4-O-α-maltotetraosyl-2-deoxy-D-glucose (G_4-D), 3-O-α-maltotetraosyl-L-sorbose (G_4-S), 4-O-β-maltotetraosyl-D-glucose (G_4β-G), α-maltotetraosyl-β-D-fructose (G_4-F), α-maltotetraosyl-p-nitrophenol (G-φ), and maltopentaitol

(G_4-GOH), whose reducing end residue relevant to the subsite 5 are α-D-xyloside (-X), α-2-deoxy-D-glycoside (-D), α-L-sorboside (-S), β-D-glycoside (β-G), α-D-fructoside (-F) and α-D-sorbitorate (-GOH), respectively. The optimum pH for the substrates G_5, G_4-X, G_4-D, G_4-S, G_4β-G and G_4-d was neutral and that for G_4-OH and G_4-F was acidic. The results indicate that only six-membered ring residues including a phenyl group are recognizable by the subsite 5 and steric compatibility at the subsite 5 with the substrates is important for the enzyme activity showing a neutral pH optimum.

A point-mutated HPA, H201N, in which the histidine at position 201 is replaced by asparagine, was prepared and the catalytic activity for the synthetic substrates was examined, since the histidine residue is located around the subsite 5 and suggested by the chemical modification study to be important for the substrate recognition. The mutant H201N was turned out to exhibit only acidic optimum pH for all the substrates; the subsite 5 of the mutant enzyme recognized none of their reducing end residues. This means that interaction between the histidine at position 201 and the substrate is essential for the amylase activity to be optimal at neutral pH region, in addition to the steric fitness. Furthermore, regulation of the catalytic power and the optimum pH through the substrate recognition at the subsite 5 was qualitatively explained by the stabilization effect of a peptide loop containing the histidine at position 201 at the active site.

REFERENCES

1) Fischer, E. H. and Stein, E. A. (1960) *The Enzymes*, 2nd ed. Academic Press, New York, 4, 313-343.
2) Svensson, B. (1988) *FEBS Lett.*, **230**, 72-76.
3) Newcomer, A. D. and McGill, D. B. (1966) *Gastroenterology*, **51**, 481-488.
4) Shiozaki, K., Tanaka, K., Omichi, K., Tomita, N., Horii, A., Ogawa. M., and Matsubara, K.(1990) *Gene*, **89**, 253-258.
5) Nogi, Y., Shimada, H., Matsuzaki, Y., Hashimoto, H., and Fukasawa, T. (1984) *Mol. Gen. Genet..*, **195**, 29-34.
6) Jigami, Y. Toshimitsu, N., Fujisawa, H., Uemura, H., Tanaka, H., and Nakasato, S. (1986) *J. Biochem.. (Tokyo)*, **99**, 1111-1125.
7) Suzuki, K., Ichikawa, K., and Jigami, Y. (1989) *Mol. Gen.Genet.*, **219**, 58-64.
8) Fujisawa, T., Otsuki, M., Okabayashi, Y., Nakamura, T., Fujii, M., Tani, S., Koide, M., Hasegawa, H., and Baba, S., (1989) *Suizo* (Japanese) 4, 31-37.
9) Kushner, S. R.(1978) *"Genetic Engineering"* ed. by Boyer, H. W., and Niscosia, S., Elsevier, 17
10) Morinaga, Y., Franceschini, T., Inouye, S., and Inouye, M. (1984) *BIO/TECHNOLOGY*, **2**, 636-639.
11) Broach. J. R., Li, Y.-Y., Wu, L.-C. Chen, and Jayaram, M. (1983) *"Experimental Manipulation of Gene Expression"*. Academic Press. New York, 82-117.
12) Ichikawa, K., Nakahara, T., Uemura, H., and Jigami, Y. (1989) *Agric. Biol. Chem. (Tokyo)*, **53**, 1445-1447.
13) Sherman, F., Fink, G. R., and Hicks, J. B.(1982) *"Methods in Yeast Genetics"* A Laboratory Manual, Cold Spring Harbor Laboratory, Cold Spring Harbor, New York, 61- 62.
14) Mastuura, K., Ogawa, M., Kosaki, G., Minamiura, N., and Yamamoto, T.(1978) *J. Biochem. (Tokyo)* , **83**, 329-332.
15) Kitahata, S., Okada, S., and Fukui, T.(1978) *Agric. Biol. Chem. (Tokyo)*, **42**, 2369-2374.
16) French, D., Levine, M. L., Pazur, J. H., and Norberg, E. (1949) *J. Am. Chem. Soc.*, **71**, 353-356.
17) Dygert, S., Li, L.H., and Thoma, J.A. (1965) *Anal. Biochem.*, **13**, 367-374.
18) Elodi, P., Mora, S., and Kryzteva, M., (1972) *Eur. J. Biochem.* **24**, 577-582.
19) Miyanohara, A., Tho-e, A., Nozaki, C., Hamada, F., Ohtomo, N., and Matsubara, K.(1983) *Proc. Natl. Acad. Sci. USA*, **80** 1-5.
20) Kondo, H., Nakatani, H., and Hiromi, K.(1990) *Carbohydr. Res.*, **204**, 207-213.
21) Robyt, J. F., and French, D. (1970) *J. Biol. Chem.*, **45**, 3917-3927.
22) Matsuura, Y., Kusunoki, M., Harada, W., and Kakudo, M. (1984) *J. Biochem.(Tokyo)*, **95**, 697-702.
23) Koshland, D. E., Jr. and Neet, K. E. (1968) *Ann. Rev. Biochem.*, **37**, 359-410.
24) Ichikawa, K., Komiya, K., Suzuki, K., Nakahara,T., and Jigami, Y.(1989) *Agric. Biol . Chem. (Tokyo)*, **53**, 2687-269.
25) Nishide, T., Emi, M., Nakamura, Y., and Matsubara, K.(1986) *Gene*, **50**, 371-372
26) Sato, T., Tsunasawa, S., Nakamura, Y., Emi, M., Sakiyama, F., and Matsubara, K.(1986) *Gene*, **50**, 247-257.
27) Yoshizawa, S., Moriuch, S., and Hosoya, N. (1975) *J. Nutr.Sci. Vitaminol*, **21**, 31-37.

CHAPTER V   Roles of Histidine Residues in Human Pancreatic α-Amylase

Catalytic residues of mammalian α-amylases were regarded to be two carboxyl residues which are identical with those of TAA (1 - 4). There are many functional differences, however, between PPA and TAA in optimum pH (5, 6), regulation with an activator (6-8) and a proteinaceous inhibitor (9), and effects of chemical modifications (10, 11, CHAPTER I) etc.. These differences may be related to physiological significance of mammalian α-amylases for the catalytic action in small intestine. It is expected that functional characteristics of mammalian α-amylases must be reflected in the roles of particular amino acid residues, since X-ray crystallographical studies show that the active site structures of PPA and TAA resemble each other.

The author targeted histidine residues in α-amylases because the activity and specificity of PPA are controlled sensitively by the chemical modification of histidine residues (11, CHAPTER I). There are three histidine residues (101, 201, 299) in the active site of mammalian α-amylases, according to the information on the three-dimensional structure of PPA and the sequence homology among mammalian α-amylases (1, 2). The structural gene of HPA has been obtained (12) and HPA is able to be produced using yeast (CHAPTER IV). From the sequence homology (83%) of PPA and HPA (1) functional characters of HPA must be identical to those of PPA. In this chapter, three mutant HPAs of which each histidine residue (101, 201, 299) was converted to asparagine residue were synthesized and the functional roles of the histidine residues were examined.

MATERIALS AND METHODS

Materials. HPA and the plasmid (YEp-HPASIG) containing the GAL10 promoter, the HPA structural gene, and the signal sequence is the same as that described in CHAPTER IV. G_6OH is the same as that described in CHAPTER II. G_2-PNP was purchased from Calbiochem corp. AF-Epoxy TOYOPEARL 650M was purchased from Toyo Soda Mfg. Co., Ltd.

Construction and purification of mutant HPAs. Mutant HPA genes were constructed in M13mp19 vector by site-directed mutagenesis using the method of Kunkel (13). The sequence of the mutant gene was checked by dideoxy sequencing (14) throughout the entire coding region. Three mutant HPAs (H101N, H201N and H299N) of which each histidine residue (101, 201 and 299) was converted to asparagine residue were prepared, respectively. Production of the mutant HPAs was carried out with the same method described in CHAPTER IV. After the removal of the yeast from culture medium with centrifugation, mutant HPAs

were precipitated with 0.75 saturation of ammonium sulfate. The precipitates were dissolved with phosphate buffer (pH 6.9, 20 mM) containing 0.1 mM $CaCl_2$ and purified with α-CD affinity chromatography (AF-Epoxy TOYOPEARL 650M). Enzyme assay and assay condition are the same as that described in the previous chapter.

RESULTS

Hydrolytic activity of mutant HPAs

About 1 mg of purified mutant HPAs were obtained from 1L culture medium. The purified mutant HPA's showed 58-61 kDa component in SDS-PAGE which is identical to that of wild-type HPA. The difference in the molecular weight predicted from the amino acid sequence (55-kDa) was responsible for glycosylated protein, as indicated by Shiozaki et al. (12). These mutant HPAs specifically cross-reacted with HPA-antibody used in clinical analysis of human serum α-amylase (15). These mutant were stable in cold neutral buffer solution for at least a few months.

Amylase activity of mutant HPAs was measured with G_6OH as a substrate. The hydrolytic position of G_6OH by wild-type HPA and mutant HPAs was the same as that by PPA (CHAPTER II). The kinetic parameters obtained are shown in Table I. Increase of K_m value and slight decrease of k_{cat} value of H201N HPA reflect the fact that His201 locates at the substrate binding site relatively far from the catalytic site (2). The values of k_{cat} were decreased extensively by change of His101 and His299. Remarkable decrease of k_{cat} value of H101N HPA is significant for the catalytic mechanism because it locates at the catalytic site (2). Maltosidase activity of H101N, H201N, and H299N showed 1, 1120, and 3% of the wild-type activity, respectively.

The optimum pH of the wild-type HPA is 6.9 for amylase activity and 5.2 for maltosidase activity (CHAPTER II). Fig. 1 shows the pH profiles of amylase and maltosidase activities for wild-type and mutant HPAs. The optimum pH for the amylase activity of H201N HPA was changed to 5.2 from 6.9, whereas those of the others stayed around neutral pH. As for maltosidase, H201N HPA stayed 5.2 but H101N and H299N were shifted to 6.9. Then the author examined the pH profiles of H201N HPA for the synthesized substrates, described in CHAPTER IV, on the same cleavage pattern as in Fig. 5 (CHAPTER IV), and found that its optimum pH is independent of the substrate being acidic for all substrates examined as seen in Fig. 2. The pH profiles of H101N and H299N HPAs for the synthesized substrates were not observed successfully since their amylase activities were so small that their transglycosylation activities could not be ignored.

Table I. Kinetic parameters of wild-type and mutant HPAs for amylase activity.

	wild-type	H101N	H201N	H299N
Amy.				
k_{cat} (s^{-1})	410 ± 24	3.28 ± 0.10	107 ± 6.7	12.5 ± 0.63
K_m (mM)	0.85 ± 0.15	0.42 ± 0.05	2.75 ± 0.32	0.83 ± 0.13
Mal.				
k_{cat} (s^{-1})x10^3	40.0 ± 6.8	0.651 ± 0.100	448 ± 66	1.24 ± 0.15
K_m (mM)	4.2 ± 1.2	3.4 ± 0.5	15.1 ± 2.4	5.0 ± 0.8

Amylase (Amy.) and maltosidase (Mal.) activities were measured in the buffers (20 mM sodium phosphate, pH 6.9) containing 30 mM NaCl at 30°C with reductometry using maltohexaitol and absorbance of released PNP at 400 nm using G_2-PNP as a substrate, respectively.
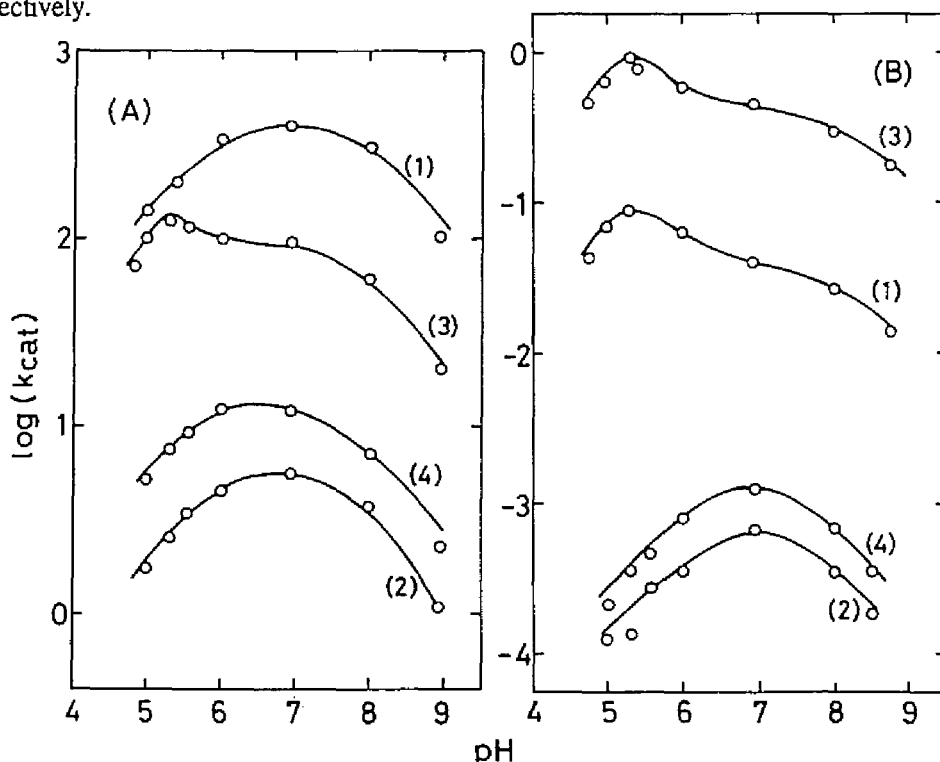
Fig. 1 pH Profiles of amylase (A) and maltosidase (B) activities for wild-type HPA (1) and HPA mutants (H101N (2), H201N (3), H299N (4)). Amylase activity was measured in the buffers (20 mM sodium acetate buffer (pH 4-5.7), 20 mM sodium phosphate buffer (pH 6-8), and 20 mM sodium borate buffer (pH 8.5-9)) containing 30 mM NaCl at 30°C with reductometry using maltohexaitol (G-G-GG-G-GOH) as a substrate. The reaction for amylase activity is; G-G-G-G-G-GOH → G-G-G + G-G-GOH, where G is a glucose and -GOH is a sorbitol bound to the reducing end of maltooligosaccharides. Maltosidase activity was measured under the same conditions as that of amylase activity with a spectrophotometrical method using p-nitrophenyl α-D-maltoside (G-G-PNP) as a substrate. The reaction is G-G-PNP → G-G + PNP where -PNP is a p-nitrophenol bound to the reducing end of maltose.
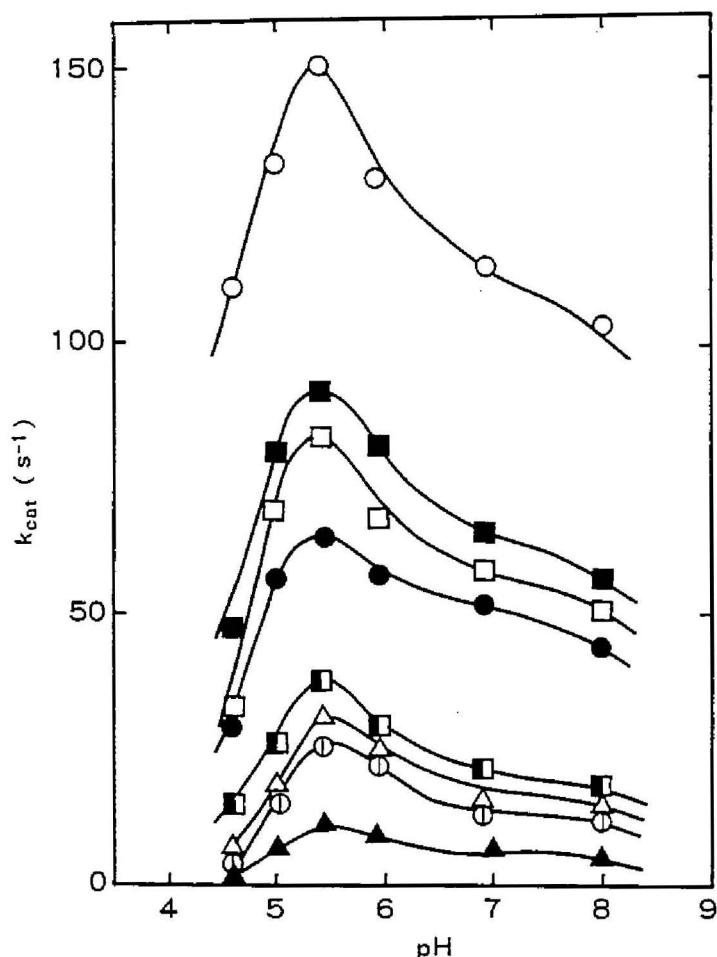
Fig. 2. pH profiles of cleavage activity of H201N HPA for the hetero-oligosaccharides. The values of kcat were based on the reaction from the productive binding mode where the substrate's terminal analog is located on the subsite 5, as shown in Fig. 5 (CHAPTER IV). The reaction was carried out at 30°C.
($\bigcirc$)G_5; ($\square$)G_4-S; ($\bullet$)G_4X; ($\blacksquare$)G_4-D; ($\oplus$)G_4-ϕ; ($\triangle$)$G_4\beta$-G;　($\blacksquare$)G_4-GOH; ($\blacktriangle$)G_4-F.

Inhibition by the proteinaceous inhibitor

Further, detailed characters of the H201N PPA were investigated, since pronounced increase of maltosidase activity was observed in this mutant only. A proteinaceous α-amylase inhibitor, phaseolamin from white kidney bean (*Phaseolus vulgaris*) inhibits mammalian α-amylases specifically (9). Both amylase and maltosidase activities of the wild-type HPA are completely inhibited by the inhibitor (Table II). In the case of H201N HPA, however, the enzyme-inhibitor complex still has both residual amylase and maltosidase activities (4% and 15% of H201N, respectively) as shown in Table II.

Effect by the activator

Mammalian α-amylases are activated by chloride ion (Cl⁻). The binding site is near the active site cleft (2, 3), and the dissociation constant is below 1 mM (7). Amylase and

maltosidase activities of the wild-type HPA were activated 44- and 3.2-fold by Cl⁻, respectively. This activation ratio was changed in H201N; 23-fold for amylase and 6.8-fold for maltosidase activities (Table II). The amplitude of activation by Cl⁻ decreased for amylase activity (52% of the wild-type HPA) and increase for maltosidase activity (210% of the wild-type HPA).

Table II. Functional change of HPAs

	wild-type	modified	H201N	modified H201N
Amy.				
k_{cat} (s⁻¹) (%)	410(100%)	6.6(1.6%)	107(26%)	12.2(3.0)
K_m (mM)	0.87 ± 0.15	-	2.75 ± 0.32	-
Mal.				
k_{cat} (s⁻¹) (%)	0.040(100%)	0.260(373%)	0.448(1120%)	0.233(582%)
K_m (mM)	4.2 ± 1.18	-	15.1 ± 2.4	-
Residual activity of E-I complex[a]				
Amy.				
k_{cat}(s⁻¹)(%)	0(0%)	0(0%)	4.26(4%)	3.75(31%)
Mal.				
k_{cat}(s⁻¹)(%)	0(0%)	0.247(95%)	0.0671(15%)	0.0820(35%)
Optimum pH[b]				
Amy	6.9	6.0	5.2	5.2
Malt.	5.2	5.2	5.2	5.2
Activation by Cl[c]				
Amy.	44 -fold	-	23 -fold	-
Mal.	3.2-fold	-	6.8-fold	-

Amylase activity (Amy.) was measured at pH 6.9 (20 mM sodium phosphate buffer containing 30 mM NaCl) with reductometry using maltohexaitol as a substrate. Maltosidase activity (Mal.) was measured in the same sodium phosphate buffer with a spectrophotometrical method using p-nitrophenyl α-D-maltoside as a substrate.

[a] Enzyme-inhibitor (E-I) complexes were formed at pH 6.5 and 25° C for 5 h. Complete formations of E-I complexes were confirmed changing excess inhibitor concentration.
[b] Determined from pH profiles (Fig. 1).
[c] Each ratio was determined at pH 6.9 comparing k_{cat} values in 20 mM sodium phosphate buffer in the absence or presence (30 mM) of NaCl.

Chemical modification of histidine residue

Increase of maltosidase activity and decrease of amylase activity has been observed by chemical modification of histidine residues of PPA and TAA with diethyl pyrocarbonate (DEP) (10, 11, CHAPTER I). The author confirmed that the maltosidase activity of the wild-type

HPA was increased by the chemical modification of histidine residues with DEP. The result was similar to that of PPA. However, maltosidase activity of the mutant enzyme, H201N HPA, was rather decreased to 50% with the chemical modification by DEP (Table II).

DISCUSSION

The drastic shift of optimum pH from 6.9 to 5.2 for amylase activity by conversion of His201 indicates that His201 which is located about 5 Å far from the catalytic center plays an important role for controlling optimum pH of HPA. So far, slight optimum pH shifts have been observed mainly when the pK values of the catalytic residues are affected by neighbor charged residues (16 - 18). In the case of PPA and HPA, optimum pH is able to be changed by the substrate recognition of subsite 5 without change of the pK values. Therefore, His201 of HPA is one of the important residues which recognizes the substrate at subsite 5 and contributes to the control of the optimum pH at pH 6.9. Furthermore, the subsite 5 of mammalian α–amylase recognizes the substrates not only by the fitness of its size and shape (CHAPTER IV) but also by the interaction with His201. The interaction might be attributable to the van der Waals force between the imidazole ring of His201 and the terminal residues of the substrates. Similar interaction was observed in the case of lysozyme (19). Since both His101 and His299 are located near the catalytic center of PPA, they may be related to the catalytic mechanism directly or indirectly in spite of weak residual activities (20, 21). From the data for the increase of maltosidase activity by the conversion of His201 and the chemical modification of wild type HPA and H201N HPA, it is shown that His201 in all the modifiable histidine residues solely contributes to the increase in maltosidase activity of the wild-type HPA. Both amylase and maltosidase activities of wild-type HPA were inhibited by the inhibitor (phaseolamin) completely. However, both activities of H201N HPA were not inhibited completely and only amylase activity of mod-HPA was inhibited completely by the inhibitor, as in the case of PPA (11). These results show that His201 of HPA is essential for complete inhibition by the inhibitor and the inhibition mechanism for mod-HPA by the inhibitor is different from that for H201N HPA. Furthermore, His201 is related to the activation by Cl⁻ which is unique to mammalian α-amylases, although it locates far from the binding site of Cl⁻ (2, 3). Since Cl⁻ binds Arg195 (one of the Cl⁻ binding residues), the loop containing Arg195, Asp197 (one of probable catalytic residues), and His201 must be locally stabilized by Cl⁻ for the formation of the active conformation (2). It is speculated that configuration of Asn201 in H201N is arranged with the binding of Cl⁻ at Arg195. His201 of HPA plays important multi-functional roles in the catalytic activity and regulation of HPA; control of optimum pH, conversion of the substrate specificities, change in the inhibition mode of a proteinaceous inhibitor, and modulation

of activator effect by Cl⁻. The above roles of His201 should be peculiar not only to HPA but also to whole mammalian α-amylases due to close sequence homology among them. In general, histidine residue may play important roles multi-functionally when it is located at the suitable position in the active site of an enzyme owing to the unique characters of the imidazole group in its structure. In the case of α-amylase, histidine residues (101, 201, and 299) are conserved from microorganism to mammal. Therefore, it is reasonable to speculate that in the course of evolution, His201 has acquired unique multi-functional roles which are significant physiologically for the control of starch digestion in small intestine of mammal.

SUMMARY

Functional roles of histidine residues at the active site in HPA were examined by protein engineering. Three histidine residues at 101, 201, and 299 were converted to asparagine residues, respectively. It was found that His201 played multi-functional roles concerning so many functions; substrate binding, control of optimum pH, change in substrate specificity, activation by chloride ion, and inhibition by a proteinaceous inhibitor.

REFERENCES

1) Svensson, B. (1988) *FEBS Lett.*, **230**, 72-76 (1988)
2) Buisson, G., Duee, E., Haser, R., and Payan, F. (1987) *EMBO J.*, **6**, 3909-3916
3) Buisson, G., Duee, E., Payan, F., and Haser, R. (1987) *Food Hydrocolloids*, **1**, 399-406
4) Matsuura, Y., Kusunoki, M., Harada, W., and Kakudo, M. (1984) *J. Biochem. (Tokyo)*, **95**, 697-702
5) Matsubara, S., Ikenaka, T., and Akabori, S. (1959) *J. Biochem. (Tokyo)*, **46**, 425-431
6) Wakim, J., Robinson, M., and Thoma, J.A. (1969) *Carbohydr. Res.*, **10**, 487-503
7) Levitzuki, A. and Steer, M.L. (1974) *Eur. J. Biochem.*, **41**, 171-180
8) Yamashita, H., Nakatani, H., and Tonomura, B. (1991) *J. Biochem. (Tokyo)*, **110**, 605-607
9) Marshall, J.J. and Lauda, C.M. (1975) *J. Biol. Chem.*, **250**, 8030-8037
10) Kita, Y., Sakaguchi, S., Nitta, Y., and Watanabe, T. (1982) *J. Biochem. (Tokyo)*, **92**, 1499-1504
11) Nakatani, H. (1988) *Arch. Biochem. Biophys.* **263**, 364-368
12) Shiozaki, K., Takata, K., Omichi, K., Tomita, N., Horii, A., Ogawa, M., and Matsubara, K. (1990) *Gene*, **89**, 253-258
13) Kunkel, T. A. (1985) *Proc. Natl. Acad. Sci. USA*, **82**, 488-492
14) Sanger, F., Nicklen, S., and Coulson, A. R. (1977) *Proc. Natl. Acad. Sci. USA*, **74**, 5463-5467
15) Fujisawa, T., Otsuki, M., Okabayashi, Y., Nakamura, T., Fujii, M., Tani, S., Koide,M., Hasegawa, H., and Baba, S., (1989) *Suizo (Japanese)*, **4**, 31-37
16) Muraki, M., Morikawa, M., Jigami, Y., and Tanaka, H. (1988) *Protein Engineering*, **2**, 49-54
17) Russell, A.J., Thomas, P.G., and Fersht, A.R. (1987) *J. Mol. Biol.*, **193**, 803-813
18) Sternberg, M.J.E., Hayes, F.R.F.,Russell, A.J., Thomas, P. G., and Fersht, A.R. (1987) *Nature*, **330**, 86-88
19) Muraki, M., Harata, K., and Jigami, Y. (1992) *Biochemistry* 31, 9212-9219
20) Canter, P and Wells, J.A. (1987) *Science*, **237**, 394-399
21) Lewendon, A., Murray, I. A., Shaw, W. V., Gibbs, M. R., and Leslie, A, G, W. (1990) *Biochemistry*, **29**, 2075-2080

CHAPTER VI Proteinaceous α-Amylase Inhibitors in Wheat Gluten

Wheat gluten is a viscous mixture of proteins which is water soluble extract from wheat flour. Gluten is used as an additive for food materials (bread and noodle etc.) to improve their physical characteristics. Gluten contains a lot of proteins to characterize their physical and biochemical properties. However, physiological and biochemical activities of proteins in gluten have not been sufficiently investigated. Wheat flour contains many types of α-amylase inhibitor and each inhibitors has been classified with purification and fractionation procedures (1, 2). A related material, wheat gliadin, contains a proteinaceous α-amylase inhibitor which molecular weight of about 55,000 (3, 4). In 1978, Pace et al. (5) showed preliminarily that commercial gluten contains some proteinaceous α-amylase inhibitor, although the details of the active components were not clarified. The author improved purification procedures of α-amylase inhibitors from gluten and characterized two types of proteinaceous α-amylase inhibitors. It is important to examine α-amylase inhibitors content and their specificities in gluten, concerning to toxin and drag activities as a food additive.

MATERIALS AND METHODS

Materials. Canada gluten was gift from Riken Vitamin Co. Ltd. Porcine pancreatic α-amylase (PPA) was purified with the same method described in CHAPTER 1. Human salivary α-amylase (HSA) and soluble starch were purchased from Nacalai tesque Ltd. Human pancreatic α-amylase (HPA) was gift from Toyobo Co. Ltd. DEAE and CM-Toyopearl 650 S, Toyopearl HW 50 and TSKgel G3000SW column were purchased from Toyo Soda Mfg. Co., Ltd. Other chemicals were of guaranteed or reagent grade of commercial.

Assay of amylase activity. One unit of the amylase activity is defined as the amount of enzyme that catalyzed the hydrolysis of 1 μ moles/min of glycoside bond at 30°C. Molarity of PPA was determined from the absorbance at 280 nm on the basis of a molecular weight of 55,000 and $A^{1\%} = 24.0$ cm^{-1} (6). The hydrolytic reaction for glycoside bond (G_5) by PPA was measured by use of β-(2,4 dichlorophenyl) maltopentaoside with Daiya-color AMY measurement kit (7). After appropriate time, the reaction was stopped by adding 2.0 mL of 10 mM KIO_3 to the 1 ml of the reaction mixture and the absorbance of the colored compound (produced from 2,4-dichlorophenyl-4-aminoantipyrine and KIO_3) was measured at 500 nm.

Assay of α-amylase inhibitor activity. During the purification steps, the inhibitor activity was assayed against PPA and HSA. After preincubation (30°C, 15min) of the α-

amylases and the inhibitors in phosphate buffer (25 mM, pH 6.9) containing 30 mM NaCl and 0.1 mM CaCl$_2$, remaining amylase activities were determined. The amylase reaction was initiated by addition of 1 ml of soluble starch (0.25 %) dissolved in the above buffer into the 1 ml of preincubated reaction mixture. After incubation for 15 min at 30°C, the reaction was stopped by adding 1 ml of the reaction mixture into 4 ml of 1 N acetic acid. After adding of 5 ml of 0.02 % iodine - 0.2 % potassium iodine into its stopped solution, the solution was filled up to 20 ml with distilled water and the absorbance of the solution was measured at 680 nm. Inhibition activity was calculated using following equation:

$$\text{inhibition (\%)} = \frac{(EI - E)}{(S - E)} \times 100$$

S ; the absorbance of substrate blank at 680 nm
E ; the absorbance of enzyme blank at 680 nm
EI; the absorbance of (enzyme + inhibitor) at 680 nm

One unit of inhibitor activity is defined as the amount which brings 50% inhibition of two units of amylase activity.

Analysis of the molecular weight. Analysis of the molecular weight of these inhibitors was carried out with the High Performance Liquid Chromatography (HPLC) equipped with TSKgel G3000SW column (7.5φ X 600 mm). Elution was performed with 0.1 M phosphate buffer (pH 6.5) containing 0.3 M KCl at room temperature. The inhibitors were monitored by the the UV detector with 280 nm.

Animal experiment. Male Wistar rats weighing between 130-190 g were used as treated animals for the influence of the inhibitor. Wheat starch containing the inhibitor sample was administered orally to the rats which had been fasting for 24 h. After 30 min, the blood was taken from the heart and the amount of glucose in the serum was measured with Hitachi 705 automatic glucose analyzer. Whole animal experiments have been performed at the laboratory of Toyobo Co. Ltd.

Other analytical methods. Protein content was determined by the method of Lowry - Follin (8) with bovine serum albumin as standard.

Electrophoresis was performed in polyacrylamide gel at pH 9.4, essentially as described by Ornstein and Davis (9, 10).

Amino acid composition of these inhibitors were determined by automated amino acid analyzer (Hitachi KLA-5), applying samples which were hydrolyzed with 6 N HCl at 110°C

for 12 h. The number of Trp residues were determined according to the method of Goodwin (11).

N-terminal sequence was analyzed by ABI 470A sequencer with a carboxymethyl (12) sample.

RESULTS AND DISCUSSION

Purification procedure of amylase inhibitor

Step 1. Extraction with 70% ethanol.

Gluten (20 g) was immersed with 70% ethanol (100 ml) and stirred for 3 hours at room temperature. After centrifugation (22,000 x g, 40 min) the supernatant was dialyzed against 0.2 M NaCl. Precipitate was removed by centrifugation (22,000 x g, 40 min) and then the supernatant was concentrated with ultrafilter.

Step 2. Gel filtration by TOYOPEARL HW-55.

The concentrated crude inhibitor solution from ethanol extract was applied to TOYOPEARL HW-55 column equilibrated with 0.1 M NaCl and eluted with 0.1 M NaCl solution. Elution was carried out at room temperature and monitored at 280 nm. Two peaks were eluted as shown in Fig. 1. The first peak, designated P1 demonstrated inhibitory activity to both PPA and HSA. The second peak, designated P2, demonstrated inhibitory activity to only HSA. The first peak was dialyzed against 10 mM phosphate buffer (pH 8.0) and second peak was dialyzed against 20 mM sodium acetate buffer (pH 5.5).

Purification of PPA specific inhibitor

Step 3. DEAE-TOYOPEARL column chromatography.

After removal of precipitate material in the dialyzed P1 solution by centrifugation (22,000 x g, 30 min) the supernatant solution was applied to DEAE-TOYOPEARL column equilibrated with 10 mM phosphate buffer (pH 8.0). The bound protein was eluted with a gradient (0 - 0.1 M) of NaCl in 10 mM phosphate buffer (pH 8.0) at room temperature (Fig. 2). The fractions containing inhibitor activity were collected and then concentrated with a ultrafilter. The concentrated solution was applied to TOYOPEARL HW-55 column equilibrated with 0.1 M NaCl again and the fractions containing inhibitor activity were combined, and this solution was used for characterization of properties of PPA specific inhibitor P1.
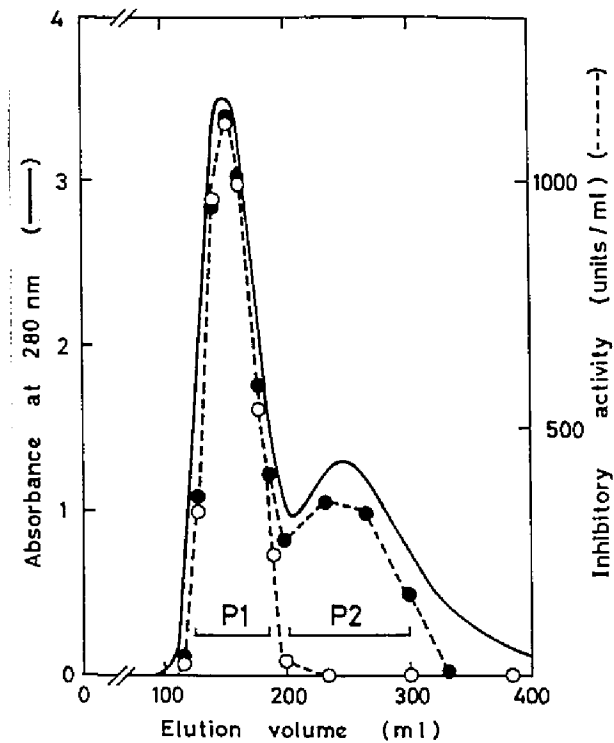
Fig. 1. TOYOPEARL HW-55 column chromatography with 0.1 M NaCl at room temperature. Column size; ϕ2.0 x 100 cm, (−) absorbance at 280 nm, (○) inhibitory activity to PPA, (●) inhibitory activity to HSA.
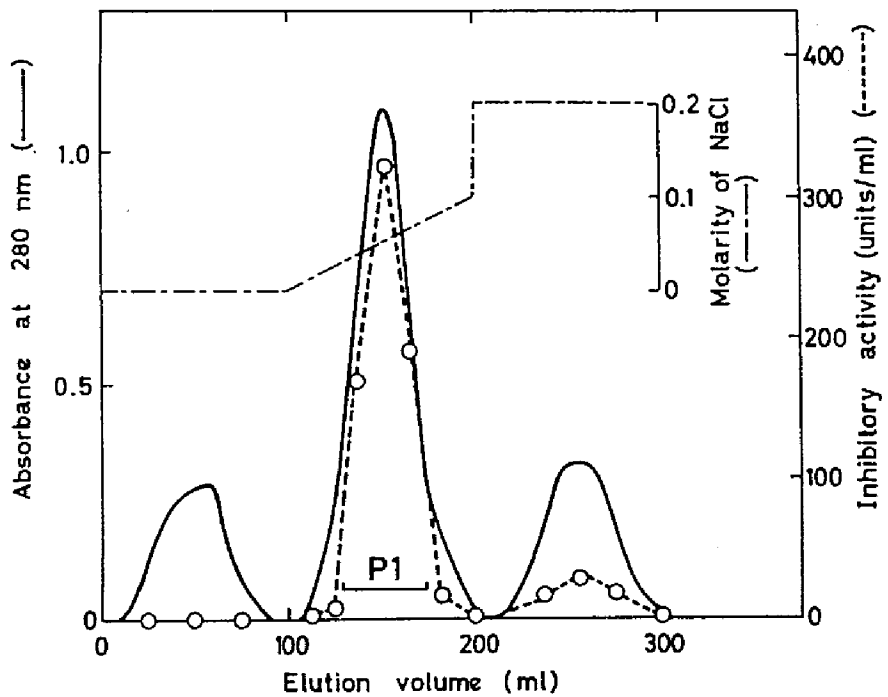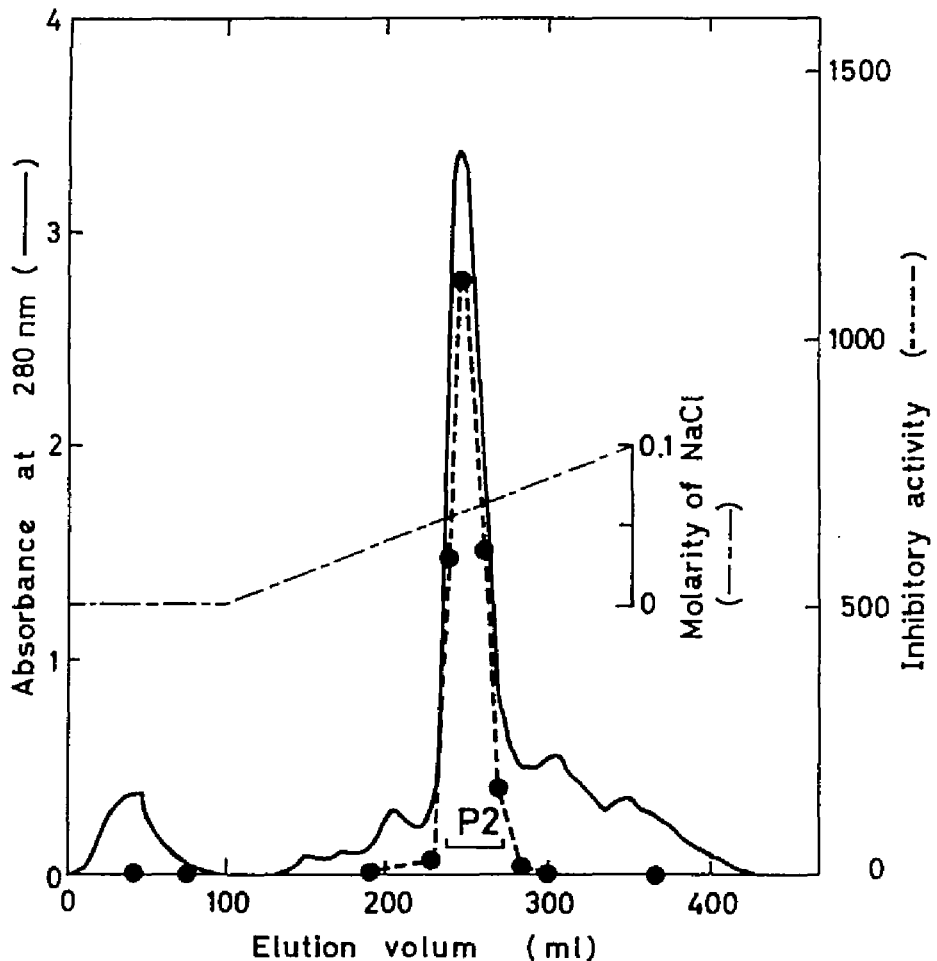

Fig. 2. DEAE-TOYOPEARL column chromatography with 10 mM sodium phosphate buffer (pH 8.0) at room temperature.
Column size; ϕ1.0 x 15 cm, (−) absorbance at 280 nm, (○) inhibitory activity to PPA.

Purification of HSA specific inhibitor

Step 3'. CM-TOYOPEARL column chromatography.

After removal of precipitate material in the dialyzed P2 solution by centrifugation (22,000 x g, 30 min) the supernatant solution was applied to CM-TOYOPEARL column equilibrated with 20 mM sodium acetate buffer (pH 5.5). The bound protein was eluted with a gradient (0 - 0.2 M) of NaCl in 20 mM sodium acetate buffer (pH 5.5) at room temperature (Fig. 3). The fractions containing inhibitor activity were collected and then concentrated with a ultrafilter. The concentrated solution was applied to TOYOPEARL HW-55 column equilibrated with 0.1 M NaCl again and the fractions containing inhibitor activity were combined, and this solution was used for characterization of properties of HSA specific inhibitor P2.

Fig. 3. CM-TOYOPEARL column chromatography with 20 mM sodium acetate buffer (pH 5.5) at room temperature. Column size; φ1.0 x 15 cm, (-) absorbance at 280 nm, (●) inhibitory activity to HSA.

The results of a typical purification process are presented in Table I. P1 was not stable at above pH 8.0 therefore the loss of the activity was observed at the purification step 3. Polyacrylamide gel electrophoresis of P1 and P2 did not show a single band at pH 9.4, and SDS polyacrylamide gel electrophoresis showed some bands which molecular weights were determined to be about 11,5000 However, HPLC with 3000 SW column analysis of them showed a single peaks and determined the molecular weight of them to be about 48,000 (P1) and 24,000 (P2) (Fig. 4). These results indicate that these inhibitor P1 and P2 have some subunits which molecular weight are 11,500. $E^{1\%}(280$ nm) of P1 and P2 was 10.0 and 10.3 cm^{-1}, respectively.

Table I. Purification of α-amylase inhibitors (P1 and P2).

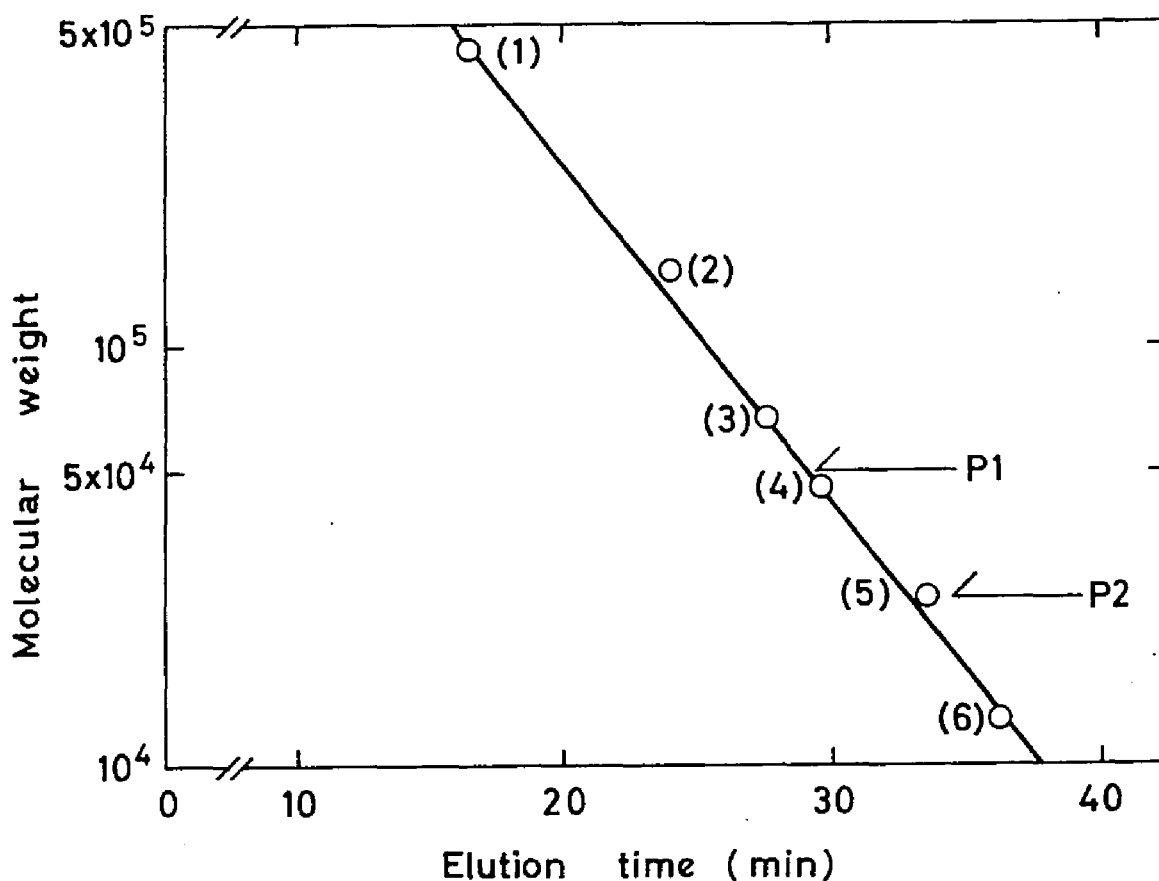| Purification step	Total protein (mg)		Total inhibitory units against PPA HPA		Recovery (%)	
Step 1 (20 g)	270		64,000	72,000	100	100
Step 2	P1	P2	P1	P2	P1	P2
	80	110	46,000	15,000	71.9	20.8
Step 3	25		13,000		20.3	
Step 3'		82		14,800		20.6
Step 4	18	70	9,300	14,000	14.5	19.4

Fig. 4. Molecular weight determination by HPLC with TOYOPEARL SW 3000 column. Elution was performed with 0.1 M phosphate buffer (pH6.5) containing 0.3 M KCl. Standard protein; (1) Ferritin (M.W., 420,000), (2) γ-Globulin (M.W., 150,000), (3) Bovine serum albumin (M.W., 67,000), (4) Ovalbumin (M.W., 45,000), (5) Chymotrypsinogen A (M.W., 25,000), (6) Cytochrome C (M.W., 12,500).

Amino acid composition of these inhibitors

The amino acid compositions of purified inhibitors P1 and P2 are summarized in Table II. Comparison with other inhibitors from same and different origin is also shown in Table II. It is clear that the total patterns are similar with each other. Primary structure of N-terminal of P2 was determined as Ser-Gly-Pro-Trp-Met-Cys-Tyr-Pro-Gly-Gln-Alα-Phe-Gln-Val-Pro- with amino acid sequencer using a carboxymethyl P2 sample. This sequence is same as that of 0.19 inhibitor from wheat kernel (13).

Table II. Amino acid compositions of α–amylase inhibitors (P1, P2) and 0.19 inhibitors from wheat flour.

| Amino acid | Inhibitor | | |
	P1	P2	0.19
Asp	7.8	6.0	5.6
Thr	5.7	3.4	2.4
Ser	5.4	7.4	5.6
Glu	11.2	11.5	10.5
Pro	12.2	7.6	7.3
Gly	8.9	12.5	8.1
Ala	5.3	16.6	13.7
Cys	1.7	2.1	8.1
Val	7.2	5.6	8.1
Met	2.5	+	2.4
I le	3.6	2.4	2.4
Leu	9.0	9.0	8.1
Tyr	2.2	4.3	4.0
Phe	2.2	1.2	1.6
Trp	4.4	1.5	1.6
Lys	2.5	2.0	2.4
His	2.0	1.2	1.6
Arg	6.5	6.2	6.5

The numbers of amino acids represent mol%.

Specificity of these inhibitors

Specificity of these inhibitors was investigated using a Daiyacolor AMY measurement set (10). These inhibitors (P1 and P2) were preincubated (30°C, 15 min) with HSA, HPA and PPA, and remaining amylase activity was measured with the above kit (Fig. 5). P1 inhibited HPA, PPA and HSA similarly. P2 did not inhibited PPA at all but HSA specifically and HPA slightly. Therefore, P2 can be used as discrimination between pancreatic and salivary α-amylase in human serum and urine using this specificity. From the data of inhibition profile and N-terminal amino acid sequence of P2, it is speculated that P2 is similar to 0.19 inhibitor.

These amylase inhibitors from wheat gluten may be consist of some similar subunits and discriminate a little difference between pancreatic and salivary amylase. The selective inhibition mechanism of P2 will be clarified in molecular level by protein engineering method using mutant human salivary and pancreatic α-amylase.
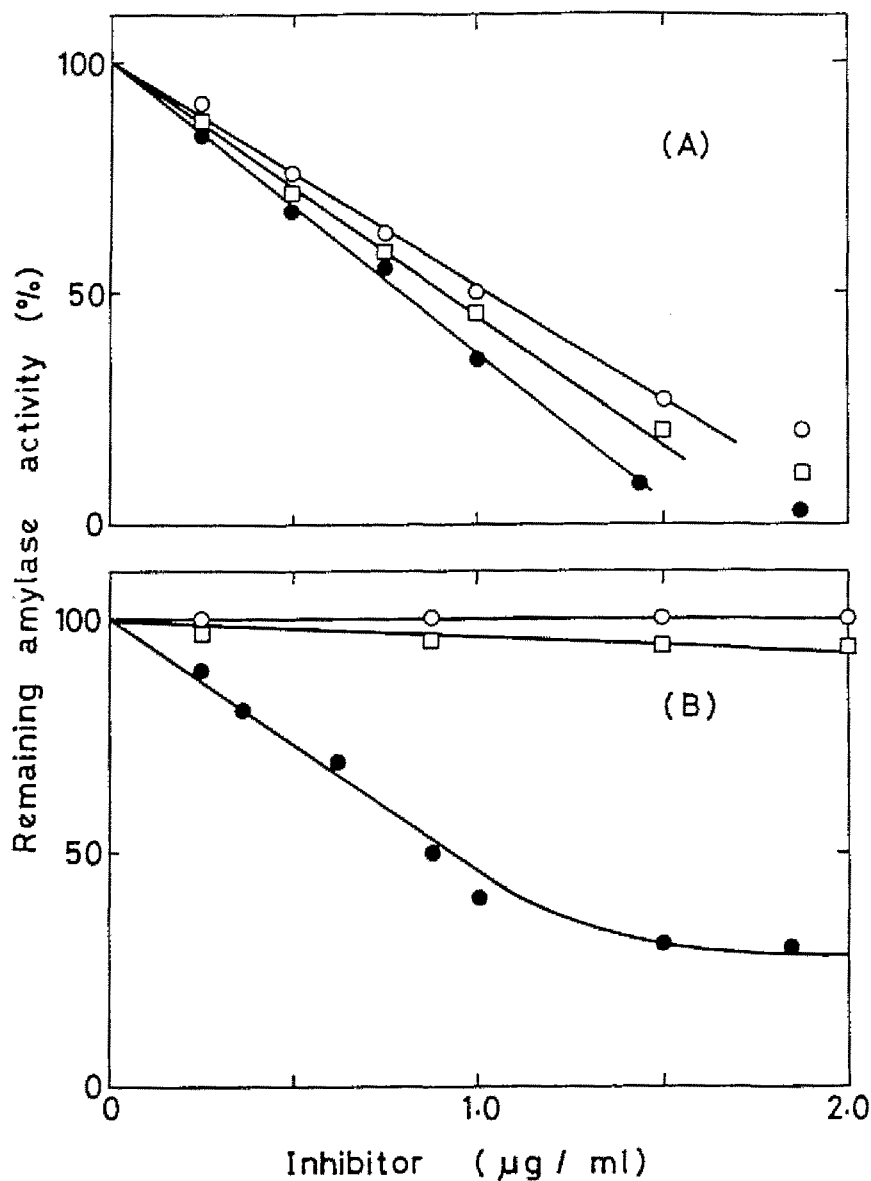
Fig. 5. Inhibition profile of P1 (A) and P2 (B) against PPA (O) (7.5 units/ml), HPA (□) (7.3 units/ml) and HSA (●) (7.2 units/ml).

The influence of P1 as a food additive

Wheat starch (2.5 g / kg (rat)) containing P1 (9.5 and 38.0 mg) was administered to the rat which was performed fast for 24 h. The amount of glucose in serum of the rat was measured after administration as shown in Table III. From this result, the inhibition (Ca. 65 %) of the increase of glucose in the serum was observed. Furthermore, every rat had been living for 7 days. After P1 (2000 mg / kg (rat)) had been administered to the rat for every 20 day, abnormal phenomena were not observed in every viscera of the rat. Therefore, LD_{50} of P1 for rat must be over 2000 mg/kg. The binding rate between human pancreatic α-amylase and P1 was about three order higher than that between human pancreatic α-amylase and

phaseolamin, a proteinaceous α-amylase inhibitor from white kidney bean (17), at pH 6.9 near the physiological condition in vivo (unpublished data). Phaseolamin was effective to reduce serum glucose blocking starch digestion (18). These results indicate that P1 and gluten itself have a possibility of a reagent or a food additive which reduces postprandial plasma glucose.

Table III. Amount of glucose in serum of rats.

Treatment	No. analyses	Serum glucose Mean + SD (mg/100ml)	Change due to starch load (mg/100ml)
Control	6	93.5 ± 6.3	-
Starch (2.5g/kg)	6	214.2 ± 7.6	120.7
Starch (2.5g/kg) + P1 (9.5mg)	6	175.8 ± 5.7	82.3
Starch (2.5g/kg) + P1 (38.0mg)	6	135.8 ± 5.6	42.3

REFERENCES

1) Buonocore, V., Petrucci, T., and Silano, V. (1977) *Phytochemistry,* **16**, 811-820
2) Strumeyer, D. H. (1972) *Nutrition Report Internat.,* **6**, 45-52,
3) Strumeyer, D. H. and Fisher,B. R.,(1973) *Fed. Proc.,* **32**, 624-
4) Strumeyer, D. H. and Fisher, B. R., (1983) *Analyt. Biochem.,* **130**, 506-513
5) Pace, W., Parlamenti, R., Ur Rab, A., Silano, V., and Vittozzi, L., (1978) *Cereal Chem.,* **55**, 244-254
6) Elodi, P., Mora, S. and Kryzteva, M. (1972) *Eur. J. Biochem.,* **24**, 572-581.
7) Nakagiri, Y., Kanda, T., Otaki, M., Inamoto, K., Asai, T., Okada, S., and Kitahata, S., (1982) *J. Japan, Soc. Starch Sci.,* **29**, 161-166
8) Lowry, O. H., Rosebrough, N. J., Farr, A. L., and Randall, R. J.,(1951) *J. Biol. Chem.,* **193**, 265-275
9) Ornstein, L. (1964) *Ann. N. Y. Acad. Sci.,* **121**, 321-349
10) Davis, B. J. (1964) *Ann. N. Y. Acad. Sci.,* **121**, 407-427
11) Goodwin, T. W. and Morton, R. A. (1946) *Biochem. J.,* **40**, 628-632
12) Crestfield, A. M., Moore, S., and Stein, W. H., (1963) *J. Biol. Chem.,* **238**, 622-627
13) Maeda, K., Kakabayashi, S., and Matsubara, H., (1985) *Biochim. Biophys. Acta,* **828**, 213-221
14) Marshall, J. J. and Lauda, C. M., (1975) *J. Biol. Chem,* **250**, 8030-8037
15) M. Bovine, B. Flourie, R. A. Rizza, V. L. W. Go and E. DiMagno, (1988) *Gastroenterology,* **94**, 387

Numerical Method to Analyze pH-Profile from Initial Velocity
                Data and Semi-Empirical Procedure to Identify Catalytic Residues
                of Enzymes Using pK and Heat of Ionization

One of the most important parts of an enzyme molecule is the active site, containing the catalytic residues. The most reliable method to determine catalytic residues is probably identification from the three-dimensional structure of the enzyme-substrate complex established by X-ray crystallography. Usually, functional amino acid residues at the substrate or substrate-analog binding site are identified as catalytic residues for the enzyme. However, when three or more functional residues are located close to the substrate binding site, identification of the proper catalytic residues may be difficult. For example, the catalytic residues of porcine pancreatic α-amylase were suggested to be a pair of aspartic acids from the three-dimentional structure at 2.9 Å resolution (1). On the other hand, detailed analysis of the pH-profile of the enzyme-catalyzed reaction using suitable oligosaccharide substrates suggested that the catalytic residues number are not two, but three, two carboxylates and a histidine (CHAPTER II). At the active site of porcine pancreatic α-amylase and a related α–amylase, Taka-amylase A, two aspartic acids, one glutamic acid, and three histidine residues are located relatively closely (1,2), so it is not easy to assign the catalytic residues on the basis of structural data only. Since identification of catalytic residues from structural points of view must correspond to functional properties, the reliability of the method to identify catalytic residues by using pH-profile and thermodynamic parameters is important. The procedures are at present not well refined. Observations of the effects of additional salts and organic solvents on rate parameters are useful in some cases, but binding or absorption of added compounds to the enzyme molecule tends to disturb exact assignment of catalytic residues (3). The author has developed a semi-empirical procedure to identify catalytic residues from pK and heat of ionization data based on thermodynamic analysis and experimental data which have been obtained on small molecules and enzymes.

METHOD

Numerical method to compute pK and heat of ionization from initial velocity data. Initial velocity data implicitly contain full information on thermodynamic parameters. The equation of initial velocity v can be represented in the form containing apparent thermodynamic parameters as follows:

$$\mathrm{d}p/\mathrm{d}t = v\,(e^0,\, s^0,\, T,\, \mathrm{pH};\, k_{cat}{}^0,\, K_m{}^0,\, K_1{}^0,\, K_2{}^0,\, \ldots,\, E^{\neq},\, \Delta H_m{}^0,\, \Delta H_1{}^0,\, \Delta H_2{}^0,\, \ldots\,)\quad (1)$$

where p is the product concentration, e^0 and s^0 are initial concentrations of the enzyme and substrate, respectively, T is the absolute temperature of the sample solution, k_{cat}^0 and K_m^0 are intrinsic rate parameters independent of temperature, assuming the Arrhenius and van't Hoff equations defined in eq. (2), respectively, and K_1^0, etc. are intrinsic ionization constants for ionic amino acid residues. The corresponding activation energy for k_{cat} is shown as $E^{\neq}$, and standard enthalpy change for K_m, heat of ionization for K_1, etc. are shown as ΔH_m^0, ΔH_1^0, etc.,

$$k_{cat} = k_{cat}^0 \exp(-E^{\neq}/RT)$$
$$K_m = K_m^0 \exp(-\Delta H_m^0/RT)$$
$$K_1 = K_1^0 \exp(-\Delta H_1^0/RT)$$
$$K_2 = K_2^0 \exp(-\Delta H_2^0/RT) \qquad (2)$$

where R is the gas constant (1.987 cal·K^{-1}·mol^{-1}). The apparent from of v and number of parameters vary with the reaction mechanism. Actually, a preliminary pH profile at the standard temperature should be analyzed to determine parameters to be estimated and to deduce a suitable rate equation to be applied. The procedures can be summarized as follows.

1. Analysis of pH-profile at the standard temperature: pH-dependence of k_{cat}, K_m, and k_{cat}/K_m.

2. Determination of a rate equation based on a suitable mechanism to fit experimental data on pH-dependency.

3. Extension of the rate equation to a general equation using eq. (2).

4. Least-squares analysis of initial velocity data using the general equation as a function of substrate and enzyme concentrations, pH, and temperature. Restriction conditions to set upper and lower limits of parameters are added, if necessary, for rapid convergence to reasonable values.

Practically, input data are a set of s_0, T, pH and v/e_0, and then output parameters (k_{cat}^0, K_m^0, etc. and $E^{\neq}$, ΔH_m^0, ΔH_1^0, etc.) are obtained without Arrhenius and van't Hoff plots. Numerical calculation with a non-linear least-squares method has been carried out with the program system SALS using Gauss-Newton variation (4), on a FACOM-M780 computer. The data on porcine pancreatic α–amylase were analyzed as described in "RESULTS AND DISCUSSION".

Relation between pK and ΔH^0 for acidic and basic residues. Acid-base dissociation and association reactions can be formulated as follows,

$$XH \rightleftharpoons X^- + H^+ \tag{3}$$

$$K = [X^-][H^+]/[XH] \tag{4}$$

where XH and X^- are conjugate acid and base, respectively, and K is the dissociation constant. Standard enthalpy and entropy changes, ΔH^0 and ΔS^0, are related as follows (5).

$$\Delta H^0 = T\Delta S^0 + 2.303\ RT\ \mathrm{p}K \tag{5}$$

when values of standard entropy change, ΔS^0, are restricted to a limited range, the plot of ΔH^0 versus pK must be distributed as a band with slope 1.4 kcal (25°C) or 1.5 (30°C). Data for aliphatic carboxylic acids, imidazole derivatives, thiol derivatives, and aliphatic amines listed in Table I are approximately distributed in the form of eq. (5) under the condition $0.6 > \Delta S^0 > -40$ e.u. Acid and bases listed in Table I are model compounds for aspartic acid, glutamic acid, histidine, cysteine, and lysine residues. Model compounds for arginine were not considered here because the pK values are in the more alkaline region than those of lysine residue and are relatively unimportant for catalytic residues. The identify and pK value of tyrosine residue are easily determined by spectroscopic titration (6).

RESULTS AND DISCUSSION

The validity of the present numerical computing method was examined using recent data on porcine pancreatic α-amylase, based on the mechanism shown in CHAPTER III. The substrates are maltopentaitol and maltohexaitol synthesized from maltopentaose and maltohexaose, respectively, of which the reducing ends are converted to sorbitol (CHAPTER II). The equation of initial rate deduced from the mechanism in CHAPTER III is as follows,

$$k_{cat} = \frac{(k_1 \cdot K_1)/[H^+] + (k_2 \cdot K_1 \cdot K_2)/[H^+]^2}{1 + (K_1 + K_2)/[H^+] + (K_1 \cdot K_2)/[H^+]^2 + (K_1 \cdot K_2 \cdot K_3)/[H^+]^3} \cdot \frac{e^0\ s^0}{K_m + s^0} \tag{6}.$$

The experimental data (148 points) were analyzed using the mechanism and equation. Estimated rate and thermodynamic parameters with standard deviations are shown in Table II. Estimated values in Table II are quite compatible with those of the literature (CHAPTER II). The catalytic residues have been assigned to be two carboxyl and one histidine residues. Since free SH groups of cysteine residues are not found at the active site (1), a contribution of cysteine residues to the catalytic residues was ruled out for porcine pancreatic α-amylase. The present method can use incomplete pH-profile data, where exact data analysis to estimate experimentally pK values is impossible by traditional methods at the given temperature.

The procedure to estimate catalytic residues from pK values and heats of ionization was developed semi-empirically, combining theoretical considerations and experimental data on model compounds and enzymes. Values of pK and heat of ionization for catalytic residues of enzymes cited from the literature are listed in Table III. These data are for carboxyl and histidine residues as catalytic residues. The author assumes at first that all assignments of catalytic residues in Table III are correct. Plots of ΔH^0 *versus* pK for model compounds and catalytic residues are represented in the same graph in Fig. 1. It is clear that each residues is clustered approximately in a restricted range. Each residue is grouped in a band between two lines with slope 1.4 as calculated from eq. (8). The upper and lower ranges of ΔH^0 were determined empirically to separate each residue rationally. As a result, each residue could be classified as a parallelogram as shown in Fig. 1. The coordinates for each parallelogram are described in the legend of Fig. 1. Except two points (pK=5.22, ΔH^0=4.5; pK=7.45, ΔH^0=4.0), all the experimental values for small-molecular derivatives and enzyme residues are well classified into separated parallelograms, excluding a part of the imidazole and thiol groups. One of the points deviating from the defined area at pK=5.22 and ΔH^0=4.5 is an inaccurate datum of which the experimental error for ΔH^0 is ±3.2 (7). The other deviating datum at pK=7.45 and ΔH^0=4.0 for *Bacillus amyloliquefaciens* α-amylase using amylose as a substrate had been assigned as a histidine residue (8), but is now regarded rather to be a carboxyl residue since it deviates relatively far from the defined area for the histidine residue, and belong to the area for carboxyl residues. Recent investigations using site-directed mutagenesis on a related enzyme, *Bacillus stearothermophilus* α-amylase, suggest two aspartic acids as catalytic residues (9). Reexaminations for these enzymes using proper substrates such as maltooligosaccharides are needed to identify the catalytic residues more certainly. Since areas for thiol groups and histidine residues overlap partially, it is difficult to distinguish the two if pK-ΔH^0 data for an enzyme fall into the overlapping area. In such cases, available information from three-dimentional structure, chemical modification, site-directed mutagenesis, etc. should be utilized to assign the catalytic residues in addition to the present pK-ΔH^0 diagram method.

From a theoretical point of view, there is no limitation of ΔH^0 value for each residue, depending on the environment in the enzyme. However, since the active site of a free enzyme is usually at the surface of the enzyme molecule or only partially buried at the surface, the value of ΔH^0 of each catalytic amino acid residue should not deviate greatly from the values of model compounds cited in Table I. Therefore, analysis of pH-profile data is a reliable method to determine numbers of ionic amino acid residues contributing to the catalytic function, and to assign the nature of catalytic amino acid residues.

Table I. Names of model compounds, aliphatic carboxylic acids, histidine, thiols, amines, and their derivatives, of which values of both pK and ΔH^0 are known.

A) Carboxylates[a]

trimethylacetic	acetic	chloroacetic
propionic	diethylacetic	fluoroacetic
hexoic	succinic	cyanoacetic
isobutyric	lactic	oxalic (ionized)
isohexoic	glycolic	malonic (ionized)
valeric	formic	glutaric (ionized)
butyric	iodoacetic	
isovaleric	bromoacetic	

B) Imidazol derivatives[b,c]

imidazole	histidine methyl ester	4-imidazolylacetic acid (ionized)
histidine (ionized)		

C) Thiol derivatives[d,e]

acetylcysteine ester (ionized)	formylcysteine (ionized)
thiodipropionic acid (ionized)	thioglycolic acid (ionized)

D) Amine derivatives[a]

ammonium	n-butylammonium	ethylendiamine
methylammonium	hydroxymethil-	(monocation)
ethylammonium	ammonium	1.6-hexanediamine
n-propylammonium	dimethylammonium	(monocation)
diethylammonium		

Value of pK at 25°C were recalculated from original data if necessary.
[a]Bell, R.P. (1973) *The Proton in Chemistry*, Chap.3, Chapman and Hall, London. [b]Datta, S.P. and Grzybowsk, A.K. (1966) *J. Chem. Soc.* (B) 136-140. [c]Andrews, A.C. and Zebolsky, D.M. (1965) *J. Chem. Soc.* 742-746. [d]Cecil, R. and McPhee, J.R. (1955) *Biochem. J.* 60, 496-506. [e]Benesch, R.E. and Benesch, R. (1955) *J. Am. Chem. Soc.* 77, 5877-5881.

Table II. Rate parameters of the mechanism in CHAPTER I with standard deviations for porcine pancreatic α-amylase-catalyzed hydrolysis of maltopentaitol (G$_5$OH) and maltohexaitol (G$_6$OH).

	G$_5$OH	G$_6$OH
pK_1	4.78±0.04	
pK_2	5.54±0.05	
pK_3	8.62±0.02	
ΔH_1^0 (kcal/mol)	0.09±2.18	
ΔH_2^0 (kcal/mol)	1.52±2.24	
ΔH_3^0 (kcal/mol)	6.86±0.94	
k_a (s^{-1})	456±26.7	505 ±30
k_b (s^{-1})	97.8±4.21	867 ±12.6
E^*_a (kcal/mol)	19.2±1.25	20.8 ±1.54
E^*_b (kcal/mol)	20.5±1.23	16.9 ±0.28
K_m (mM)	0.231±0.022	0.849±0.036
ΔH_m^0 (kcal/mol)	-9.3 ±2.7	-0.41 ±1.0

Values of rate parameters and pKs are at 30°C.

TABLE III. pK and ΔH^0 values of catalytic amino acid residues assigned for enzyme.

pK	ΔH^0	Residue	Enzyme	Method
6.01	2.9	carboxyl	lysozyme[a]	titration
4.43	3.5	carboxyl	lysozyme[a]	titration
5.22	2.9	carboxyl	lysozyme[a]	titration
5.22	4.5	carboxyl	lysozyme[a]	titration
2.9	0	carboxyl	glucoamylase[b]	pH-profile
5.9	-0.8	carboxyl	glucoamylase[b]	pH-profile
1.51	-0.8	carboxyl	carboxyl protease[c]	pH-profile
3.80	1.2	carboxyl	carboxyl protease[c]	pH-profile
4.22	2.0	carboxyl	Bacillus α-amylase[d]	pH-profile
4.78	0.09	carboxyl	pancreatic α-amylase[e]	pH-profile
5.58	1.5	carboxyl	pancreatic α-amylase[e]	pH-profile
8.81	6.8	histidine	pancreatic α-amylase[e]	pH-profile
6.25	7.0	histidine	trypsin[f]	pH-profile
6.8	8.9	histidine	chymotrypsin[g]	titration
7.45	4.0	histidine	Bacillus α-amylase[d]	pH-profile

Values of pK at 25°C were recalculated from original data if necessary.
[a]Parsons, S.M. and Raftery, M.A. (1972) *Biochemistry* 11, 1630-1633. [b]Hiromi, K., Takahashi, K., Hamauzu, Z., and Ono, S. (1966) *J. Biochem.* 59, 469-475. [c]Oda, K. and Murao, S. (1986) *Agric. Biol. Chem.* 50, 659-663. [d]Ono, S., Hiromi, K., and Yoshikawa, Y. (1958) *Bull. Chem. Soc. Jpn.* 31, 957-962. [e]From Table II in this paper using initial rate data. [f]Gutfreund, H. (1955) *Trans. Farad. Soc.* 51, 441-446. [g]Hanai, K. (1976) *J. Biochem.* 79, 107-116
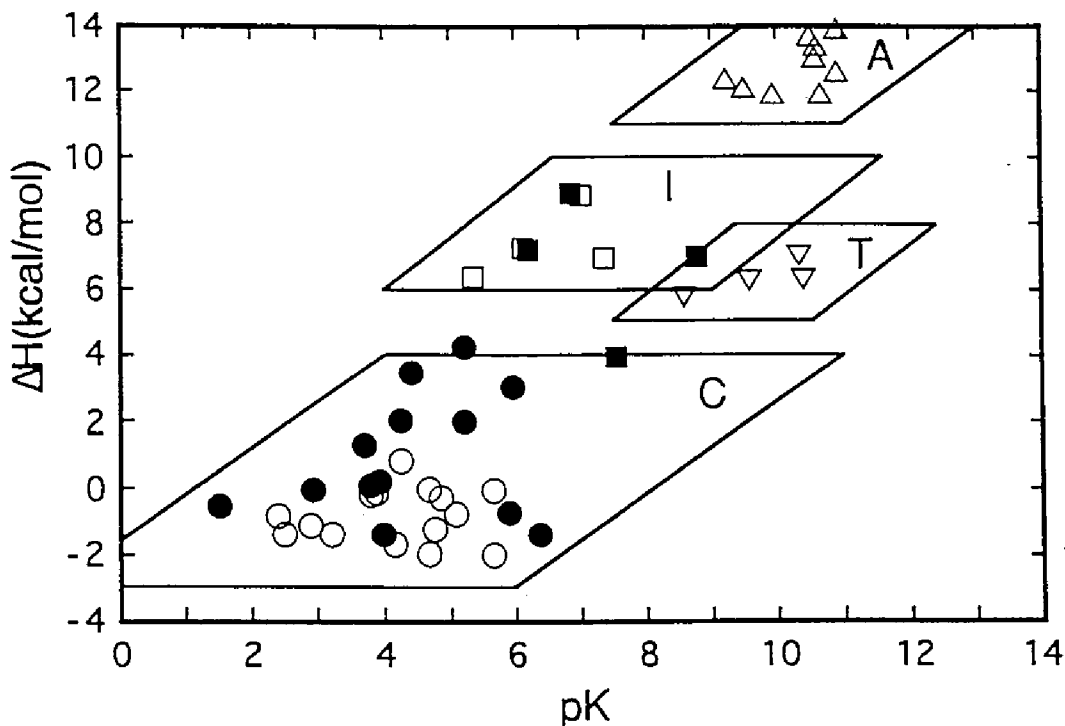
Fig. 1. Possible distribution areas of pK and ΔH^0 for catalytic carboxyl, histidine, thiol, and lysine residues of enzymes. The ranges of parallelograms C, I, T and A are for carboxyl, histidine, thiol, and lysine residues, respectively. The coordinate for each area are (4,4)-(11,4) -(6,-3)-(-1,-3) for C, (6.9,10)-(11.9,10)-(9,6)-(4,6) for I, (9.3,8)-(12.3,8)-(10.5,5.5) -(7.5,5.5) for T, and (9.6,14)-(13.1,14)-(11,11)-(7.5,11) for A. O: carboxylate, model compounds; ●: carboxylate, enzymes; □: imidazole, model compounds; ■: imidazole, enzymes; ▽: thiol, model compounds; △: amine, model compounds

SUMMARY

A numerical computing method to estimate pK and heat of ionization directly from initial velocity data was developed for systematic analysis of rate parameters. Values of rate and thermodynamic parameters were determined together with standard deviations, without using Arrhenius and van't Hoff plots. Distributions of pK and heat of ionization of small-molecular derivatives of aliphatic carboxylates, imidazoles, thiols, and aliphatic amines as possible models for catalytic residues of enzymes were analyzed from a thermodynamic point of view. Each group was classified in a parallelogram without overlapping, except for a part of the imidazole and thiol groups. It was shown that values of pK and heat of ionization of carboxylates and histidine residues involved in the catalytic activity of enzymes determined from pH-profile experiments can be classified into similar, though somewhat extended, areas to those of the corresponding small-molecular derivatives. Identification of catalytic residues using values of pK and heat of ionization is proved to be a reliable method when the procedure is properly used.

REFERENCES

1) Buisson, G., Duee, E., Haser, R., & Payan, F. (1987) EMBO *J.* 6, 3909-3916
2) Matsuura, Y., Kusunoki, M., Harada, W., & Kakudo, M. (1984) *J. Biochem.* 9 5, 697-702
3) Parsons, S.M. & Raftery, M.A. (1972) *Biochemistry* ,1 1, 1623-1629
4) Nakagawa, T. & Oyanagi, Y. (1980) in *Recent Developments in Statistical Inference and Data Analysis* (Matsushita, K., ed.) pp. 221-225, North Holland Publishing, Amsterdam
5) Bell, R.P (1973) *"Proton in Chemistry* "pp. 72-85, Champan and Hall, London
6) Cantor, C.R. & Schimmel, P.R. (1980) *"Biophysical Chemistry* "pp. 376-379, W.H. Freeman and Company, San Fransisco
7) Parsons, S.M. & Raftery, M.A. (1972) *Biochemistry* , 1 1, 1630-1633
8) Ono, S., Hiromi, K., & Yoshikawa, Y. (1958) *Bull. Chem. Soc. Jpn.*, 3 1, 957-962
9) Vihinen, M. & Mantsala, P. (1990) *Biochem. Biophys. Res. Commun.*, 1 6 6, 61-65

SUMMARY AND CONCLUSION

Roles of histidine residues

In the active site of PPA and possibly other mammalian α-amylases, three histidine residues (101, 201, and 299) and three carboxyl residues (Asp197, Glu233, and Asp300) are located (1). One of the histidine residues, His201, is located a little far from the catalytic center (around subsite 4 and 5) and plays important multi-functional roles which are specific to mammalian pancreatic α-amylases. His201 relates to substrate recognition, control of optimum pH, increase of maltosidase activity by chemical modification, activation by chloride ion and inhibition by proteinaceous α-amylase inhibitor. From the pH-profile analysis, one of the histidine residues has to be proposed as one of catalytic residues. His201 can not contribute to the active center directly. His299 is the neighbor residue of Asp300, one of the possible catalytic carboxyl residues. However, the imidazole group of His299 is not directed to the catalytic site (1). Although H299N HPA loses amylase activity (3% of that of wild-type), it is regarded to be indirect effect disturbing the action of Asp300. On the other hand, His101 is very close to the catalytic site geometrically according to the three-dimensional structure of PPA (1); the imidazole site is directed to the catalytic site and close to the carboxylate of Asp197. H101N HPA lost amylase activity (0.8% of that of wild-type). Therefore, His101 is the most probable catalytic residue which had been suggested by us from pH profile analysis (CHAPTER II and III).

Catalytic mechanism of PPA and HPA

HPA has 83% homology with PPA in overall amino acid sequence, and its amino acid residues at the active site correspond almost completely to those of PPA (2). Therefore, the catalytic mechanism of HPA and PPA must be common to each other. Comparison between the steric structures and amino acid sequences of PPA HPA and TAA, Asp300 of PPA and HPA correspondents to Asp297 of TAA which is in hydrophobic environment and may exist in ionized form (2-4). Asp297 of TAA has been regarded to be the negatively charged side chain as a general base, to stabilize the carbonium ion intermediate (3, 4) in the process of the catalytic reaction. From the X ray analysis study of PPA (1) and sequence homologies of α-amylases (2), the author assumes here that Asp300 of PPA and HPA is also negatively charged throughout the catalytic process like Asp 297 in TAA. On the other hand, the two residues, Asp197 and His101, are candidates for proton donors of PPA and HPA toward the glycoside bond to be hydrolyzed. In the proposed three catalytic residue model, there are four different protonation stages, $EH_aH_bH_c$, EH_bH_c, EH_c and E, (H_a, H_b and H_c are protons bound at Asp300 (pK_1), Asp197 (pK_2) and His101 (pK_3) of the deprotonated enzyme, E, respectively) (CHAPTER

III) in PPA. Among them, EH_bH_c and EH_c are active around pH 5.2 and 6.9, respectively. Therefore, PPA has at least two different hydrolytic mechanisms in regard to roles of proton donor residues. Combining the three dimensional structure of PPA and our works, four representative possible mechanisms for the PPA's initial stage of hydrolysis, extended from original mechanism proposed by Fischer and Stein (1), are shown in Fig. 1. At the EH_bH_c state, the proton donor residue is Asp197 (A) or His101 (B) and at the EH_c state, it is His101 (C) or His101 cooperated with Asp197 through probable hydrogen bonding (D). The pK_3 values of PPA (8.62) (CHAPTER III) larger than the normal pK values (6-7) for model imidazole derivatives (5) suggests that the model (D) with His101 affected by Asp197 is more reliable than the (C) without such affection. There are four possible alternation paths between EH_bH_c and EH_c, as illustrated with hollow arrows in Fig. 1. The path (A) − (C) needs an exchange of the proton donor residue from Asp197 to His101. The path (A) − (D) needs a proper proton transfer from His101 to deprotonated Asp197 at the EH_c state. The path (B) − (D) assumes that the proton donor residue is His101, and Asp197 contributes to arrange directly the function of His101 at the state of EH_c. The path (B) − (C) contains the direct contribution of deprotonated Asp197 to proton transfer from His101 to the substrate at the EH_c state. From the previous reports (1, 4) and pK_3 value of PPA (8.62), the path (A) − (D) is the most probable. On the other hand, the other model in which the proton dose not come from amino acid directly but from water coordinated at the active center in the EH_c state can be proposed, as shown in Fig. 2. In this model, protonated His101 and deprotonated Asp197 assist the water to give its proton to the substrate. This model was similar to that of phosphorylase (11) and suitable to explain the following efficient hydrolytic process using the coordinated water conserving the α-anomeric form.

The fact that H101N HPA exhibits very little catalytic activity does not conflict with present models, provided that a proton may come from other ionic residues which are located near the active site such as Glu233 and His299 or from a water molecule which may be trapped near or at the space made by the change of His101 to Asn101 as shown in Fig. 3. When His101 was changed to Leu, amylase activity was disappeared completely (unpublished data). This result supports the above speculation (Fig. 3). There are some examples that mutant enzymes (by protein engineering methods) without native proton donor residues still have residual catalytic activities with the help of a water molecule or the substrate (6, 7). Furthermore, the results that both the two mutant HPAs of which Asp197 and 300 were changed to Asn had no amylase activity (unpublished data) support the mechanism described above.
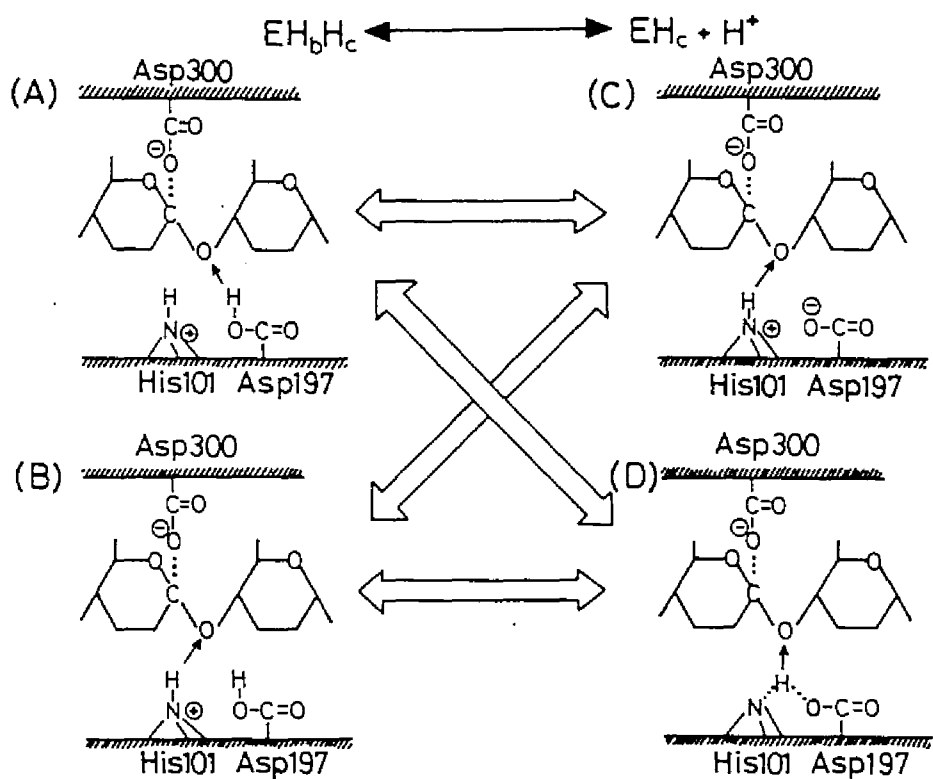
Fig. 1. Proposed mechanism of action of mammalian α-amylase at the initial stage. (A) or (B) is the active form complex of EH_bH_c and substrate of which Asp197 and His101 are protonated. (C) or (D) is the active form complex of EH_c and substrate of which His101 is protonated.
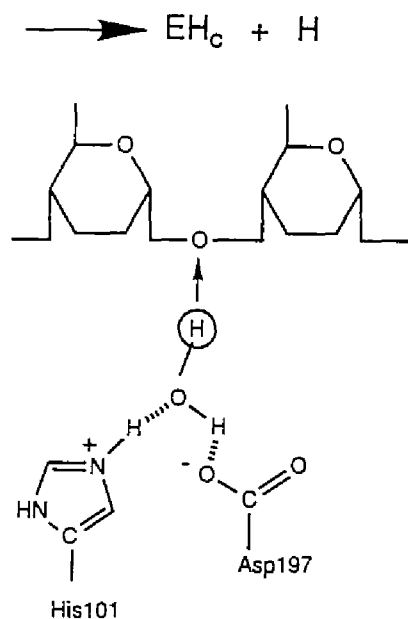

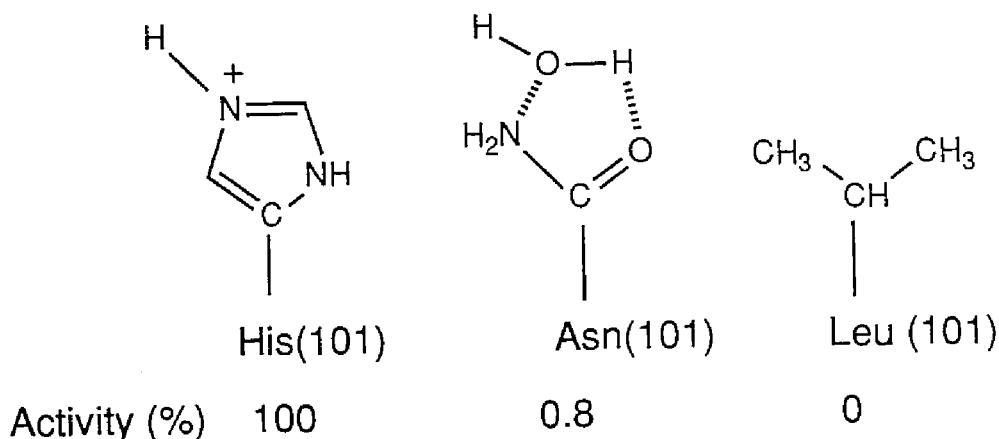Fig. 2. Proposed mechanism of the catalysis with the coordinated water at EH_c state.

	His(101)	Asn(101)	Leu (101)
Activity (%)	100	0.8	0

Fig. 3 (A) Imidazole ring of His; (B) A part of Asn and trapped water; (C) A part of Leu (water is not trapped).

Mammalian α-amylases are activated by the binding of chloride ion which also causes the shift of optimum pH (8, 9). In the case of PPA, chloride ion binds at Arg195, Lys257 and Arg337 (1). The loop containing Arg195, Asp197 and His201 is located along the catalytic site and the substrate binding site (subsite 5) (CHAPTER V) can be stabilized by binding both to the chloride ion through its Arg195 (10) and to the substrate around the subsite 5 through its His201 (CHAPTER V). The stabilization of the loop must be necessary for PPA's activity with neutral optimum pH, since the activity requires the presence of chloride ion and occupancy of the subsite 5 with suitable substrate. The function of His101 is controllable through Asp197 on the loop. Consequently, the efficiency of the catalytic activity form EH_c with neutral optimum pH must be enhanced by the stabilization of the loop. That is, a part of the substrate bound to the subsite 5 can act as an activator or a modulator of the enzyme function by stabilizing the loop through interaction with His201. A schematic mechanistic model exhibiting the correlation of chloride ion, the subsites, the loop and the participating amino acids is shown in Fig. 4. It is clear that both interactions between the substrate bound at subsite 5 and His201 and between chloride ion and Arg195 contribute almost equally to the activation and control of optimum pH, through the stabilization of the loop. Effects of synthesized substrates upon the activity is well explained by the model in Fig. 4 where His201 plays an important role to recognize the substrate at the subsite 5. Since at EH_c state His101 plays principal roles, it is natural to speculate that subtle configuration change of Asp197 through loop stabilization affects the proton transfer efficiency of the His101 connected to Asp197 with a hydrogen

bonding bridge as shown in Fig. 1. The very close sequence homologies among porcine, human and rat α-amylases fairly suggest the same recognition and control mechanisms.
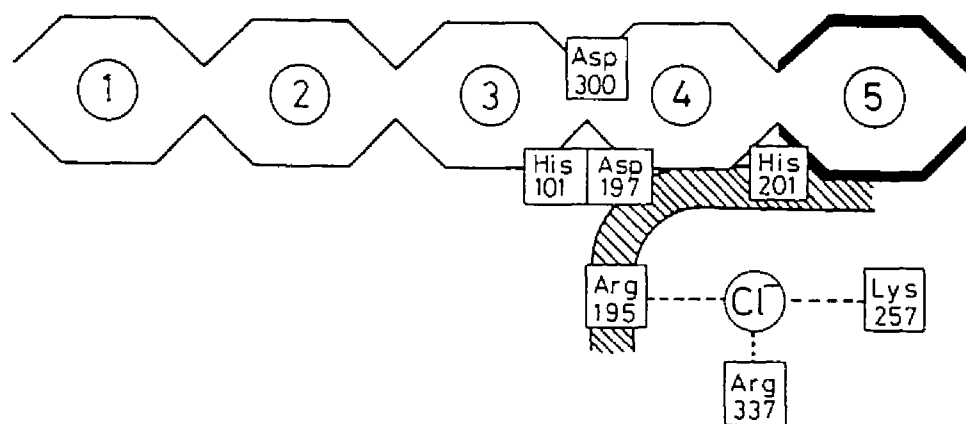

Fig. 4 Schematic active site model of PPA. Subsites per glucose residues of the substrate are numbered 1 to 5 from the nonreducing end. Catalytic site composed of Asp300, Asp197 and His101 is located between subsite 3 and 4. Chloride ion (Cl⁻) binds at Arg195, Lys257 and Arg337. Shaded band along the active site shows a loop containing Arg195, Asp197 and His201.

Inhibition mechanism by proteinaceous α-amylase inhibitors

From the data for the mutant HPAs and X-ray analysis of PPA, it was revealed that His201 which can be modified by DEP is located around subsite 4 and 5 in mammalian α-amylase. By considering that His201 relates to the binding of the α-amylase inhibitor (phaseolamin) (CHAPTER V), the author speculates that inhibition mechanism of mammalian α-amylase by phaseolamin as follows.

In the case of native enzyme, phaseolamin bind to the enzyme occupying subsite 4-5 as shown in Fig. 5 (A). Starch, amylose and other oligosaccharides are not able to bind to the active site of the enzyme which the inhibitor binds to in the productive binding mode (Fig. 5 (B)). Therefore, both amylase and maltosidase activities are inhibited completely.

In the case of modified PPA and HPA by DEP, amylase activity was decreased by the decrease of the affinity in subsite 4 and 5 by the chemical modification. Furthermore, the steric hindrance of modified His201 (etoxyformylated His201) disturbs the acceptance of subsite 4 and 5 for G. However the steric hindrance does not inhibit the acceptance of subsite 4 for φ, because φ is smaller than G. The part of phaseolamin which binds to subsite 4 in the native enzyme as shown in Fig 5 (A) is not able to bind to it in modified one because of the modified

His201 (Fig. 5 (C)). Therefore in the modified HPA, subsite 4 does not influenced by phaseolamin, but subsite 5 was occupied by phaseolamin. Consequently, only ϕ can be accepted in subsite 4 of modified enzyme and modified enzyme-phaseolamin complex and only maltosidase activity of the modified enzyme was observed without inhibition by phaseolamin. The selective inhibition of amylase activity of modified enzyme by phaseolamin can be explained with the above speculation.

In the case of mutant HPA (H201N) neither amylase and maltosidase activities were not inhibited by phaseolamin completely. This result indicates that the part of phaseolamin which binds to the character of His201 in α-amylase dose not bind to Asn201 rigidly. Therefore, the part of the phaseolamin which relates to the complete inhibition exists flexibly around subsite 4 and 5 in the complex, and complete inhibition for neither amylase and maltosidase are not observed.

In the case of P1 inhibitor purified from wheat gluten, both amylase and maltosidase activities were inhibited completely in spite of the chemical modification and site directed mutation in mammalian α-amylases (unpublished data). Therefore, it was revealed that the inhibition mechanism by P1 is different from that by phaseolamin.
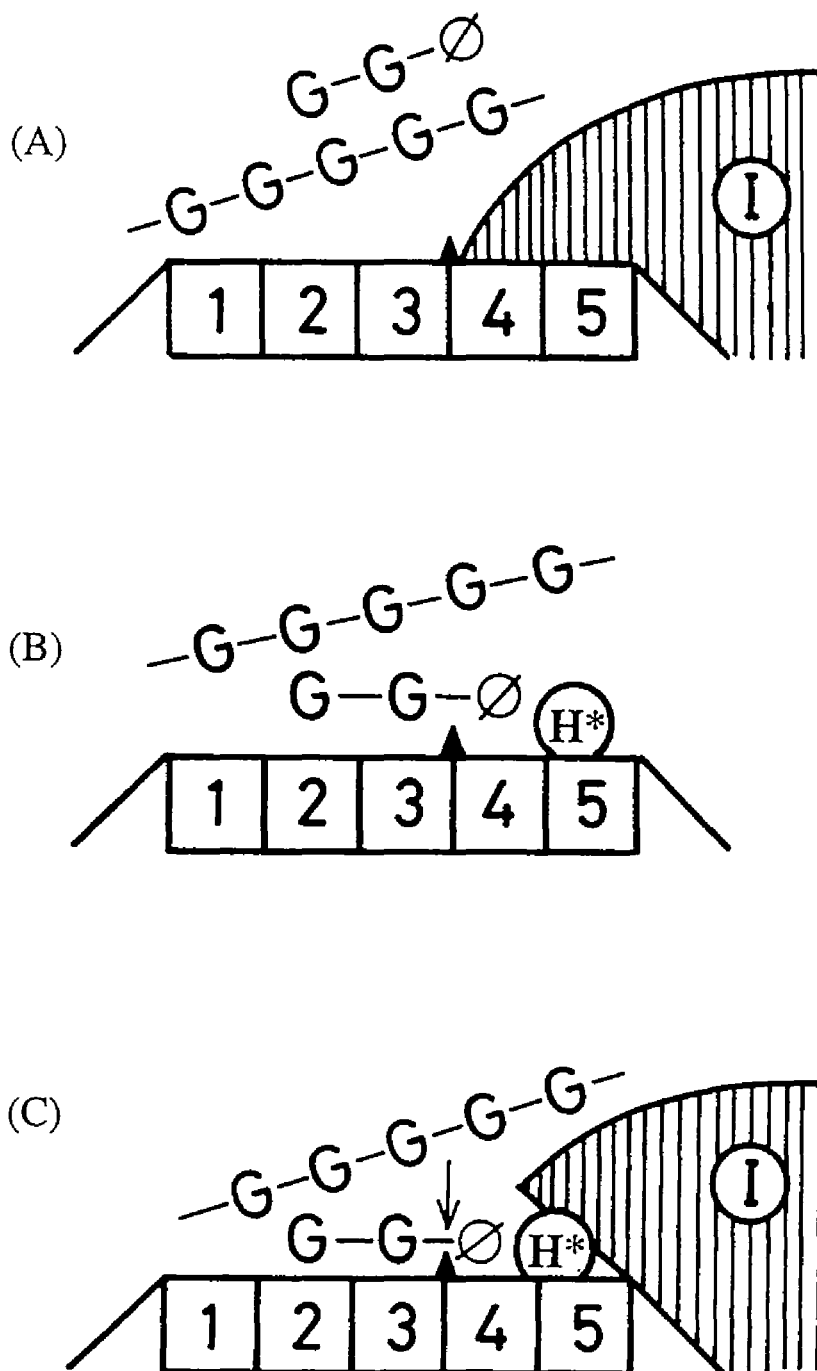
Fig. 5 Binding model of mammalian α-amylase and phaseolamin. (A), (B) and (C) show the binding model of phaseolamin and native mammalian α-amylase, modified mammalian α-amylase and the binding model of phaseolamin and modified mammalian α-amylase, respectively. I, H*, G and φ represent phaseolamin, modified His201, glucose and p-nitrophenol, respectively.

REFERENCES

1) Buisson, G., Duee, E., Haser, R., and Payan, F. (1987) *EMBO Journal,* **6**, 3909-3916 399-406

2) Svensson, B. (1988) *FEBS Lett.,* **230**, 72-76

3) Fischer, E.H. and Stein, E.A. (1960) *The Enzymes* , 4, 313-343

4) Matsuura, Y., Kusunoki, M., Harada, W., and Kakudo, M. (1984) *J. Biochem. (Tokyo),* **95**, 697-702

5) Nakatani, H. and Ishikawa, K. (1991) *J. Biochem.,* **109**, 440-443

6) Canter, P and Wells, J.A. (1987) *Science,* **237**, 394-399

7) Lewendon, A., Murray, I. A., Shaw, W. V., Gibbs, M. R., and Leslie, A, G, W. (1990) *Biochemistry,* **29**, 2075-2080

8) Wakim, J., Robinson, M., and Thoma, J.A. (1969) *Carbohydr. Res.,* **10**, 487-503

9) Levitzuki, A. and Steer, M.L. (1974) *Eur. J. Biochem.,* **41**, 171-180

10) Yamashita, H., Nakatani, H., and Tonomura, B. (1991) *J. Biochem. (Tokyo),* **110**, 605-607

11) Johnson, L. N., Acharya, K. R., Jordan, M. D., and McLaughlin, P. J. (1990) *J. Mol. Biol.,* **211**, 645-661

ACKNOWLEDGMENTS

LIST OF PUBLICATIONS

(A) Main publications

1. Ishikawa, K. and Hirata, H. (1989) "New Substrate Specificity of Porcine Pancreatic α-Amylase", *Arch. Biochem. Biophys.*, **272**, 356-363

2. Ishikawa, K., Matsui, I., Honda, K., and Nakatani, H. (1990) "Substrate Dependent Shift of Optimum pH in Porcine Pancreatic α-Amylase-Catalyzed Reactions", *Biochemistry*, **29**, 7119-7123

3. Ishikawa, K., Matsui, I., Honda, K., Kobayashi, S., and Nakatani, H. (1991) "The pH Dependence of Action Pattern in Porcine Pancreatic α-Amylase-Catalyzed Reaction for Maltooligosaccharide Substrates", *Arch. Biochem. Biophys.* **289**, 124-129

4. Ishikawa, K and Nakatani, H (1991) "α-Amylase Inhibitors from Wheat Gluten", *Agric. Biol. Chem.* **55**, 2891-2892

5. Nakatani, H. and Ishikawa, K. (1991) "Numerical Method to Analyze pH-Profile from Initial Velocity Data and Semi-Empirical Procedure to Identify Catalytic Residues of Enzymes Using pK and Heat of Ionization", *J. Biochem.*, **109**, 440-443

6. Ishikawa, K., Matsui, I., Honda, K., and Nakatani, H. (1992) "Multi-Functional Roles of Histidine Residues in Mammalian α-Amylase", *Biochem. Biophys. Res. Commun.*, **183**, 286-291

7. Ishikawa, K., Matsui, I., Honda, K., Kobayashi, S., and Nakatani, H. (1992) "Substrate Recognition at the Binding Site of Mammalian Pancreatic α-Amylases", (in submission to *Biochemistry*)

(B) Related publications

1. Matsui, I., Matsui, E., Ishikawa, K., Miyairi, S. and Honda, K. (1990) "The Enzyme and Molecular Characteristic of *Saccharomycopsis* α-Amylase Secreted from *Saccharomyces cerevisiae*", *Agric. Biol. Chem.*, **54**, 2009-2015

2. Matsui, I., Ishikawa, K., Miyairi, S., Fukui, S. and Honda, K. (1991) "Subsite Structure of *Saccharomycopsis* α-Amylase Secreted from *Saccharomyces cerevisiae*", *J. Biochem.*, **109**, 566-569

3. Matsui, I., Ishikawa, K., Miyairi, S., Fukui, S. and Honda, K. (1991) "An Increase in the Transglycosylation Activity of *Saccharomycopsis* α-Amylase Altered by Site-Directed Mutagenesis", *Biochim. Biophys. Acta,* **1077**, 416-419

4. Matsui, I., Ishikawa, K., Miyairi, S., Fukui, S. and Honda, K. (1992) "Alteration of Bond-cleavage Pattern in the Hydrolysis Catalyzed by *Saccharomycopsis* α-Amylase Altered by Site-directed Mutagenesis ", *Biochemistry* , **31**, 5232-5236

5. Matsui, I., Ishikawa, K., Miyairi, S., Fukui, S. and Honda, K. (1992) "A Mutant a-Amylase with Enhanced Activity Specific for Short Substrates", *FEBS Lett.,* **310,** 216-218

(C) Review

1. Ishikawa, K (1990) "New Substrate Specificity of Porcine Pancreatic α-Amylase by Chemical Modification", *Tanpakushitu Hybrid III,* (Kyouritu Syuppan) 222-230